Development and Characterization of Grouts for Sealing and Sensing Applications

A Dissertation

Presented to

the Faculty of the Department of Civil and Environmental Engineering

University of Houston

In Partial Fulfillment

of the Requirements for the Degree

Doctor of Philosophy

in Civil Engineering

by

Shiva Sunder

December 2012

DEVELOPMENT AND CHARACTERIZATION OF GROUTS FOR SEALING AND SENSING APPLICATIONS

Shiva Sunder

Approved:

Chairman of the Committee
Cumaraswamy Vipulanandan, Professor,
Civil and Environmental Engineering

Committee Members:

Ashraf S. Ayoub, Associate Professor,
Civil and Environmental Engineering

Kaspar J. Willam, Professor,
Civil and Environmental Engineering

Shuhab Khan, Associate Professor,
Earth and Atmospheric Sciences

Gangbing Song, Professor,
Mechanical Engineering

Suresh K. Khator,
Associate Dean,
Cullen College of Engineering

Abdeldjelil "DJ" Belarbi,
Professor and Chairman,
Civil and Environmental Engineering

ACKNOWLEDGEMENTS

I would like to express my sincere thanks to those who have helped me during the course of my research in the past four years. I would like to express my sincere gratitude to my advisor, Dr. Cumaraswamy Vipulanandan, for his valuable guidance and encouragement throughout the course of this study. I would also like to express my thanks to my dissertation committee members, Dr. Ashraf S. Ayoub, Dr. Kaspar Willam, Dr. Gangbing Song and Dr. Shuhab Khan for their precious time and suggestions.

My thanks also go to the graduate students, Srisothinathan Pakeetharan, Ahmed Mohammed, Jeannot Ahossin Guezo, Aram Mohammed, Danistan Joseph, Siva Vinay Moturi, Kalaiarasi Vembu, Deepthi Kumar Sugumar, Harendra Sivaram, Prashanth Puvirajasingham, Saravanan Ravichandran, Dongmei Pan, Jia Liu, Naveed Salehi, Navaneeth Narayanan, Wei Qiao, Emrah Demircan, Burak Kazez and Balakrishnan Ramesh for their assistance, companionship and encouragement.

I would like to extend my deepest gratitude to the faculty and staff of the Department of Civil and Environmental Engineering for their unflinching support. The help and support rendered by Jeffrey Miller and Gerald McTigret will never be forgotten. Special thanks goes to Cherish Wallace, Stephanie Woods, Stephanie Williams, Justin Burton and Charlene Holliday.

I acknowledge the financial support given by CIGMAT, THC-IT and the Department of Civil and Environmental Engineering. Finally, my special thanks go to my family and friends for their tireless support when it was most required.

Development and Characterization of Grouts for Sealing and Sensing Applications

A Dissertation

Presented to

the Faculty of the Department of Civil and Environmental Engineering

University of Houston

In Partial Fulfillment

of the Requirements for the Degree

Doctor of Philosophy

in Civil Engineering

by

Shiva Sunder

December 2012

ABSTRACT

Greater use of cement and polymeric grouts in sealing applications demands further enhancement in the physical, mechanical and sensing properties from the time of mixing through pumping, final setting and entire service life. Hence, the cement and polymeric grouts (acrylamide, acrylic and polyurethane) were modified using various solutions and particle fillers. The self sensing capabilities for the grouts and grouted sands have been developed (resistivity and dielectric parameters) with applied stress. For the purpose of enhancing piezo-resistive and dielectric sensing capabilities of the grouts, a small amount of conductive fibers were used in the grout mix. Test protocols were developed to evaluate the sealing of leaking waste water pipe joints and decommissioning oil pipelines.

The addition of surfactants had a significant effect on the polymeric grouts (maximum increase up to 4 hrs with the addition of Cationic surfactant). The bleed in the cement grout was reduced to zero with the addition of 10% clay. The pullout test developed was sensitive to the addition of admixtures in the grout and grouted sand. The compressive strength of the polymeric grout increased by over 50% with the addition of anionic surfactant. The optimum clay content was 5% based on the strength enhancement of cement grout.

The dielectric constant of the chemically grouted sand varied from a value of 4 to 1200 with the addition of conductive fibers. With stress application on grouted sand with fibers, the dielectric constant varied from 1200 to 4200, a 250% increase as compared to a variation of 4.3 to 5.8 which was a 34% increase for the sample without fibers. The dielectric constant of the cement grout decreased by about 25% with the addition of clay.

Application of polymeric grout was studied in large scale model tests. The polymeric grout was effective in sealing the lateral leaking joint with a leak of 1220 gpd to 0 gpd. The use of polyurethane grout was effective in sealing material in the decommissioning of simulated oil pipelines. A phenomenological model based on gas production and hardening properties of grout was developed to predict the confined expansion pressures developed during the curing of polyurethane grout. Also non-linear stress strain models were used to predict the behavior of grouted sand. Effect of additives on stresses on the sensing properties of the grouts and grouted sand were quantified.

TABLE OF CONTENTS

LIST OF FIGURES

LIST OF TABLES

CHAPTER 1 INTRODUCTION

Grouts are being used in a number of applications to solve short-term and long-term problems. Soil stabilization and leak control through grouting has been a popular technique where the void spaces in the soil are filled using a viscous liquid which has the ability to undergo a phase transformation to solid. Based on how the fluid is injected into the ground, grouting can be classified as permeation grouting, compaction grouting, hydrofracture grouting and jet grouting (Gallavresi, 1992). However, from the materials perspective, the grouts can be divided into two broad categories, they are, chemical grouts (true solutions) and suspended solid grouts (like cement grouts) (Karol, 1982; Vipulanandan and Shenoy, 1992).

1.1. Problem Statement

The widespread usage of cement and polymeric grouts in various applications demands further enhancement in the physical, mechanical and sensing properties from the time of mixing through pumping to final setting and during the grout's service life. The study of the complex chemistry and physics in the process of setting of these grouts are absolutely important in understanding their short term and long term behavior. The knowhow on the nature of their behavior enhances the field of research to modify their composition for various applications. In the past, grouts were primarily used for the purpose of soil stabilization with the main objective, being strength enhancement and permeability reduction, but as years passed, they were used in varied applications, most common among them being, sealing pipeline leaks.

For a population of around 2 million, Houston has around 1.8 million lateral pipeline joints. Therefore, Infiltration/inflow is often one of the major issues that result in the underground pipeline leak. Infiltration/Inflow is defined as the entrance of storm water through pipeline joints and fissures. Similarly, decommissioning is a term frequently used in the offshore industry to abandon the currently dormant offshore structures. It is important to note that the old pipelines that are to be removed or replaced contain inside them, a notable amount of oil waste. Hence decommissioning of old pipeline is to be done without contaminating the ocean. This facilitates the need to seal the pipelines before being cut and removed from the ocean floor. It is also essential to develop grout materials with sensing capabilities. For this purpose, the grouts that are used to fill the cracks and fissures and also leaking joints are to be inherited with self sensing property which acts as a good indicator during the times of leaks or material failure.

Therefore, this research mainly focuses on the use of admixture modified grouts for sealing onshore waste water pipeline and offshore oil pipelines. An attempt has also been made to develop grout materials with self sensing capabilities. The sealing methodology is opted to minimize the infiltration/inflow leaks on the waste water pipelines (sealing from outside) and decommissioning/abandoning the portion of offshore oil pipeline (sealing the inner cross section of the pipeline).

1.2 Objectives

The overall objective of this research was to develop grout materials for sealing and sensing applications. The specific objectives of this study are as follows.

1) Modify and characterize the chemical grouts for sealing and sensing applications.

2) Modify the cement grout with sensing properties

3) Model the curing and mechanical behavior of modified grouts.

1.3 Organization

This Dissertation is an organization of the study investigating the behavior of modified chemical and cement grouts for sealing and sensing applications which have been summarized in 7 chapters. Chapter one introduces the reason behind this study by defining the problem statement and the potential objectives that this research is driven toward. Chapter two gives a detailed background on the basic concepts that have been used in this study with supporting information from the literature. Chapter three focuses on the existing and newly developed testing methodologies that have been applied to characterize the grout materials. Chapter four discusses the effect of addition of surfactants on the chemical grouts and the grout performance in sealing lateral leaking joint. Chapter five focuses on the development of clay-cement grout and the effect of clay on the sensing properties of cement grout. Chapter six discusses the modeling of the uni-axial stress development during the expansion of polyurethane grout during gelling. The stress-strain behavior of the chemical grout has also been modeled. Chapter seven draws the important observations and conclusions of this study.

CHAPTER 2 BACKGROUND AND LITERATURE REVIEW

Introduction

This chapter provides a comprehensive review of the basic concepts that have been used in the proposed research in addition to the past and recent works related to the current study. A detailed investigation on the process of grouting, types of grouts and admixtures, the chemistry of grout materials, the concept of sensing with special significance to dielectric behavior of the grouts and sealing has been carried out.

2.1 Cement Grouts

Cement grouts have been used in the field of civil engineering since 1930s (Shenoy, 1991). They have multiple applications and hence there is continued interest in modifying the grout. The main interest in the applicability of the cement grout is heavily dependent on the penetrability of the grout into fissures or cracks. For this purpose, researches have been conducted on the ultrafine cement grouts to increase the applications of cement grouts. So, investigation on the flow-ability of the cement grout is essential when modified by the addition of admixtures. The hydration process and the hydrated products are believed to exert major control over almost all the important engineering properties of cements such as strength, elasticity, shrinkage, creep, permeability and durability (Taylor and Arulanandan, 1974). Water-Cement Ratio is one of the prime governing factors which influence the behavior of the cement grout. Insufficient water content in the grout is one of the main contributing factors for incomplete hydrated gel formation. Recent researches have proved that by adding additives, the properties of cement grouts can be

altered to desired satisfaction which makes it more appropriate for the multiple applications.

Effect of the adsorptive behavior of surfactants in the surface of Portland cement was studied by Zhang (2001). The main functions of adding additives with respect to surface activity are to improve viscosity, to reduce water, to act as air-entraining admixture and to reduce shrinkage. Adsorbance, contact angle and zeta potential were measured on adding ethoxylated fatty alcohol sulfate (AES ,anionic), Cetyl piridinium chloride (CPC, cationic), ethoxylated alkyl phenol (TX-10, nonionic) and NS (polymeric). It was noted that, AES was adsorbed fast and belongs to LS type adsorption. CPC was adsorbed slowly. TX-10 was not adsorbed. All the hydrophobic chains of the surfactants were present on the surface of the Portland cement. Zeta potential measurements indicated that both cationic and anionic surfactants can be adsorbed o the cement surface. Role of most commonly used admixtures with cement grout have been discussed in the next section.

2.1.1 Admixtures

Admixture is a material added in small quantities during the process of mixing to modify the properties of the concrete (Buekett, 1998). These admixtures can also be used to modify the properties of cementitious and chemical grouts as modification of the grout mix proportions are being extensively carried out to alter the grouts for various applications with desired properties. Generally, the maximum limit of admixture is kept under 5% by the weight of cement with the exception for mineral admixtures such as silica fume and blast furnace slag (Buekett, 1998).

Metakaolin (MK): it is a pozzolanic material, which is a thermally activated alumino-silicate material. It is manufacturd by the process of calcination of kaolin clay at a temperature of 700–850 ˚ C (Sabir et al, 2001). The use of metakaolin clay increases the strength, reduces the shrinkage and increases the durability.

Surfactants: When surfactants are added to a solution will lower the surface tension of the solution. Critical micelle concentration (CMC) is that concentration of the surfactants in the solution above which the micelles are formed. Hence, if the concentration of surfactant added to the solution exceeds the CMC of the surfactant, no change in the surface tension of the solution can be observed. Below the CMC, the addition of surfactant concentration decreases the surface tension of the solution. Structure of surfactant contains both hydrophobic and hydrophilic groups which make them soluble in water and various other organic chemicals. Based on the charge carried by the surfactants, they are classified as cationic, anionic, zwitterionic and non-ionic surfactants. Table 2-1 summarizes the research works done in the recent past which highlight the role played by the admixtures to modify different properties of the Cement grout.

2.1.2 Cement Chemistry

Cement grouts are formed by the process of hydration. And as time progresses the process of hydration continues and eventually the grouts attain strength. The mechanism of the hydration of cement grout can be explained by the following set of equations (Papadakis et al., 1991),

$$2C_3S + 6H \longrightarrow C_3S_2H_3 + 3CH, \qquad (2\text{-}1)$$

$$2C_2S + 4H \longrightarrow C_3S_2H_3 + CH, \quad (2\text{-}2)$$

$$C_4AF + 2CH + 2CSH_2 + 18H \longrightarrow C_8AFS_2H_{24}, \quad (2\text{-}3)$$

$$C_3A + CSH_2 + 10H \longrightarrow C_4ASH_{12}, \quad (2\text{-}4)$$

$$C_4AF + 4CH + 22H \longrightarrow C_8AFH_{26}, \quad (2\text{-}5)$$

$$C_3A + CH + 12H \longrightarrow C_4AH_{13}. \quad (2\text{-}6)$$

Portland cement paste is is composed of lime (CaO), silica (SiO_2), alumina (Al_2O_3 and ferric oxide (Fe_2O_3) with small percentages of alkali oxides, magnesia gypsum and sulfur trioxide. The main compounds in the ordinary Portland cement are tricalcium silicate (C3S), dicalcium silicate (C_2S), tetracalcium aluminoferrite (C_4AF) and tricalcium aluminate (C_3A). C_3A attributes to the setting of cement as it hydrates rapidly. C_3S and C_2S contribute to the early and long term strength of the cement by hydrating more rapidly and slowly respectively. Thus 7 day strength of the cement is governed by the hydration of C_3S.

Table 2-1: Summary of studies on admixtures in cement grouts

S.No.	Reference	Grout	Admixture	Admixture Composition	W/C Ratio	Measurement	Properties	Result	Remarks
1	Huang (2001)	70% Type 1 Portland Cement (PC) + 30% FA	Polypropelene Fiber (PP) Superplasticizer (SP)	PP and SP - 0 and 1%	W/[C+FA] = 0.4 - 0.8	Mixing – ASTM C 938, Rheology Working Properties Strength Durability	Viscosity, Comp. strength, Setting Time, Bleeding, Permeability, Sulfate attack	PP increases resistance to cracking and alters the durability addition of SP nullifies the adverse effects of PP	No electrical characterization
2	Shannag (2002)	Type 1 PC	Natural Pozzolan (NP) SF Napthalene Formaldehyde sulfonated (SP)	SF - 0-0.15% NP - 0 - 0.15% SP - 0.02%	0.33	Flowability Durability Strength; ASTM C 305, ASTM C 109, ASTM C 939, ASTM C 191, ASTM C 940, ASTM C 942	Flow time Comp. Strength Sulfate resistance, Bleeding, Setting Time	No Bleeding High Flowability good resistance to Sulfate attack High compressive strength	50 mm cubes for Strength – 3, 7, 28 and 56 days
3	Krishna -moorthy et al (2002)	PC	Flyash (FA) Blast Furnace Slag (BFS) Silica Fume (SF)	FA - 20 - 40% BFS - 20-40% SF - 5-10%	0.25-0.4	Flowability Strength Durability	Flow time Comp. Strength Water Absorption	Compressive Strength increases with time Water absoprtion Decreases with time	Optimum SP Figured Strength of concrete before and after grouting was reported

Table 2-1: Summary of studies related to admixture influence on cement grouts (Continued)

S.No.	Reference	Grout	Admixture	Admixture Composition	W/C Ratio	Measurement	Properties	Result	Remarks
4	Svermova et al (2002)	PC	VMA SP Limestone Powder (LSP) - repl cement	VMA - 0.02-0.07% SP - 0.3 - 1.2% LSP - 12-45%	W/B = 0.35 - 0.42	Fluidity Rheology Strength	Rheology Comp. Strength Bleeding	Validating test result using statistical models. Ratio of predicted to experimental values varied from 0.83 to 1.05	Modified Bingham Model Used. Statistical Linear and Log Models
5	Tan et al. (2004)	Type 2 PC	Bentonite (B) SF FA	B - 0 - 3% SF - 0 - 20% FA - 10 - 40%	W/S = 0.75 - 1.25	Bleeding	Bleeding	Silica Fume - most effective for Bleeding. Optimum mix - 20% SF, 3% B, 10% FA. FA not contribute much to bleeding	Full and Factorial Design used S/N Ratio used
6	Eriksson et al (2004)	PC	SP	SP - 0.5 and 1%	0.6 - 1%	Rheology Penetrability	Viscosity, Yield Stress	Deviations due to Ageing of cement and Environmental Conditions	Importance of Test Conditions and Storage

Table 2-1: Summary of studies related to admixture influence on cement grouts (Continued)

S.No.	Reference	Grout	Admixture	Admixture Composition	W/C Ratio	Measurement	Properties	Result	Remarks
7	Anagnosto-poulos (2007)	Microfine PC – Clay	Acryllic Resin (AR) MethylMethacrylate Ester (MMA)	AR and MMA - 0.3%	W/[C+clay] = 2 and 1	Flowability Strength Durability	Setting time Comp. Strength Flowability Shear Bond Str. Sedimentation Resist. to Wet -Dry Cycles and Sulfate attack.	Reduces Flow time increases the setting time MMA decreases strength durability and strength improved	No Model was used
8	Sahmaran et al. (2008)	PC	Natural Zeolite (NZ) Polycarbozyllic ether (SP) Welan Gum (VMA)	NZ - 20 - 40% SP - 0.25-1.00% VMA - 0.05-0.15%	0.6	Rheology	Setting time Viscosity Flowability	VMA and NZ-increased Flow time and decreased Slump flow, apparent viscosity decreases with shear rate	Modified Bingham Model was used.
9	Nguyen et al (2011)	Portland Cement (PC)	Polycarboxylate (HRWRA) Polysacchride (VMA)	HRWRA - 0 - 0.5% VMA - 0 - 1.0%	0.35-0.45	Rheology	Yield Stress	Shear Thinning Behavior Exp. Decrease as HRWRA increases Lin. increase as VMA increases.	Regression Model Developed

Table 2-1: Summary of studies related to admixture influence on cement grouts (Continued)

S.No.	Reference	Grout	Admixture	Admixture Composition	W/C Ratio	Measurement	Properties	Result	Remarks
10	Sonebi et al. (2013)	PC	Metakaolin (MTK) Superplasticizer (SP) VMA	MTK - 6% - 20% (Repl. Cement) SP - 0.3-1.4% VMA - 0.01-0.06%	W/B = 0.4	Rheology Strength	Yield Stress Flow Time Setting Time Plastic Viscosity Comp. Strength	SP - increased Fluidity, Reduced yield stress, VMA - increased flowtime, yield stress, plastic viscosity MTK - reduced setting time, increases compressive strength, increases flow time, yield stress, plastic viscosity.	Modified Bingham Model used. Quadratic Model Developed
Remarks		PC, PC with Clay or FA studied	VMA - Most common admixture	Admixture - Polymer Fiber Pozzolanic	W/C - 0.4 - 0.8 Typical	Rheology - Yield Stress most commonly follows Bingham Model SP - extensive used for enhancing the flow properties Clay had a deep impact on the pure cement grout Regression models used to develop to support the results			

2.2 Chemical Grouts

2.2.1 History

The First chemical grout was invented by Jeriorsky and his work was patented in 1886 where he developed the sodium silicate grout with a coagulant as one of its components (Karol, 1990). Amongst the chemicals used for grouting, acrylamide grouts take one of the prime spots. Since 1950s, acrylamide grouts have been repeatedly used in USA in grouting applications for stabilizing the soil and for resolving pipeline leaks (Vipulanandan and Ozgurel, 2009; Ozgurel, 2004). In 1989, around 43% of the chemical grouts that were used in USA were acrylamide grouts (Weideborg et al., 2000). Polyurethane grouts are a type of high viscous chemical grouts which have been used in U.S.A since early 1970s. It was developed in Germany during the time of World War II.

2.2.2 Acrylamide and Polyurethanes

Chemical grouts/resins not only serve as grout materials as they are, but they are often mixed with cement grouts for improving the characteristics of the composite grout system. Acrylamide grouts are aqueous solutions having more than two chemical components. Considering chemical grouts, their penetrability is primarily dependent on the viscosity of the solution that enables a reasonable flow of the grout at applied permissible pressures (Karol, 1982). Grouting with chemical grouts is effective for sands with permeability as low as 10^{-4} cm/s (Christopher et al, 1989). A six year laboratory study was done by Haug et al (1998) to investigate the effect of confining pressure on the performance of chemical grout in salt water. Acrylamide (AV-100) and acrylate (AV-

400) grouts were studied. The test was performed at confining pressures of 0, 3.4 and 6.9 MPa. The purpose of using different confining pressures was to simulate different mining conditions. Visual inspection and weight loss measurements were done at periodic intervals. It was observed that AV-100 grout samples performed satisfactorily during the first 2 years, but rapid deterioration in the weight was observed during 3^{rd} to 5^{th} year at confining pressure of 3.4 and 6.9 MPa. The deterioration was not severe during the sixth year though. Risk assessment of acrylamide grout used in a tunnel construction was critically reviewed by Weideborg et al. (2001). The study focused on monitoring the environmental risk caused by the non-polymerized monomers during the use of acrylamide based agent, Rhoca Gel. The drainage water from the tunnel was collected and examined with respect to acrylamide. The study concluded poor degree of polymerization if diluted with water. If the monomers are not completely polymerized, the chemical effect might take a toll on the aquatic habitat. However, it can be noted from this study that proper injection method ensuring complete degree of polymerization is essential for complete results and functioning of the grout used.

Polyurethanes find their main use in mining applications with the primary use being sealing water joints and ground. Polyurethane grouts once gelled forms thick foam which is impervious to water. The polyurethane grout can be either hydrophobic (water repellent) or hydrophilic (water attractive). They are generally two component system where water is one of the components in the case of hydrophilic grouts. Since the polyurethanes are generally a two component system, they can be injected in the site in two different ways. They are, “one shot system” where the components are mixed prior to injection of the grout ensuring pre-polymerization of the grout prior to injection and “two

shot system", where, one component is injected first and then the second component is injected later ensuring the polymerization to take place at the site (Mattey, 2001).

Synthesis of hydrophilic polyurethanes was investigated by Kojio et al (2009). For making hydrophilic Pus, hydrophilic polymer glycol like poly (oxyethylene) glycol and a hydrophilic chain extender with functional grouts like sulfonic acid and quaternary ammonium groups are generally incorporated. The currently used raw materials which are diisocyanates are all hydrophobic in nature. Hence, for generating high water-absorbing PUs, it is mandatory to have a hydrophobic part in the molecular structure. PU elastomers (PUEs) were synthesized by prepolymer method where, 1,2-bis (isocyanate) ethoxy ethane (TEGDI) and 4,4`-diphenylmethane diisocyanate (MDI) were added to nitrogen dried poly(ethylene oxide-co-propylene oxide) copolyol (EOPO) with specific formulation ratios. On agitating the mixture under nitrogen environment, a drop of dibutyl tindilaurylate (DBTL) was added as a catalyst to initiate and accelerate the reaction. Then a mixture of 1,4-buthanediol (BD) and 1,1,1-trimethylol propane (TMP) was added into the prepolymer as a crosslinking agent. This gives a highly viscous product which is a polyurethane elastomer.

Polyurethane foam as a grouting system was developed to enable the installation of access tubes for the measurement of the movement of a gamma-emitting tracer in the unsaturated zone of the chalk, but will also allow neutron moisture measurements to be made to greater depths in fissures component rocks than has been possible previously which was studied by Black (1976). A two-component (mixed at equal volumes) polyurethane foam was used. The final density of the foam was about 0.04 g/cu.cm and

the diffusion coefficient was 1E-6 sq.cm/sec.the high viscosity of the grout prevenets fissure penetration. Since the density is extremely low, the gamma-ray attenuation is insignificant.

It is to be noted that the typical pressure at which the chemical grouts are injected into the ground is less than 10 psi. However, the pressure at which the grout is injected depends on other factors namely, the type of soil and its other properties such as the density, moisture content, height of the water table and grout properties such as its viscosity, flowability, setting time, number of components of the grout etc.,. Some of the recent works investigating the use of chemical grouts have been summarized in Table 2-5.

Table 2-2: Summary of relevant Literature on Chemical Grouts

S.No.	Reference	Type of Grout	Purpose of Research	Chemical	Soil and other imp. Component	Testing	Sample Dimensions	Result	Remarks
1	Maher and Ro (1994)	Inorganic Polymer	Improving soil behavior under loading conditions	Sodium Silicate (SS) (30-60%), acrylate (30-50%) and polyurethane (10-20%)	Ottawa 20-30 sand	Resonant column test, cyclic triaxial test	2 in. x 7 in. cylinders	addition of SS increased the shear modulus and decreased damping ratio, shear modulus increased with increasing confining stress	chemical grout addition reduces the cyclic prestraining in sands
2	Zelanko and Karfakis (1997)	Polymer	Mining conditions	Polyester	gravel (1 in. passing limestone), resin to catalyst = 50:1	compressive strength, tension test, field evaluation	2 x 4 cylinders (without gravel) 4 x 8 cylinders (with gravel)	compressive strength = 14000 psi tensile strength (avg) = 940 psi	less hazardous to nature, limited expansion without foaming
3	Snuparek and Saucek (2000)	Polymer	Pumpability issues	Polyurethane - 2 component	-	Viscosity, Compression, Tension	cylinders - compression - 53 mm dia. depth:thick -ness = 2:1 beams - tension	difference in viscosity - decreases exponentially with increase in temperature. Comp.Str. Decreases as foaming factor increases	strain-hardening behvior, bulging, large scale model for fissure grouting

Table 2-2: Summary of relevant Literature on Chemical Grouts (continued)

S.No.	Reference	Type of Grout	Purpose of Research	Chemical	Soil and other imp. Component	Testing	Sample Dimensions	Result	Remarks
4	Gallagher and Mitchell (2002)	Inorganic	Deforma -tion properties on loose sand	colloidal silica (5 - 20%), sodium chloride, hydrochloric acid	Monterey sand 0/30, poorly graded, medium to fine	Cyclic triaxial test, compression test	3in. X 6.25 in. cylinders	strain decreases as % colloidal silica increases, compressive str: 4 -222 kPa.	addition of colloidal silica enhances the strength of grouted sand
5	Axelsson (2005)	Inorganic	Grouting in low permeable rock	Silica sol	-	shrinkage comp. strength shear strength flexural strength	40 x 40 x 160 mm - shrinkage 55 mm dia x 50 mm - strength	Shrinkage decreased with time at all humidity Strength from 1 to 1000 kPa over 1 month	Grout behavior predicted well with Mohr-Coloumb failure criteria
6	Anagnos topoulos (2005)	Polymer	For ground improve -ment	Acryllic resin (0 and 30%) methylene mathacrylate ester (0 and 30%)	Sand-Gravel Mixture cement (20 and 100%) silty clay (0 and 80%)	Comp. strength permeability	Gr. Sand Columns - 150 cm tall (cut and tested), 1.5 cm diameter	Strength and modulus decreases as dist from grouting pt. increases. Coeff. Of prem. Increases as dist from grouting pt increases.	latexes influence setting resulting in adverse effect on 7 day strength.

Table 2-2: Summary of relevant Literature on Chemical Grouts (continued)

S.No.	Reference	Type of Grout	Purpose of Research	Chemical	Soil and other imp. Component	Testing	Sample Dimensions	Result	Remarks
7	Vintzileou and Fezans (2008)	Inorganic	Enhance durability, protect frescoes, mosaics	Lime-pozzolan mortar, Silicious river sand and limestone gravels	-	Tested after 1, 3, 6, 9 and 12 months Large scale load test - Compression or diagonal compression	Limestone agg - 1.5-2.0 cm binder:agg = 1:1.5 water:binder = 0.65	Out of plane deformation tensile strength of masonry increases	Grout injected to the masonry to improve the strength
8	Akiyama and Kawasaki (2012)	Polymer	Counter -measure for Lique -faction	Monoammonium phosphate (MAP) Diammonium phosphate (DAP) - AP stock Calcium nitrate (CN) Calcium acetate (CA) - C stock	Toyoura Sand C stock:AP stock = 1:1	Change in pH, vscosity Comp. strength	195 cm^3 of sand and 73 ml of grout	pH increases from acidic to neutral DAP:CN - 500 cP, AP:CA - 50 - 100 cP strength - 15 - 45 kPa	DAP:CA strength increases with time in all other cases, negligible change

Table 2-2: Summary of relevant Literature on Chemical Grouts (continued)

S.No.	Reference	Type of Grout	Purpose of Research	Chemical	Soil and other imp. Component	Testing	Sample Dimensions	Result	Remarks
9	Baltazar et al (2012)	Inorganic	Consolida -tion of old masonry - study of injectability	Hydraulic lime naphthalene - SP polycarboxylate - SP	-	Rheology, water retention, stability test	Water/ Binder = 0.5	apparent viscosity increased with time water retention time > 2000 s CV for stability < 0.3 - stable mix	Method of mixing greatest influence on stability
Remarks		chemical - Inorganic and Inorganic	Varied applications	Polymers - soil applications and inorganic - Rock applications.	Mainly cohesion-less soils	Mechanical and Rheology	Cylindrical samples	Chemical grouts enhance the stress strain properties of soil, compressive strength is the key parameter to be investigated with the viscosity which contributes to the flowability and pumpability.	

2.2.3 Acrylamide and Polyurethane Chemistry

In understanding the properties of grouts, it is very important to investigate the mechanism of formation of the grout. This also provides a clear understanding on the effect of admixtures (if any) added to the grout for modifying the grout. Hence this section briefly explains the process of setting of the grouts under investigation which is chemically driven.

The term polymerization is defined as the mechanism by which monomers react to form long chained cross linked three dimensional networks called polymers. The formation of polymers can happen in two possible ways. The two different types of polymerization are step polymerization or chain polymerization. Step polymerization is one in which the polymers are formed in steps as the reaction takes place by the interaction of the functional groups in the monomers. However, the chain polymerization is associated to the monomers getting to each other and forming long chains. It is also associated to the formation of unsaturated bonds during the reaction. Free radical polymerization is an important type of chain polymerization where the polymers are formed in chains by the addition of free radicals. It is to be noted that the gelling of acrylmide resin takes place by the process of free radical polymerization. Free radical polymerization has three steps:

Step 1: Initiation: the initiators provide the free radicals which get transferred to the monomers in the reaction

Step 2: Propagation: in this time the polymer chain grows. The chain length depends upon the number of free radicals and the monomer units.

Step 3: Termination: In this step, the polymerization reaction stops owing to the depletion of the monomer units since all the monomers are used up during the propagation phase to form polymer chains. The free radical copolymerization of acrylamide monomer is given by the following equation (Menter. P, 2005).

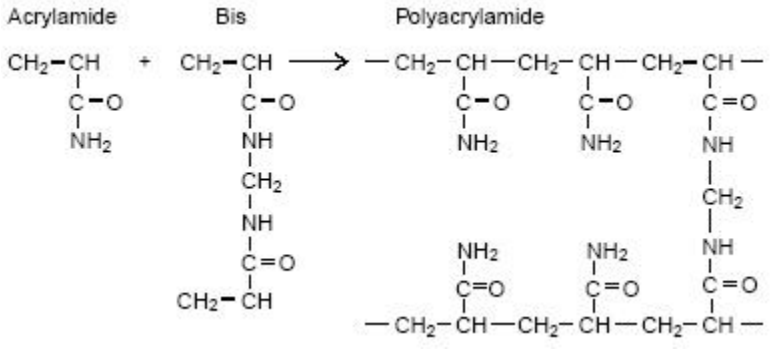

. (2-7)

Hydrophilic polyurethanes are formed by a relatively less complicated process where, the iso-cyanate group in the resin reacts with the water molecule to produce a highly unstable compound which decomposes itself to produce carbon-di-oxide gas and amine. This reaction continues till the ingredients are worn out. The property of expansion during the process of gelling is mainly because of the production of carbondi-oxide gas as a result of exothermic polymerization reaction which expels the polyurethane foam product with the intension to escape to the atmosphere. The following equation explains the polymerization reaction of polyurethane grout,

$$\underset{\text{(Urethane Monomer)}}{\text{R-NCO}} + \underset{\text{(Water)}}{H_2O} \longrightarrow \underset{\text{(Carbamic Acid)}}{\text{R-NH-COOH}} \longrightarrow \underset{\text{(Amine)}}{\text{R-NH}_2} + CO_2\uparrow, \quad (2\text{-}8)$$

R-NCO + R-NH2 ⟶ -(-R-NH-CO-NH-R-)-. (2-9)
(Urethane Monomer) (Amine) (Poly-urethane)

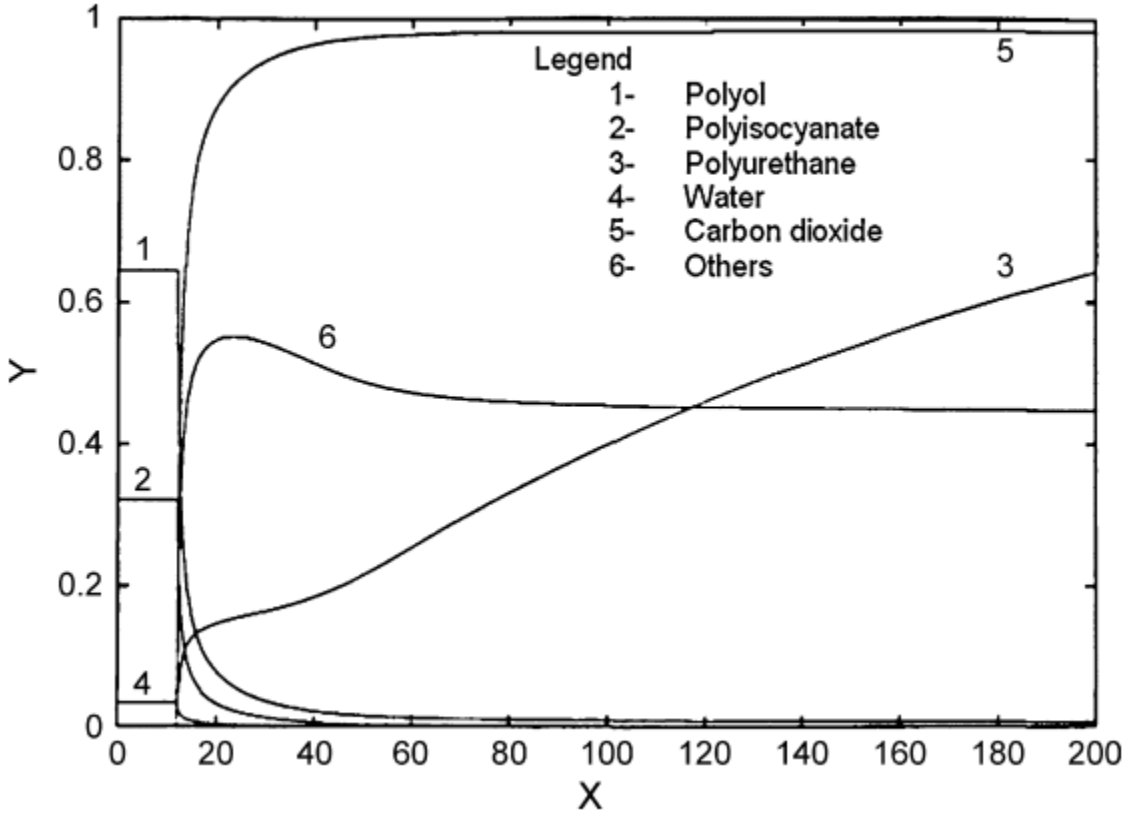

Figure 2-1: Evolution of various reactants during PU – polymerization (Lefebre, 1993).

Bikard et al. (2007) studied the polymerization reaction of a two component polyurethane chemical. They investigated the expansion during the polymerization reaction (gelling) and also during curing (strengthening). A phenomenological model developed mainly depended on the evolution of gas phase during the chemical reaction. The model was mainly based on the diphasic compressible fluid (liquid/gas phase). It is to be noted that, as shown in the Figure 2-1, the evolution or the production of carbon-

dioxide takes place at an exponential rate eventually the curve follows the path of exponential decay.

2.3 Sealing

2.3.1 Infiltration/Inflow

Infiltration/inflow (I/I) is the process by which ground water/ storm water enters the waste water sewer pipelines due to defective construction or defects in the pipe owing to cracks, fissures or pipeline breakdowns. Primary reason for the I/I to enter the waste water pipelines is the displacement or misalignment of lateral joints. The larger the crack opening or the joint displacement, more the discharge of water collected. It is to be noted that for population of about two million, Houston is supposed to have about 1.8 million lateral pipeline joints. I/I not only causes damage to the underground pipeline but also causes severe damage to the soil. Heavy runoff maight cause erosion of the top-soil stratum. It adversely affects the equilibrium of the soil properties and the underlying water table. The mechanism of erosion is accelerated by high groundwater levels caused due to infiltration forcing more water through the soil spaces at greater velocities and under more turbulent conditions (Ozgurel, 2004). Though, sanitary sewer evaluation surveys such as smoke testing, TV inspection and dye testing methods are available to detect the I/I damages, it is necessary to rectify the problem by sealing the pipelines on a permanent basis. According to Wells (1997), the leaks in sewer pipelines can be rehabilitated in several ways such as; chemical grouting, pipe- relining (slip lining) and pipe-bursting (Ozgurel, 2004).

2.3.2 Decommissioning

The word “Decommissioning” was predominantly used ever since the Brent Spar Controversy (1995 – 98). Decommissioning refers to dismantling the existing installations which are either non operative or non productive followed by immediate site rehabilitation. It is to be noted that there are over 7500 offshore petroleum installations located at different parts of the world out of which 4500 are placed in the Gulf of Mexico (Parente et al., 2005). It is also to be noted that there are approximately 40000 miles of pipeline along the shore of United States of America (Smith, 2002). On the Outer Continental Shelf (OCS) an average of 5.37 miles of pipeline are being reused and 268.67 miles are being decommissioned annually (Smith, 2002). With over 50% of the offshore structures located at the Gulf of Mexico, it is a real challenge to make an effective reuse of the abandoned structures by decommissioning them.

According to Department of Interior (DOI), an offshore pipeline can be decommissioned in place only if it does not cause a hazard to navigation, commercial fishing operations or interfere with the other uses in the Outer Continental Shelf (OCS). Therefore, it is very essential that the pipelines are properly sealed to not let the stagnant oil and petroleum products to interfere with the aquatic environment before decommissioning. It is also to be noted that if the pipeline is out of service for more than 60 months, it is to be decommissioned (Smith, 2002). Since, this gives an allowance for the pipeline to be non-operative yet situated at place for 5 years, it is susceptible to various possible ways of deterioration with corrosion being the most prevalent way. So, it

is highly recommended to identify and address this issue of decommissioning the non-operative pipelines at the earliest.

2.4 Concept of Dielectric and Piezo-Resistivity

2.4.1 Dielectric Property of a Material

Ability of a body to store charge (q) when subjected to an electric field is called capacitance. When the applied voltage is V, capacitance, C can be calculated by,

$$C = q/V. \quad (2\text{-}10)$$

Relative Permittivity (E_r) or relative dielectric constant is the ratio of electrical energy stored by a body at applied voltage to that stored in vacuum. If C_{body} is the capacitance of the material at room temperature and pressure and C_{vacuum} is the capacitance of the same material in vacuum, then relative di-electric constant can be calculated by the formula,

$$E_r = C_{body} / C_{vacuum}. \quad (2\text{-}11)$$

In other words, static dielectric constant (E) is a material property which is dependent on the electric di-pole moment per unit volume (Wen and Chung, 2001) which is a product of permittivity of the free space (E_0) and the relative di-electric constant (E_r). Therefore, relative permittivity (E_r) can also be represented as,

$$E_r = E/E_o. \quad (2\text{-}12)$$

Wen and Chung (2001) reported two ways of obtaining the dielectric constant of the material. In the first setup, the dielectric constant is obtained by the coaxial cable method where the material is allowed to come in contact with the electromagnetic wave and the wave reflected or absorbed is used to get the dielectric constant. Secondly, the most convenient way of obtaining the relative dielectric constant is the formation of

parallel plate capacitor circuit, where, two conducting circular plates acting as the electrodes sandwich the material under study, which is termed as the dielectric. On passing AC current through the electrodes and getting the capacitance values of the dielectric (insulator), the dielectric constant can be obtained.

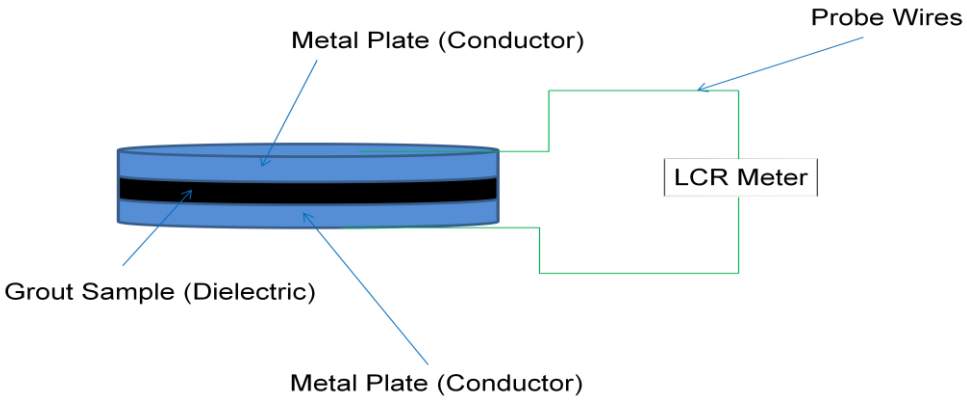

Figure 2-2: Parallel Plate Capacitor.

Figure 2-2 shows the parallel plate capacitor. The material (grout sample) which serves as the dielectric is sandwiched in between two metal plates (electrodes) and are connected to the LCR meter to obtain the capacitance between the plates (dielectric) on passing AC current. Thus, is A is the cross sectional area of the dielectric and L is the height of the dielectric, then the capacitance can be given by the equation,

$$C_{body} = E_r \cdot E_0 \cdot (A/D) \qquad (2\text{-}13)$$

Rearranging equation 2-13 we get,

$$E_r = C_{body} / [E_0 \cdot (A/D)]. \qquad (2\text{-}14)$$

It is to be noted that the permittivity of the free space, E_o is always a constant = 8.854×10^{-12} F/m. Taylor and Arulanandan (1974) studied the relationships between the electrical and physical properties of cement pastes. Since the capacitance measure and thus the

dielectric constant is obtained by passing AC current to the material, the effect of frequency at which the current is passed is to be accounted for. Figure 2-3 gives you the typical trend of the change in apparent dielectric constant with respect to change in frequency.

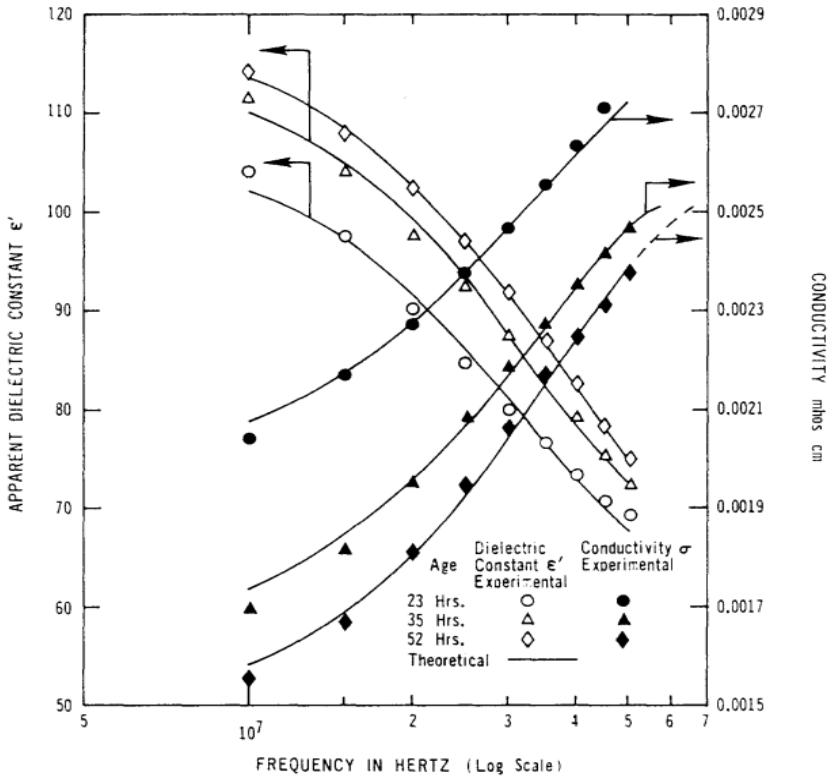

Figure 2-3: Variation of Dielectric constant with frequency (for cement paste – W/C = 0.35) (Taylor and Arulanandan, 1974).

2.4.2 Concept of Piezo-resistivity

Electrical resistance is a measure which signifies the current flow resisting capacity of the material. On the contrary, conductance is the measure by which the material allows the current to pass through it. Resistivity or the specific electrical resistance (ρ) can be calculated by

$$\rho = R.A/L. \qquad (2\text{-}15)$$

Where, R is the resistance in ohms, A is the cross-sectional area of the material through which the current is passed and L is the total height of the material. It is to be noted that the higher the value of resistivity, poor electrical conductor the material is, and vice versa. Piezo-resistivity can be defined as the ability of the body to exhibit change in the resistivity values on being subjected to stress. Thus, if

$$\rho = f(\sigma). \tag{2-16}$$

Then, the material is considered to be a piezo-resistive material. The four-probe method and the two-probe method are the two mostly commonly used methodologies to capture the resistance of a material. In the four-probe method, the electric current is allowed to pass through the two external electrodes and the corresponding voltage is obtained through measurement from the inner electrodes. Thus the resistance is calculated by the formula,

$$R = V/I. \tag{2-17}$$

Where, V is the voltage generated and I is the current that flows through the material. In two-probe method, the two probes are inserted into the material and the resistance is directly measured from the material by applying the current in the same probes. Past studies showed that the scatter obtained through the two probe method was more than that obtained with the 4-probe method. However, Prashanth (2010), studied the influence of contact resistance in polymeric composite using the two probe method with Infra-red spectroscopy and proved that the contact resistance is less than 1% bulk resistance and thus it can have negligible effect on the measured electrical resistance of the material. Table 2-3 shows the recent works investigating the self sensing properties of the cementitious materials.

Table 2-3: Summary of Recent Studies to Investigate the Electrical Properties of Cementitious Grouts

S.No.	Author	Material Used	electrical Properties	Proceedure	Material Proportions and Properties	Result	Remark
1	Sihai Wen and D.D.L Chung (1998)	Cement - matrix Composite Continuous carbon fibers	Piezoresistivity	DC electrical resistance in the stress direction during tensile testing	W/C - 0.45 Continuous Carbon Fiber	Resistance increased on stress increase; Reversible effect was observed; sudden increase was observed when the modulus decreased	The increase was due to fiber-matrix interface degradation
2	Sihai Wen and D.D.L Chung (2000)	Cement paste, silica fume, latex	Electrical resistance during Compressive loading	Compressive testing acc. ASTM C109-80; DC electrical resistance - using 4 probe method. Copper wires - electrical contacts	Silica Fume and latex - 15% - replacement of cement. w/c = 0.23 and 0.35	Resistance increased during Loading and unloading. Addition of silica fume and latex decrease the resistance during the first cycle.	This research was used to emulate the damage monitoring mechanism of cement paste.
3	Sihai Wen and D.D.L Chung (2001)	Cement Paste Silica Fume Latex Carbon Fiber	Dielectric Constant (k)	Application of AC electric field to parallel plate capacitor electrodes while the specimen was sandwiched.	0.5-1% fiber 15% Silica Fume 20% Latex W/C = 0.23 and 0.35	K value on Silicafume addition (29 to 21) Steel Fiber addition (29 to 20) Latex addition (29 to 35) Carbon Fiber addition (21 to 54)	Increasing Carbon Fiber after the threshold quantity decreases the constant
4	Sihai Wen and D.D.L Chung (2002)	Cement Paste, Steel Fiber, Carbon Filaments	Dielectric Constant on application of stress	Same as above; Stress applied in the direction parallel to the impedence measurement; repeated loading	1% short carbon fibers 3% - carbon Filament Silica fume, methyl cellulose and defoamer, polyvinyl alcohol	k value increases non linearly and reversibly to the stress upto 6.4 Mpa	Change in k relates to piezoelectric effect

Table 2-3: Summary of Recent Studies to Investigate the Electrical Properties of Cementitious Grouts (Continued)

5	Nathan Schwarz, Matthew Dubois and Narayan Neithalath (2007)	Cement paste plain and coarse galss powder	Electrical Conductivity	EIS - LCR meter; impedence. Effective conductivity measuered using bulk resistance measured by applying AC field to 2 electrodes that sandwich the sample	W/S - 0.32 and 0.42 10%, 20% and 30% replacement by glass powder	Increase in glass powder increases the conductivity.	Result can be related to various phases in the microstructural development
6	R. Potong, R. Rianyoi N. Jaitanong R. Yimnirum A. Chaipanich (2011)	PZT ceramic + Portland Cement composite	Dielectrical Properties	Impedence meter	PZT ceramic was mixed with portland cement to form 1-3 connectivity PZT-PC composite using a dice and fill technique. W/C = 0.5	Increase of PZT content increased the Dielectric constant from 100 to 1000.	The result was compared to parallel, series and cubic model.
7	S. D. Hutagalung N. H. Sahrol Z. A. Ahmad M. F. Ain M. Othman (2011)	Portland cement MnO2	Dielectric interference	HP 16435A Dielectric Material Test Fixture and HP RF impedence /material analyzer.	0.1, 0.5, 1, 5, 10 wt % of MnO2. W/C = 0.35	As the frequency increased dielectric constant increased. MnO2 increase, increased the di-electric constant	Dielectric loss was also measured

Table 2-3: Summary of Recent Studies to Investigate the Electrical Properties of Cementitious Grouts (Continued)

8	H.A. Mesbah A. Yahia K.H. Khayat (2011)	Self consolidating concrete - Portland Cement, Fly Ash - F or Silica Fume. Polycarboxylate HRWR Cellulose based VMA	Electrical Conductivity	Multi-Probe at 4 diff. Heights frequency = 1 KHz measuring diff in conductivity at diff depths of the specimen	HRWR - 30% wt VMA - 0.3% wt of cement	Conductivity increased initially and then was constant throughout. Top Pair - 1.4 ms/cm as the depth decreased the conductivity value cecreased.	Similar trends were observed for other mixes
9	Xiaosheng Wei, Lianzhen Xiao and Zongjin Li (2012)	Cement paste Cement mortar	Compressive Strength using resistivity	From the known 28 day compressive strength values for the mortars and the resistivity of cement can be used to get the compressive strength of cement pastes. Resistivity measured using the transformer principle.	W/C 0.4	Calibration curve of compressive strength vs electrical resistivity was obtained	
10	A. Lubeck A.L.G Gastaldini D.S. Barin H.C. Siqueria (2012)	White PC. High early strength PC ground granu-lated blast-furnace slag.	Electrical Resistivity Compressive strength	4-probe method - AC current, voltage measured	In concrete - 100% white PC 50 and 70% slag mortar content = 52% (fines added acc.). W/B ratio = 0.3, 0.42, 0.55	As the WPC % decreased, comp. str. Decreased. Replacement with slag increased the resistivity.	addn of activator also increased the conductivity

CHAPTER 3 MATERIALS AND METHODS

3.1 Introduction

This chapter summarizes the materials used and the testing methodologies to characterize the grouts and various applications. a detailed review of all the laboratory tests to characterize the grouts and the large scale models developed in cigmat laboratory for various application tets have been included. Applications of interest for the current study are as follows,

1) Leak control in buried pipe joints
2) Enhancing the sensing properties
3) Decommissioning of old oil pipelines.

3.2 Materials

3.2.1 Chemical Grout

Three types of polymeric chemical grouts, acrylamide, acrylic and polyurethane grout were studied. Acrylamide and acrylic grouts were selected due to their low viscosity, water soluble tendency, low permeability and rapid setting (Ozgurel, 2004). Acrylamide grout was modified using surfactants to investigate the improvement in its working and mechanical properties. Acrylic grout was used to examine the long term performance and durability in sealing applications. Polyurethane grout was used to investigate its performance as a sealing material for decommissioning of pipelines.

3.2.1.1 Acrylamide Grout

Acrylamide (C_3H_5NO) resin undergoes gelling by a mechanism called free radical polymerization. Acrylamide grouts are two component grouts where one of the components is an aqueous solution of the resin mixed with an activator (TEA) and the other component is an aqueous solution of the catalyst (APS). The acrylamide resin used in this study was AV-100 (a product of Avanti International). It is a white colored granular solid which is soluble in water. It is a blend of acrylamide monomer and methylene bisacrylamide. The activator used in this study was a viscous colorless liquid which acts as a buffer chemical and initiates the free radical polymerization reaction. It is to be noted that, the activator is composed of triethanol amine which has the primary dispersant (surfactant) and ethylene glycol. The catalyst used was ammonium persulfate. The catalyst was a white crystalline powder which is finer than AV-100 resin. The catalyst is responsible for accelerating the chemical reaction. The chemical formula of acrylamide monomer, methylene bisacrylamide, ammonium persulfate (catalyst), triethanol amine (activator) and ethylene glycol are given in Figure 3-1.

3.2.1.2 Acrylic Grout

Acrylic grout is a polymeric grout which has very similar properties compared to acrylamide grout. AV-118 Duriflex grout was used as an acrylic grout in this study. The major components of AV-118 Duriflex grout awere acrylamide monomer (C_3H_5NO) and formaldehyde (H-CHO). It undergoes the free radical polymerization to undergo phase transformation from liquid to solid. A mix of triethanolamine and ethylene glycol was used as the activator and sodium persulfate was used as a catalyst. The catalyst is a white

granular material which is an oxidizing agent which triggers the polymerization reaction. Generally it is diluted to 1 to 3% in water to form an aqueous solution.

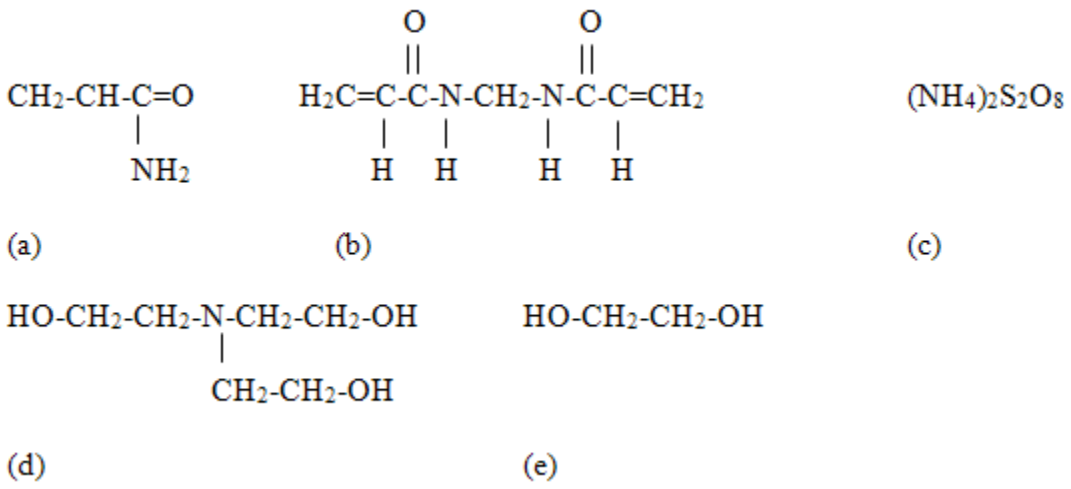

Figure 3-1: Chemical Notation of Components of Acrylamide Grout.

3.2.1.3 Polyurethane Grout

The polyurethane grout investigated in this study was the AV-202 Grout from Avanti International. AV 202 is a mix of diphenylmethane diisocyanate ($C_{15}H_{10}N_2O_2$), toluene diisocyanate ($CH_3C_6H_3(NCO)_2$ with their higher oligomers. The AV 202 is a two component hydrophilic foam grout. The resin has a tendency to cure and expand while reacting with water. In this study the grout was used for decommissioning the pipelines (filling the pipes with expanding grouts). To evaluate the performance of this grout, different mix proportions were studied. The resin was mixed with water, seawater, or oil solution The solutions used were tap water with a pH value ranging from 6.5 to 8, sea water (water collected from the Galveston Sea or the Vegetable oil solution (10% by weight of oil in aqueous mix). For initial screening purposes, the gelling time tests were

done at resin:solution ratios of 1:1, 4:1, 9:1 and 12:1 with different additives including cement, meta-kaolin clay and cationic and anionic surfactants.

3.2.2 Cement Grout

Type I/II portland cement was used in this study. The W/C ratio was kept constant at 0.6 or 1. Cement grout was also modified with a special type of clay to enhance its use for various applications. W/C ratio, quantity of clay used in the cement grout and the type of tests done to evaluate the modified grout properties are the key topics discussed in the forthcoming sections.

3.2.3 Admixtures

Surfactants: The surfactants used in this study were of two types. An anionic surfactant, (sodium dodecyl sulfate (SDS, $C_{12}H_{25}SO_4Na$)) and a cationic surfactant (cetyl tri-methyl ammonium bromide (CTAB, $[CH_3 (CH_2)_{15} N (CH_3)_3] Br$) were mixed with the acrylamide resin. The critical micellar concentration (CMC) of CTAB was 0.4g/L and that of SDS was 2.3 g/L (Harendra and Vipulanandan (2008)).

Metakaolin Clay: ASTM specified Type I/II Portland cement was used. Commercially available Meta-kaolin clay which had a coefficient of gradation (Cc) of 0.85 and coefficient of uniformity (Cu) of 3.68 and d_{50} of 0.0019 mm was used in this study. Clay was added to cement with respect to the weight of cement and mixed to get a uniform solid medium. Figure 3-2 shows the grain size distribution of the clay.

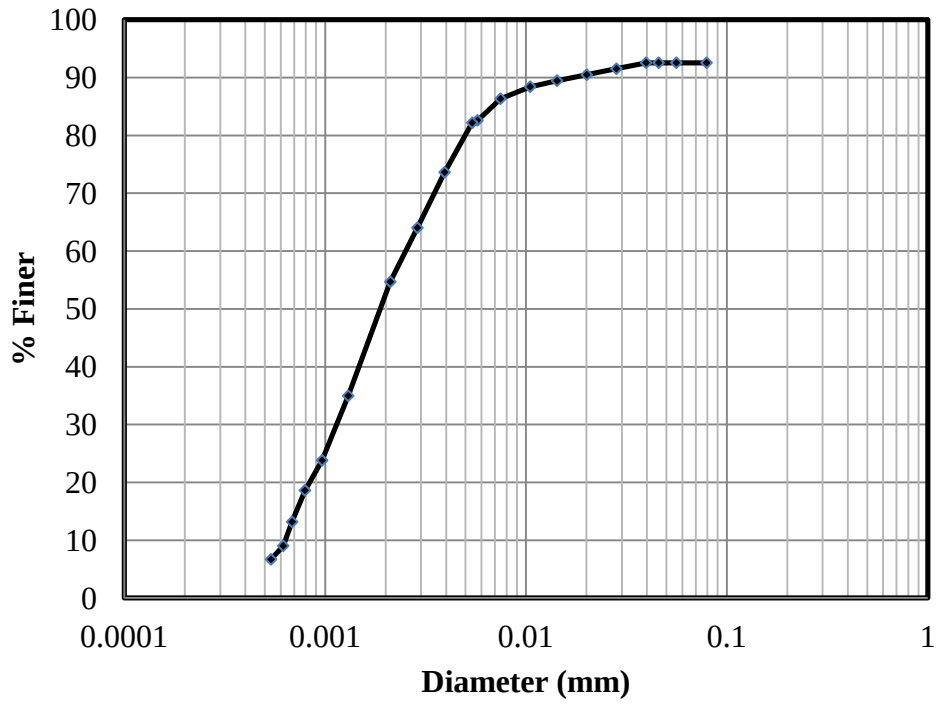

Figure 3-2: Particle size distribution of Meta-Kaolin Clay.

Carbon Fiber: Commercially available PAN based short carbon fibers were used in the grout mix. 0.5% by weight of the cement of carbon fibers was added in the grout mix. The fibers had the tensile strength of 3800 MPa, tensile modulus of 228 GPa and density of 1180 kg/m^3.

3.2.4 Sand

In this study, sand was used to prepare the chemically grouted sand specimens and also to perform the model tests. Hence the sand used was characterized based on the particle size distributions. The results obtained for the particle size distribution tests are summarized in this Chapter. Typical grain size distribution for the sand is shown in Figure 3-3. Also the particle sizes of the typical sand used in this study is summarized in Table 3-1.

Table 3-1 Summary of Particle Size Distribution for Sand

Trial	**d10** (mm)	**d50** (mm)	**d90** (mm)	**Cu**	**Cc**
1	0.45	0.87	2.0	2.44	0.78
2	0.35	1.07	2.1	4.00	0.94
3	0.36	1.1	2.1	3.92	0.99
Mean	0.39	1.01	2.07	3.45	0.90
Std. Dev	0.045	0.10	0.05	0.72	0.09
COV	0.12	0.10	0.02	0.21	0.10

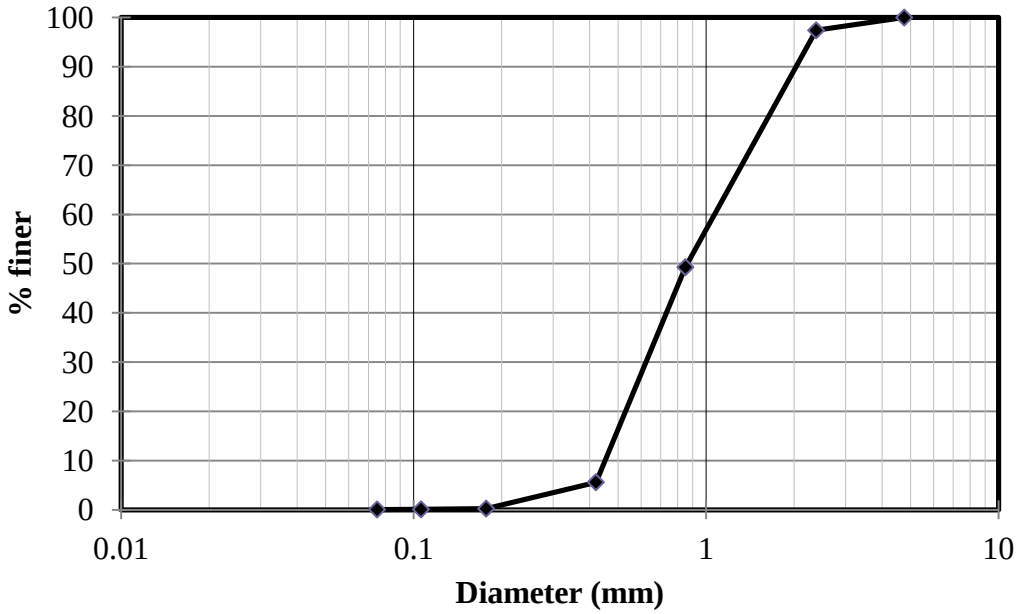

Figure 3-3 Typical Grain Size Distribution curve for Sand (Trial 1).

3.3 Test Methods

3.3.1 Mixing Procedure

Acrylamide and Acrylic grout: Acrylamide grout had two components of aqueous solution. One component was an aqueous solution of the resin and the activator while the other was an aqueous solution of the catalyst. 10% by weight of the total

solution of the resin was taken as the standard for all the grout mixes. 0.5% of catalyst and the activator was also fixed as the results gave convincing setting times and strengths for the solidified grout. The surfactant concentration varied from 0.5 – 4% by weight of the total solution. The mixing procedure is shown in Figure 3-4. The aqueous solution thus formed by mixing the two components solidified with time to form the grout.

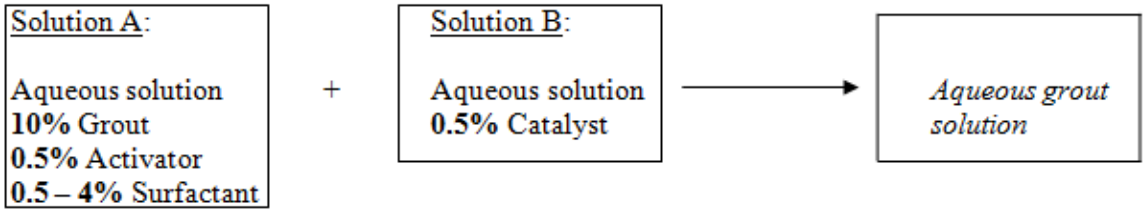

Figure 3-4: Mixing Procedure for Acrylamide/Acrylic Grout.

Polyurethane Grout: polyurethane grout, as stated earlier is also a two component grout. In this case the two components being the resin by itself and water. In this study investigations were done on testing the grout samples prepared by mixing water and resin at the ratio 1:1 and 1:4 by weight. It is also to be noted that the admixtures were added to the water component and not the resin component. And thus the ratio 1:1 and 1:4 holds good for resin: solution instead of resin: water with solution comprising of water with admixtures. W/C = 1 was fixed to prepare the solution of cement which used as one of the components added to the resin component to prepare the grout mix. When meta-kaolin clay was used as an admixture 5% of metakaolin by weight of the total grout mix was used. Likewise, 4% surfactants were also used as admixtures in the solution component. The procedure for mixing the components described in Figure 3-5.

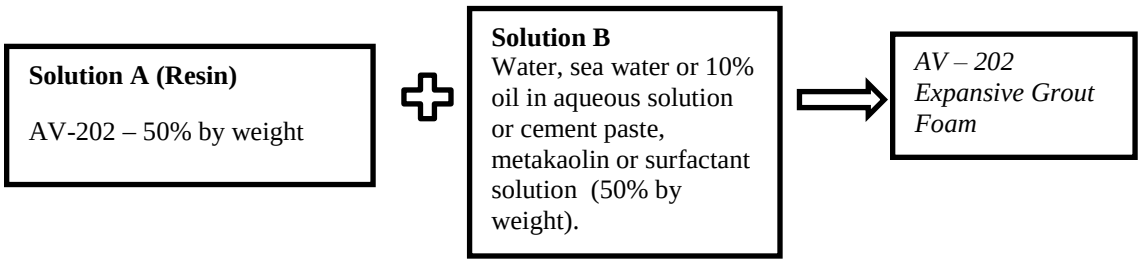

Figure 3-5 Mixing Procedure for AV-202 Grout Foam.

3.3.2 Chemical Grout and Grouted Sand

3.3.2.1 Sample Preparation

Grout: Figure 3-6 shows the mold that was utilized to make the grout specimens (acrylamide and acrylic). After polymerization, specimens were removed from the mold and stored in sealed plastic bags to prevent moisture loss. The specimens were stored in a temperature- and humidity-controlled room at 23 ± 2°C (room temperature) and 50% ± 5% humidity. In the case of polyurethane grouts, owing to their expansive behavior the top of the mold was sealed once the grout mix was poured in the mold before its setting time was reached. It was possible to study controlled expansion of the grout during the curing process.

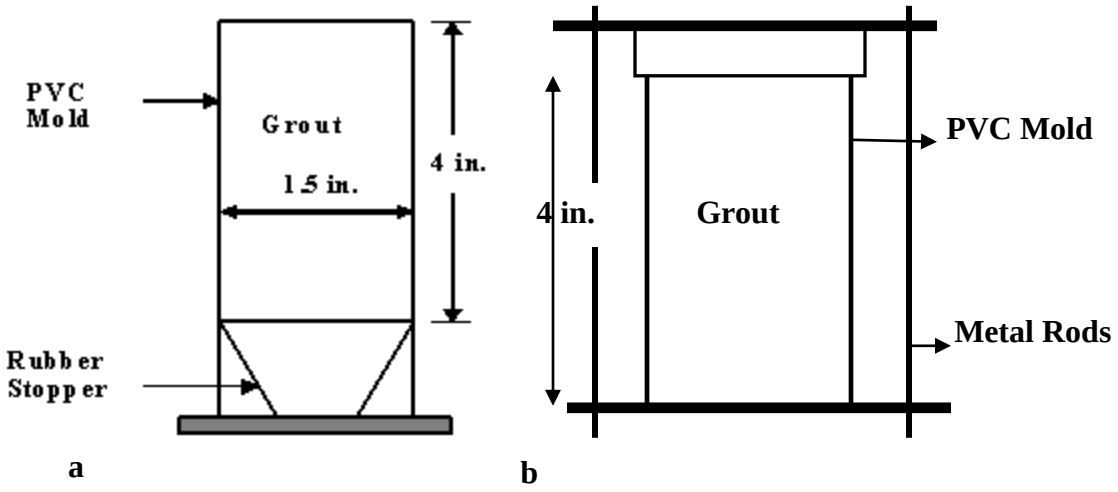

Figure 3-6. Typical mold used for preparing a) acrylamide and acrylic grout specimens; b) polyurethane specimens.

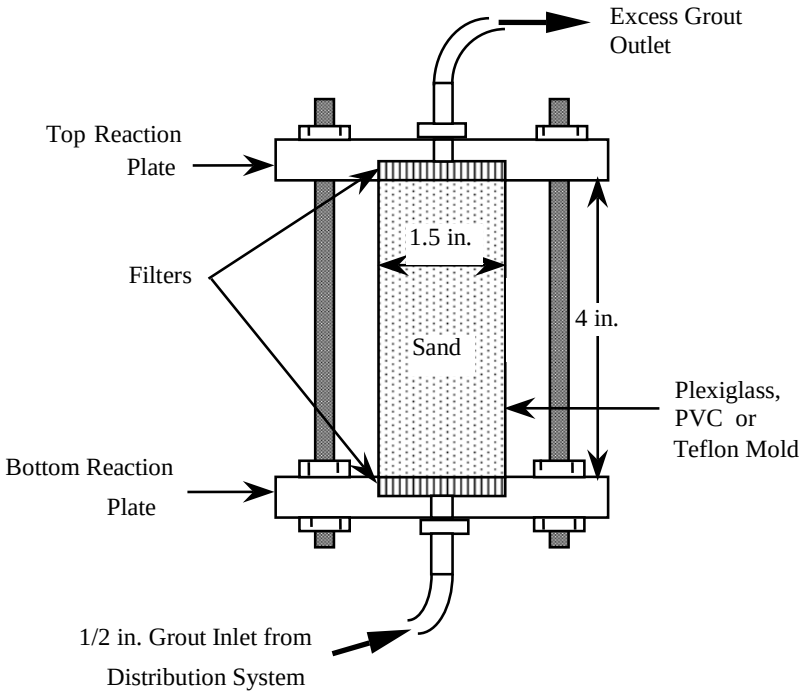

Figure 3-7. Mold for preparing acrylamide and acrylic grouted sand specimens.

Grouted Sand: Grouted sand specimens were prepared according to CIGMAT GS 1-02. The mold used to make the grouted sand is shown in Figure 3-7. Plexiglas filters were used at the inlet and outlet ends to ensure negligible loss of sand during the process of grouting. The mold was filled with sand prior to grouting and the grout mix was injected into the sand filled mold at a pressure of 1-3 psi. Once the grout solidified, the grouted sand was carefully extruded from the mold, sealed in zip-lock bags and stored in a temperature- and humidity-controlled room (23 ± 2°C and 50% ± 5% RH). Figure 3-8 shows the procedure of grouting to prepare a grouted sand sample. In the case of pullout strength test and measuring the dielectric constant of the grouted sand, sand was poured in to the mold and then the grout mix was poured to completely saturate the sand with grout and was allowed to solidify.

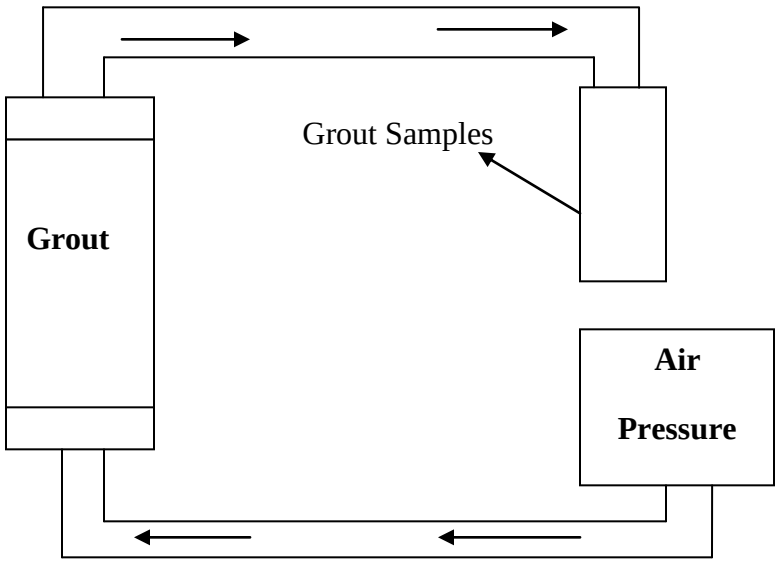

Figure 3-8. Grouting the sand filled in mold.

3.3.2.2 Viscosity

The grout viscosity was measured using the procedure outlined in CIGMAT GR 6 – 04. Cylindrical spindle type viscometer (Brookfield Dial-gage Viscometer) was used to test the viscosity of the grout (Figure 3-9). The LV Viscometer which had a spring Torque of 762.7 Dyne-cm was used in this study.

Three samples were tested for viscosity. Spindle No.1 (or 61) was used to calculate the viscosity. Viscosity of the grout was obtained by multiplying the readout value by the spindle constant relevant to the respective speed at which the selected spindle rotates.

Figure 3-9: Brookfield LVT Viscometer.

3.3.2.3 Gelling Time (Newly Developed Method)

Gelling time of the grout is defined as the time during which the grout transforms from a liquid to solid. In other words, gelling time is defined as the time when the flow

ability of the grout is completely void. Initially, in the industry, the gelling time was obtained by a fairly simple methodology. The grout mix was placed in a cup and the cup was tilted to 45º. And during this motion between horizontal to a 45º tilt of the cup, the movement of the grout mix was visually observed and when this movement is null, the corresponding time was accounted to be the gelling time of the grout. To add more science to this, the new CIGMAT standard was developed to evaluate the gelling time of the grout. The CIGMAT 8-09 gives the detailed procedure to evaluate the gelling time of the grout and is attached in appendix A.

The basic principle behind the development of gelling time test method is that, the phase transformation occurring due to polymerization is an exothermic chemical reaction. By measuring the rise in temperature of the sample, it is to be noted that, the temperature increases once the polymerization begins (when the liquid has become a solid) and then rises to a peak value (solid strengthening phase) and finally reaches the room temperature indicating the completion of the chemical reaction or in other words, all the chemicals involved in the chemical reaction for grout formation have been used up which leads to the termination of the polymerization. This phenomenon was measured using the thermocouple which was inserted into the grout immediately after the grout was mixed in a cylindrical cup and the other end of the thermocouple (probe) which was connected to the data acquisition system captured the rise in temperature with time. By relating the time with temperature, the gelling time was obtained by examining the curve. The time during which the slope of the curve began to increase rapidly from zero was taken to be the gelling time of the grout. Figure 3-10 shows the setup for the gelling time test.

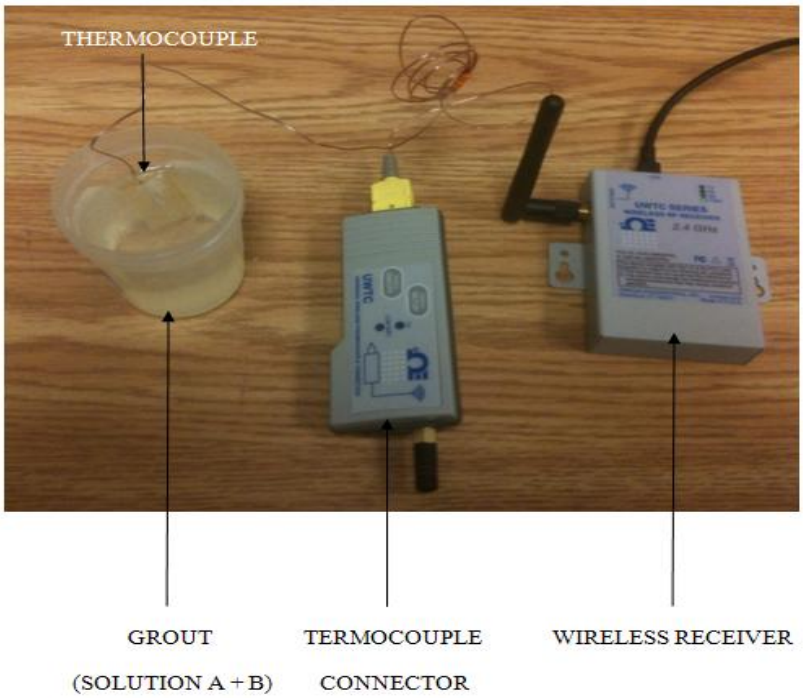

Figure 3-10: Gelling time test setup.

In the case of polyurethane grouts, however, the gelling time was determined by visual observation. Setting time of the polyurethane grout is defined as the elapsed time from the grout preparation to the time when the grout no longer flows from a beaker inclined slowly to 45º. Approximately 20 mL of freshly prepared grout was used. Care was taken not to confuse the expansion of the grout to movement of the grout. At periodic intervals, based on the observed setting of grout, the container was slowly tipped to approximately 45º to determine if the grout exhibits liquid flow properties or if the grout sample had gelled and the specimen can no longer flow from the container.

3.3.2.4 Pull-out Test (Newly Developed Methodology)

In order to rapidly determine the properties of grout and grouted sand samples in the field, the pull-out test was developed. Figure 3-11 shows the setup of the pull-out strength test of the grout and grouted sand specimens. Cylindrical molds with diameter

and height of 1.5 in. x 4 in. were used to prepare both grout and grouted sand specimens. Once the grout mix was prepared, it was immediately poured into the mold to prepare the grout specimens. For preparing the grouted sand specimens, grout mix was poured into the sand in the mold. Full saturation of the sand by the grout mix was ensured. An anchor with a ¾" head was inserted into the specimens in such a way that the head was placed at a depth of 1 in. from the top of the specimen for the first set of tests and 3 in. from the top of the specimen for the second series. The load required to pull the anchor out of the specimen was divided by the area of the failure plane gave the pull-out strength of the sample.

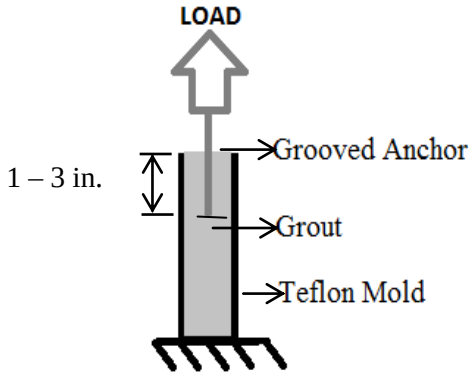

Figure 3-11: Pull-Out Strength Test Apparatus.

3.3.2.5 Compressive Stress-strain relationship

Unconfined Compressive strength test was performed on grouted sand specimens (acrylic and acrylamide grouts) according to CIGMAT GR 2-02 which is attached in appendix A. Care was taken to ensure complete grouting of the sand inside the mold. This was done by collecting at least three times the volume of voids of grout at the outlet. Once the specimens were prepared, they were cured at room condition for 7 days, the

dimensions of the samples were noted with the weight of the sample and unconfined compression tests were performed using a strength testing machine with a maximum capacity of 4000 lbs. The test was conducted at a constant strain rate of 1% / min. in the case of polyurethane grout samples that were prepared at controlled volume expansion, the same procedure was followed as stated in CIGMAT 2-02.

3.3.2.6 Sensing Properties (Newly Developed Technology)

The capacitance and resistance were measured with applied stress on the chemical grouted sand samples that were prepared with and without the addition of carbon fibers. 6 in. diameter plastic molds were used to prepare the grouted sand. 400 g of sand was poured inside the mold and 0.5% carbon fiber by weight of sand was mixed with the sand by hand and the grout mix was poured to saturate the sand. The disc was then tested for the change in capacitance (C) and resistance; the dielectric variation of the sample with respect to application of stress was investigated. Similar study was done for the samples prepared without the addition of carbon fiber. Figure 3-12 shows the setup of the test with parallel plate capacitor circuit formed using the grouted sand sample as the dielectric medium. The dielectric constant was obtained using the formula given in the equation 2-14. Resistance of the grout was also measured using the same approach and the change in resistance was calculated for varying stresses.

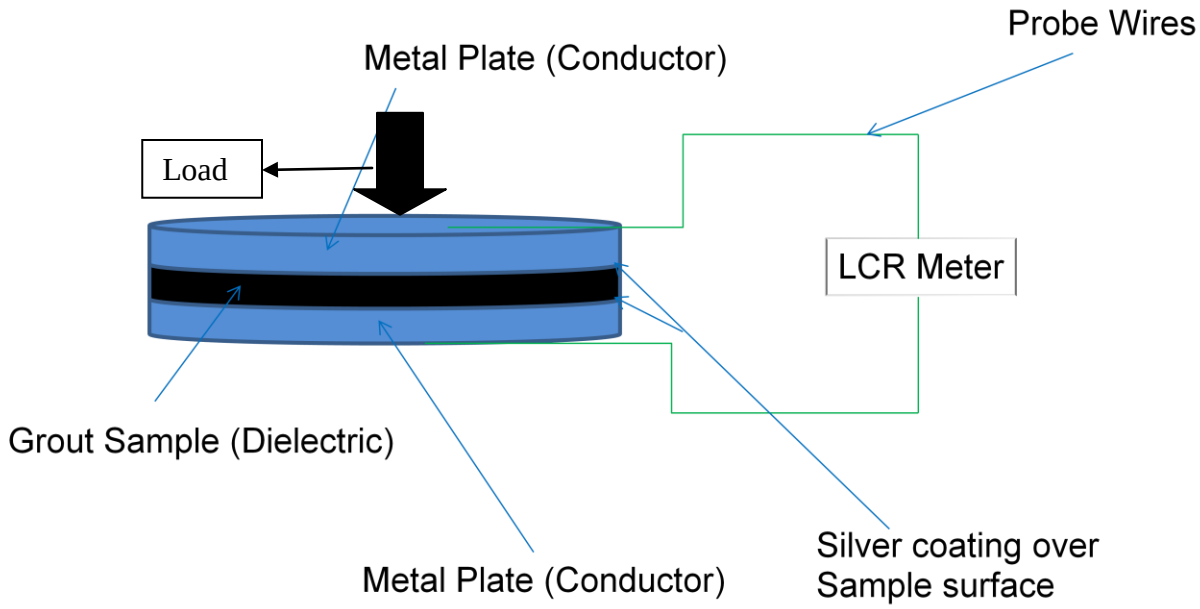

Figure 3-12: Dielectric Constant Determination.

3.4 Large Scale Models for Leak Control

3.4.1 Lateral Leak Model

3.4.1.1 Permeability Test: Three grouted sand specimens were used to determine the permeability. Specimens were prepared in Plexiglas/glass cylinders and permeated with water under a hydraulic gradient of 100 as specified in CIGMAT GR 7-02. Tests were performed at room temperature and humidity. An example calculation of the pressure application is shown below. In the case of acrylic grouted sand, the samples were prepared in 1.5 in. x 2 in. cylindrical plexiglass mold. Polyurethane grouts that were tested for permeability were prepared in 1.5 in. x 4 in. PVC mold. A suitable water pressure was applied to the top head of the grouted sand in the mold in such a way that the hydraulic gradient is 100.

For example,

Let the height of the sample, L = 4 in.

where, P (Pressure) = h. ρ. g = h. γ_w = h. (62.4 lb/cu.ft)

Since, i = h/L

h = i.L = 100 * 4 = 400 in

where, i = hydraulic gradient = 100 (needed)

Substituting value of h in P, we get,

P = h. γw = h. (62.4 lb/cu.ft) = 400 * 62.4 = 24960 lb.in/cu.ft

= (24960/1728) lb/sq.in

= 14.44 = 14.5 psi

So, a hydraulic pressure of 14.5 psi is to be applied to a 4 in. long sample to perform the permeability test with a hydraulic gradient of 100.

3.4.1.2 Water Absorption: Water absorption characteristics were evaluated for grouted sand specimens as outlined in standard procedure CIGMAT GR 3-00. The change in weight and volume of the grouted sand when exposed to tap water with the pH varying between 7 – 8 (fully submerged condition) was observed. It is to be noted that the minimum the change in weight and volume, the more durable the grout is under submerged conditions. The test was performed for one week or until the change in the volume and weight became negligible (less than 0.5% the original volume and weight). The dimensions and weight of the samples were recorded every day until the test was completed.

3.4.1.3 Shrinkage: The grouted sand specimens that were prepared using 1.5 in. x 4 in. cylindrical molds were placed under controlled conditions of humidity and at room temperature for a period of one month from the time of preparation of the grouted sand sample. Humidity of the controlled environment was measured using a digital humidity meter. The weight and dimensions of the specimens were measured before and after the test. The testing conditions are sumarized in Table 3-1.

Table 3-1 Shrinkage Test Conditions.

Parts	Temperature, Duration, and storage condition
Part C	23ºC ± 2ºC for 28 days in zip lock bags (RH = 90%± 5%)

3.4.1.4 Chemical Resistance: This test evaluated the resistance of grouted sand when exposed to chemical conditions representing various environments of applications. The test results will help when selecting suitable grouts for use in various chemical environments with varying pHs. Grouted sand specimens were prepared and the initial weight, dimensions, color, and surface appearance of the specimens was recorded. Different specimens were fully immersed in the solutions with pH 2, 7, and 10 maintained at room temperature (23 ± 2°C) for the entire exposure period. The solutions consisted of tap water with hydrochloric acid to prepare a pH 2 solution or sodium hydroxide added to achieve the pH of 10. The weight and volume change were determined and recorded for specimens at each pH after 30, 90, and 180 days, as described in Section 7.3 in CIGMAT CH 2-01. After each evaluation, compression testing was done for the specimens in accordance with Section 7.4 of CIGMAT CH 2-01.

3.4.1.5 Leaching Test: Potential contaminant leaching from solidified grout was determined by analyzing for total organic carbon (TOC) in the water exposed to the grout. The grout samples were prepared and were immersed in individual bottles containing tap water for a period of 7 days. Then the exposure water was taken and was subjected to TOC testing. In addition to this one cup with plain tap water was also used as a control medium. At the end of the exposure period, samples of water were analyzed to determine the presence of organic compounds that may have leached out from the grout. The samples were analyzed for TOC content.

3.4.1.6 Model Test

In order to simulate a leaking lateral joint, this model test (Figure 3-13) used an 8-in. diameter main pipe with a 4-in. diameter lateral pipe. Both pipes were enclosed in a rectangular steel chamber 24 in. wide, 24 in. in height and 34 in. long, filled with sand. The model was designed in such a way that the ends of the chamber allowed the 8 in. pipe to protrude and the top of the chamber was sealed with plexiglass plate which had a circular opening to allow the vertical 4 in. pipe to protrude outside the model. The reason for extra protrusions are that, the grouting of acrylic grout at the leaking lateral joint was carried out through the horizontal pipe opening and the grouting process was monitored through observations made from the vertical pipe. Valves on the outside of the test chamber enabled to saturate the sand and bleed air from the system and to apply water under pressure to evaluate the effectiveness of the grout application. It is to be noted that the sand used to prepare grouted sand samples of acrylic grout was also used to prepare

the large scale model. Two identical models were built and grouted to evaluate the consistency of the grout. Following points show the procedure for preparing the model prior to grouting the lateral joint.

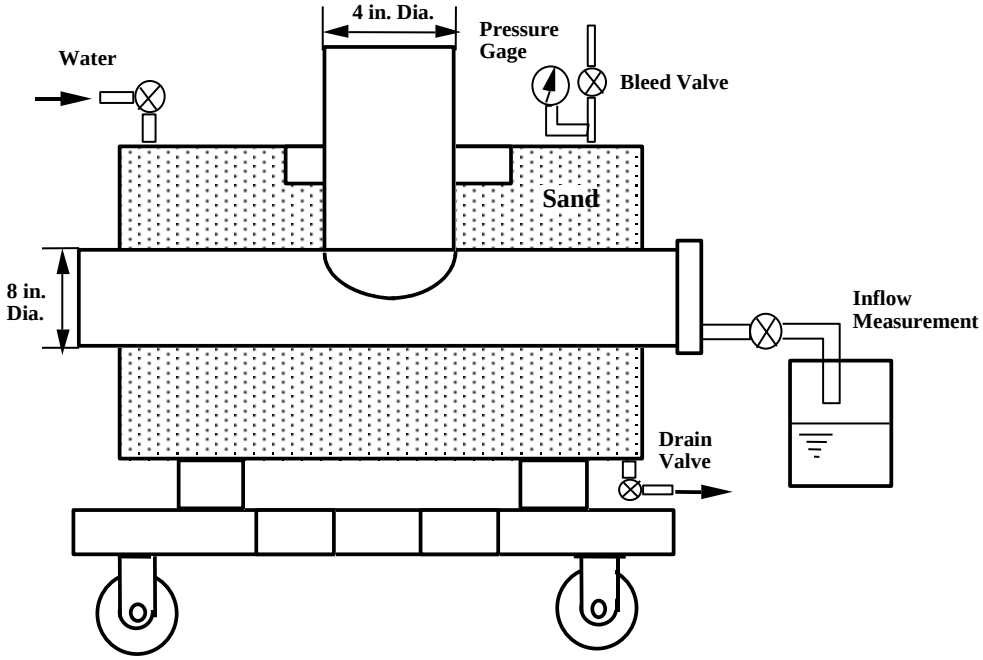

(a) Elevation View

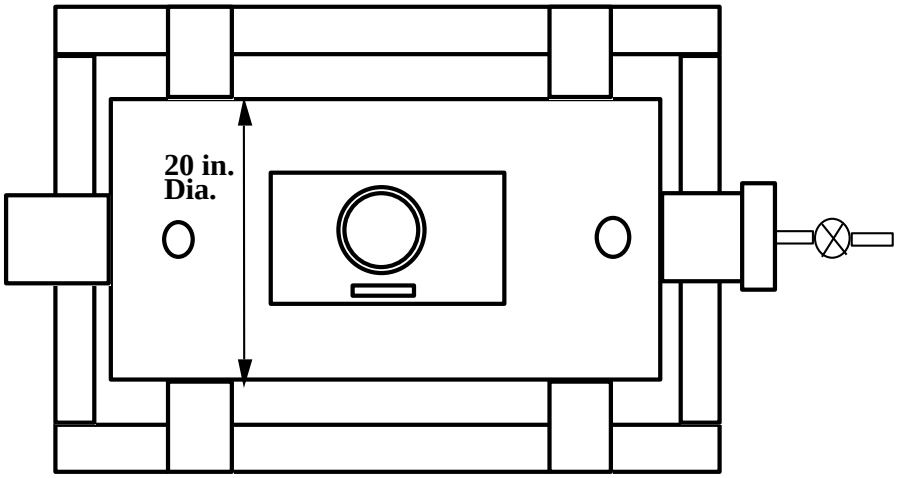

(b) Plan View

Figure 3-13. Model configuration for testing leak control at a lateral joint.

- Half of the chamber was filled by sand under loose condition (minimal compaction). The lateral pipe was then inserted in the main pipe and the rest of the chamber shall be filled with sand. Figure 3-14 (a) illustrates this step.
- Once the chamber was filled with sand, the top plexiglass cover was placed on the chamber with a rubber gasket to make the end watertight. Figure 3-14 (b) shows the fully sealed model.
- Calibration curves for joint leak rate versus pressure were developed. This was done by sealing the top of the chamber and then saturating the sand inside the chamber with water and once full saturation was ensured, the pressure of water entrance was increased to 3, 4 and 5 psi respectively. The discharge of water through the lateral joint owing to the water pressure is collected and is plotted with time. Figure 3-15 shows the I&I leak observed in one of the models.

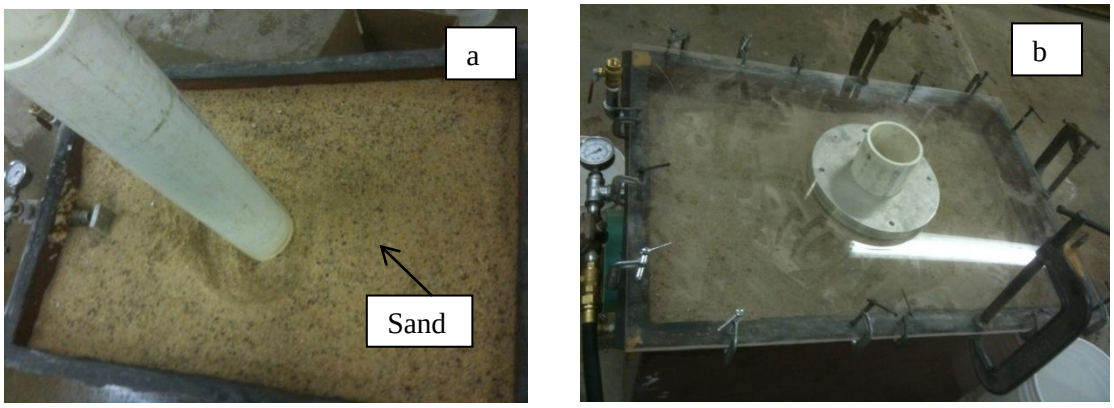

Figure 3-14: a) Top view of the chamber a) Filled with Sand and b) Top closed using a Plexiglass Plate.

Figure 3-15: Typical I&I Flow Leak in Model 3.

- Once the calibration was completed, the water was completely drained, however sand was kept under wet conditions. Figure 3-16 shows the schematic diagram of the fully built model ready to be grouted.

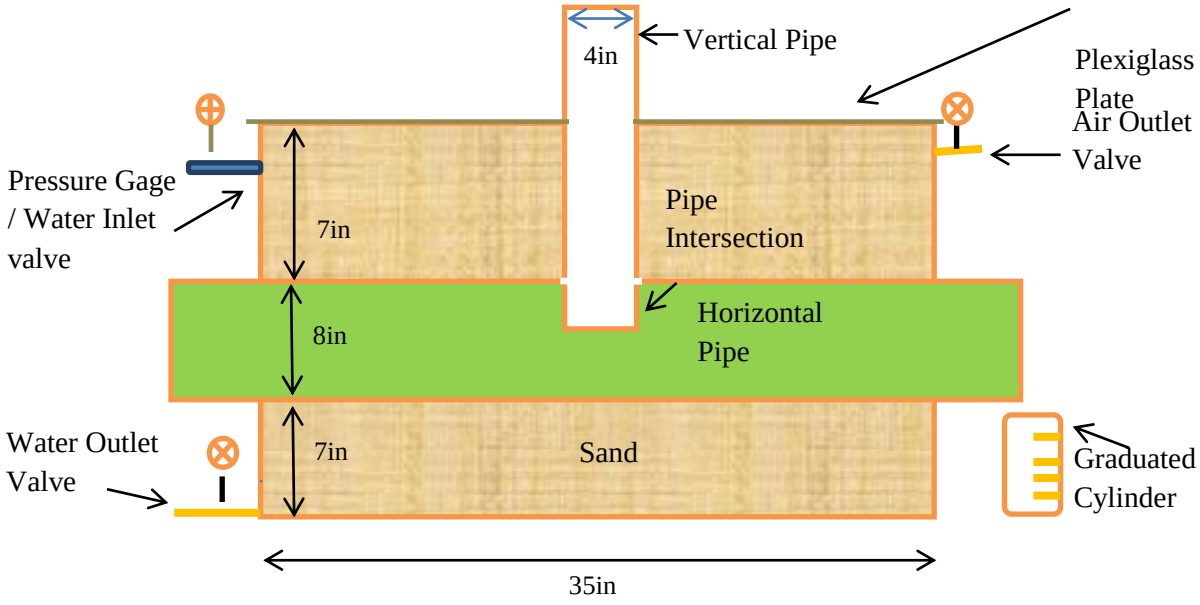

Figure 3-16: Schematic Representation of lateral leak Model.

- Then after 24 hours, grouting truck was brought to the lab and the model wad grouted. The schematic representation of the process of grouting is illustrated in Figure 3-17.

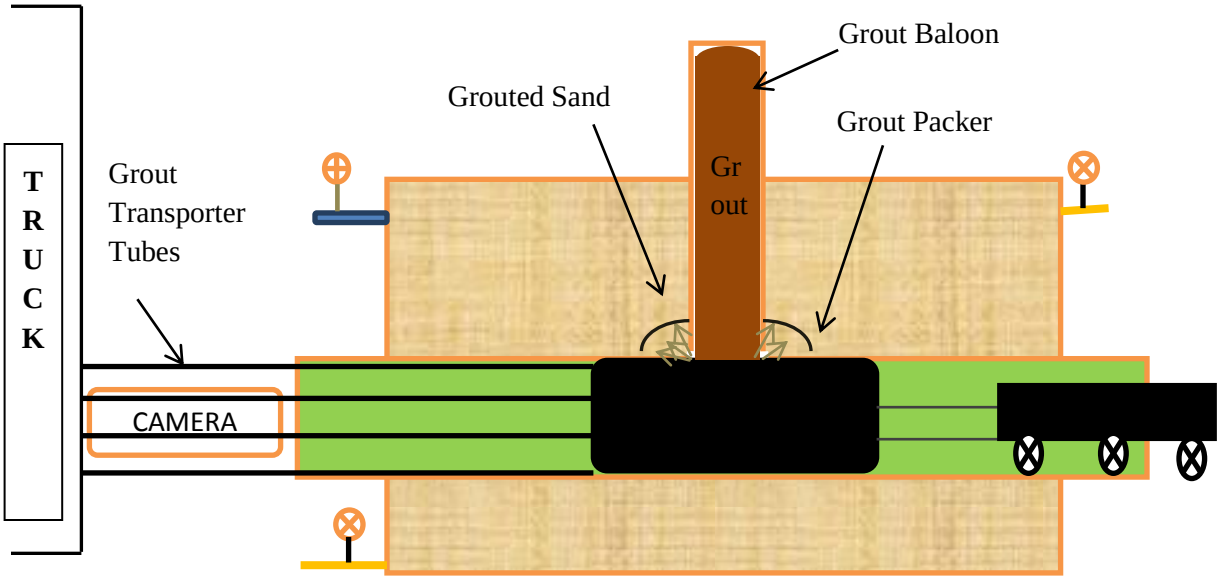

Figure 3-17: Schematic Representation of the Process of Grouting.

The time elapsed and volume of grout used during the grouting process was recorded. The following protocol was developed to evaluate the sealing ability of the acrylic grout starting from the day after grouting the joint:

1. Hydrostatic pressure of 3 psi was applied to the model held for 5 minutes; then the leak rate using a graduated cylinder and a stopwatch.
2. Step 1 was repeated at a hydrostatic pressure of 4 psi.
3. Step 1 was repeated at a hydrostatic pressure of 5 psi.
4. Saturated conditions were maintained for a period of one week.
5. Water was drained from the chamber and the dry condition was maintained for one week.

6. Step 4 and 5 were repeated.
7. Then the leak rates were again determined by repeating steps 1 – 3.

3.4.2 Decommissioning Model

3.4.2.1 Confined Compressive Strength Test (Newly developed Test):

Under confined conditions, i.e., the sample was tested for compressive strength before extruding the sample from the mold. The test was carried out at a uniform strain rate of 1%/min and was allowed to proceed till the sample failed or 15% strain was reached. The same test was also done on polyurethane grout samples after being subjected to permeability test. Figure 3-18 gives the schematic representation of confined compressive strength test of polyurethane grout samples.

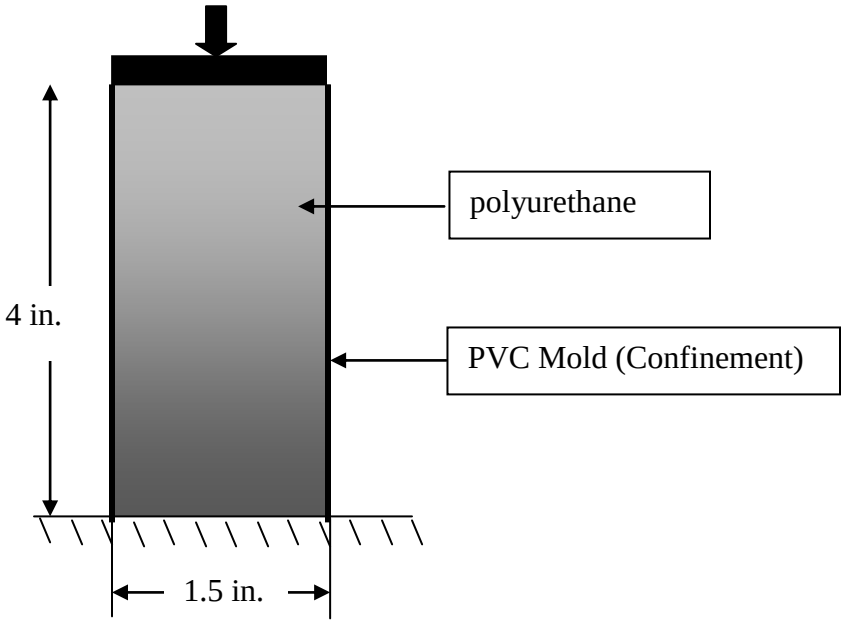

Figure 3-18 Confined Compressive Strength Test set-up.

3.4.2.2 Extrusion Test (Newly Developed Test):

Grout in Pipe Test: Different heights of samples of grout were prepared in 4 in. long PVC molds at a controlled volume expansion of 34.5%. Heights varied from 1 in., 2 in., and 3 in.. Uniformly distributed load was applied to these samples in the uni-axial direction and the deformation (strain %) with respect to the applied stress was noted. the samples were tested after 1 hr after preparation. The specimen was tested at a constant shear rate of 1%/min. Figure 3.19 shows the extrusion test set up.

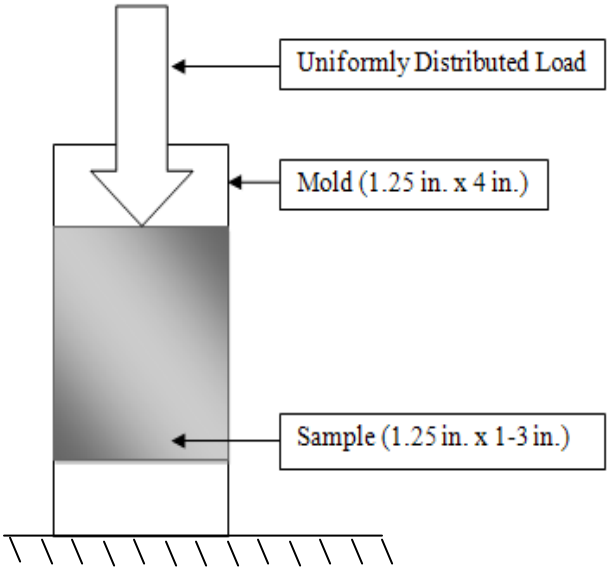

Figure 3-19 Extrusion Test – stress-deformation Set Up.

Grout in Tube: This test was developed to signify the pressure needed to extrude the grout that filled the cross section of the pipe for sealing purposes. Pipe filled with grout to a certain length and cross section can be compared to a circular pile. The forces acting on a pile like pipe filled with grout are shown in Figure 3-20. Similar phenomenon takes place in a pipe with circular cross section filled with grout occupying certain length of the pipe.it is to be noted that, the load, P taken by the grout to be

expelled from the pipe is dependent on the skin friction force, τ_s of the pipe, cross sectional area of the pipe, $\pi d^2/4$ and lateral surface area of the pipe, πdl and end bearing load, q_b.

$$p \times \pi d^2/4 = \pi dl \times \int \tau_{s(p)}.dl + \pi d^2/4 \times q_{b.} \quad (3\text{-}1)$$

On simplifying equation 3-1 we get,

$$p = 4.(l/d) \times \int \tau_s.dl + q_b \quad (3\text{-}2)$$

However, q_b = zero as there is no end bearing force in our setup.

$$\text{Hence, } p = 4.(l/d) \times \int \tau_s(p).dl. \quad (3\text{-}3)$$

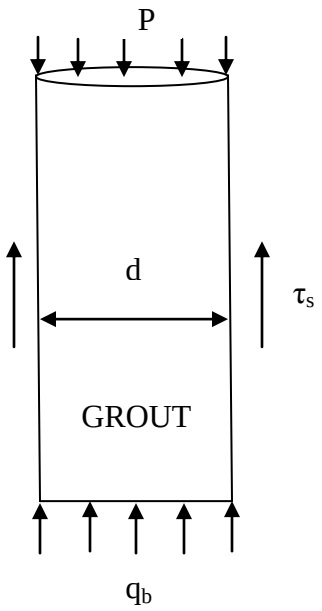

Figure 3-20 Extrusion Test Set Up.

Air/water pressure is applied to simulate the test condition. This test represents the sealing characteristics of the grouts with various pipe materials (representing cracked rocks).

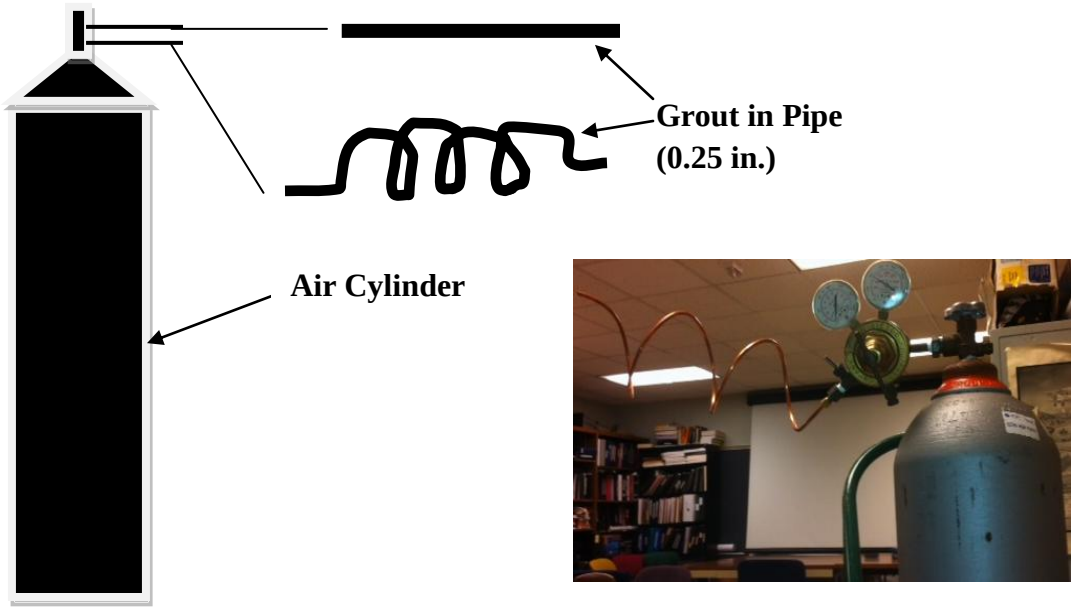

Figure 3-21 Extrusion Testing Apparatus.

3.4.2.3 Uni-Axial Expansion Test:

Pressure at controlled volume Test: The polyurethane grout was prepared using the procedure described in 3.2.2.2. During the preparation, the uni-axial grout expansion was restricted to only about 20% of the total volume of the PVC mold and then the pressure exerted by the grout owing to this restricted expansion was accounted for by placing a Load cell over the cap of the mold. The variation of pressure with respect to time was recorded for a period of 1 day.

Temperature at controlled volume Test: The polyurethane grout was prepared using the procedure described in section 3.2.2.2. During the preparation, the uni-axial grout expansion was restricted to only about 20% of the total volume of the PVC mold and then the change in temperature of the grout inside the mold was measured during the process of gelling using a thermo-couple for a period of one day.

3.4.2.4 Model Test

The main aim of this test is to examine the leak controlling (sealing) effectiveness of the polyurethane grout under study. Several cases or possible ways of installations of the grouts have been proposed in this section. Cases 1 – 4 have been illustrated in detail in figures 3.22, 3.23, 3.24 and 3.25 respectively. The tests were conducted on a three feet long PVC pipe.

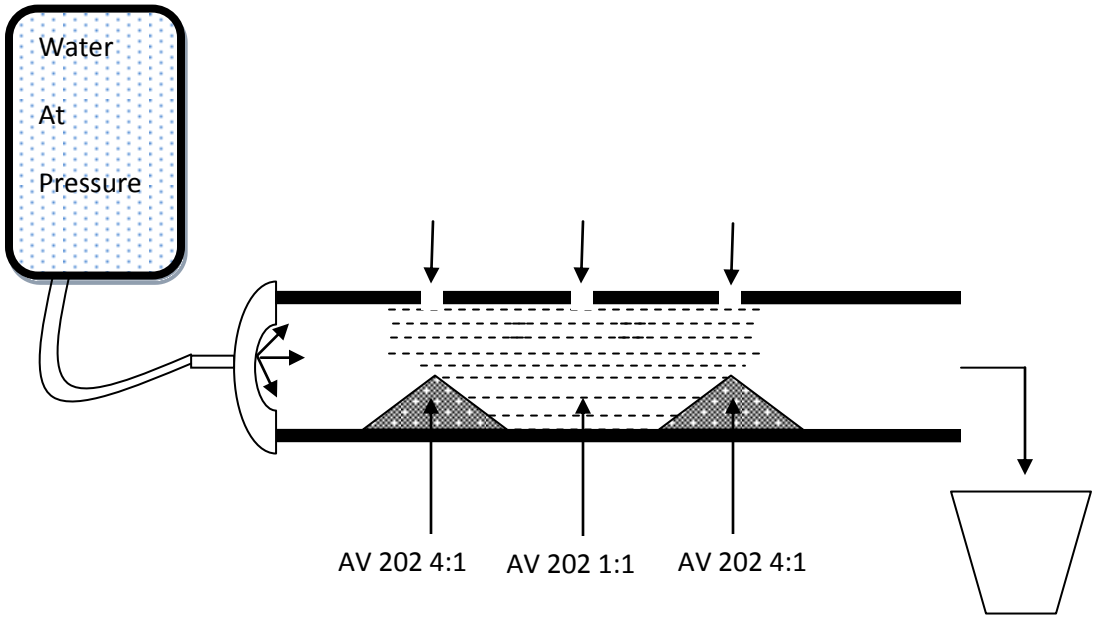

Figure 3-22. Case 1.

In case 1, three holes were drilled on the horizontal PVC pipe at six in. intervals to facilitate the grout injection. On the first and third hole, about 50 grams of polyurethane grout (W/G = ¼) were mixed and quickly injected before it set. After 5 minutes of its setting, around 200 g of polyurethane grout (W/G = 1/1) was injected into the center hole. The purpose of this set up was that the polyurethane grout (W/G = ¼) served as the barrier to stop the flow of grout injected through the center hole. After the grout had set, water at different pressures was applied from one side of the pipe to

examine the permeability of the barrier on increasing pressures. The similar concept was followed in case 2 with the only difference being the grout (W/G = 1/1) was injected through the center hole inside an elastic membrane which expands with expanding grout. The main reason for using the elastic membrane was to reduce the amount of grout used. An inverse approach was followed in case 3. Since the use of elastic membrane could contribute for interface leaks only at high pressures, the grout (W/G = ¼) was poured inside the membrane and allowed to expand (this approach was developed because, these two membrane barriers were used to eliminate the flow of the grout (W/G = 1/1) that was injected through the center hole during setting and not to control the permeability). Case 4 was developed very similar to case 3 with the only difference being sand was poured inside the center hole and the sand was grouted with acrylamide grout to add strength to the center impermeable strata. Few key points to be noted are that, in case 3, the grout was injected through the center hole in two steps to reduce the pores. The length between the holes was reduced to five in. instead of six in. to minimize the length of the impermeable grouted sand barrier.

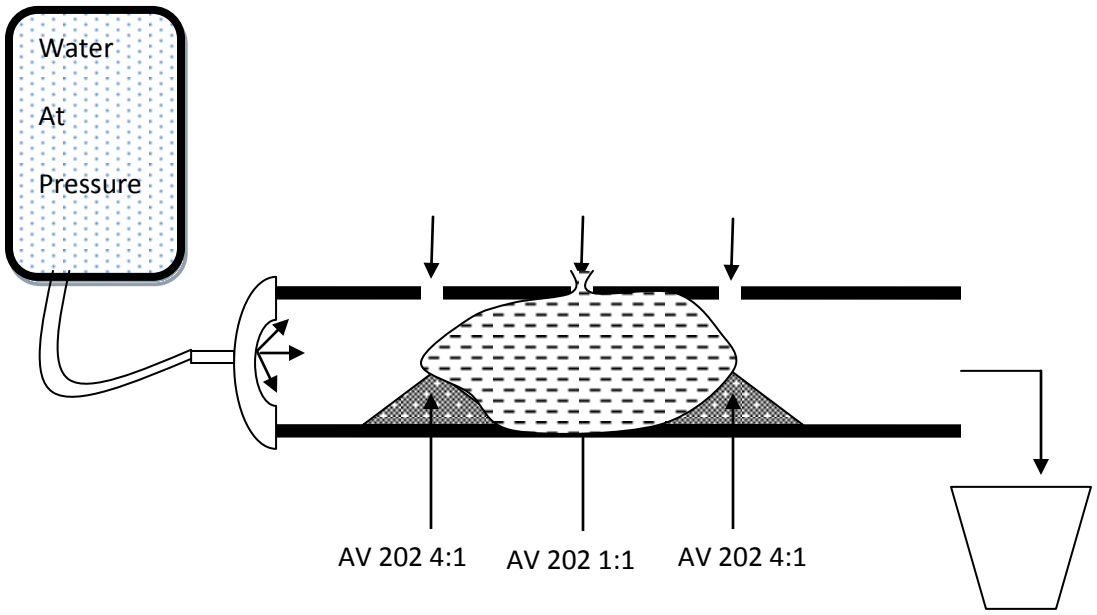

Figure 3-23. Case 2.

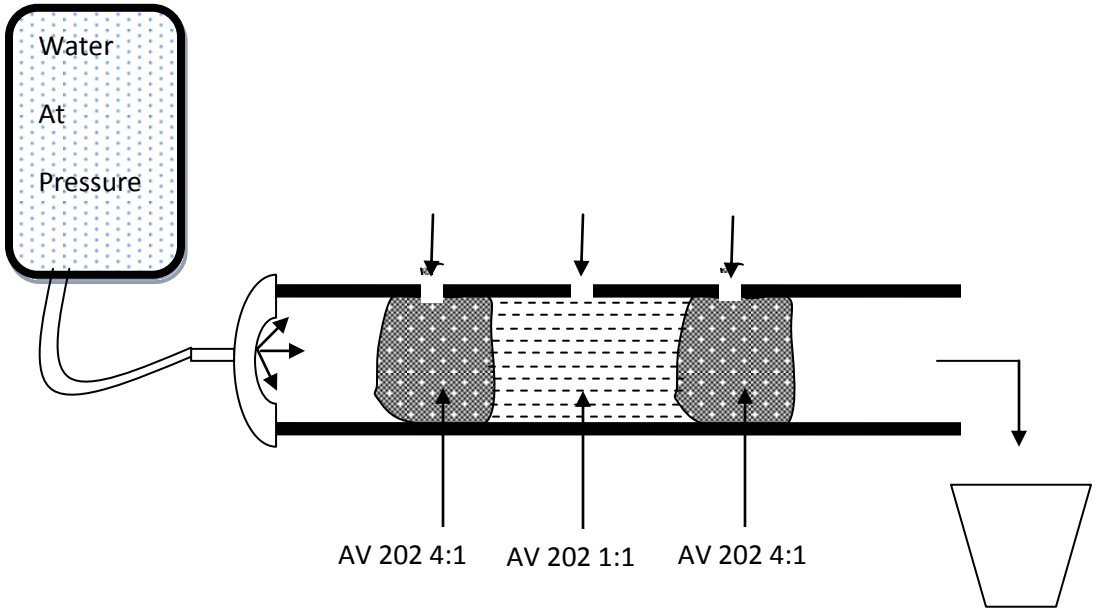

Figure 3-24. Case 3.

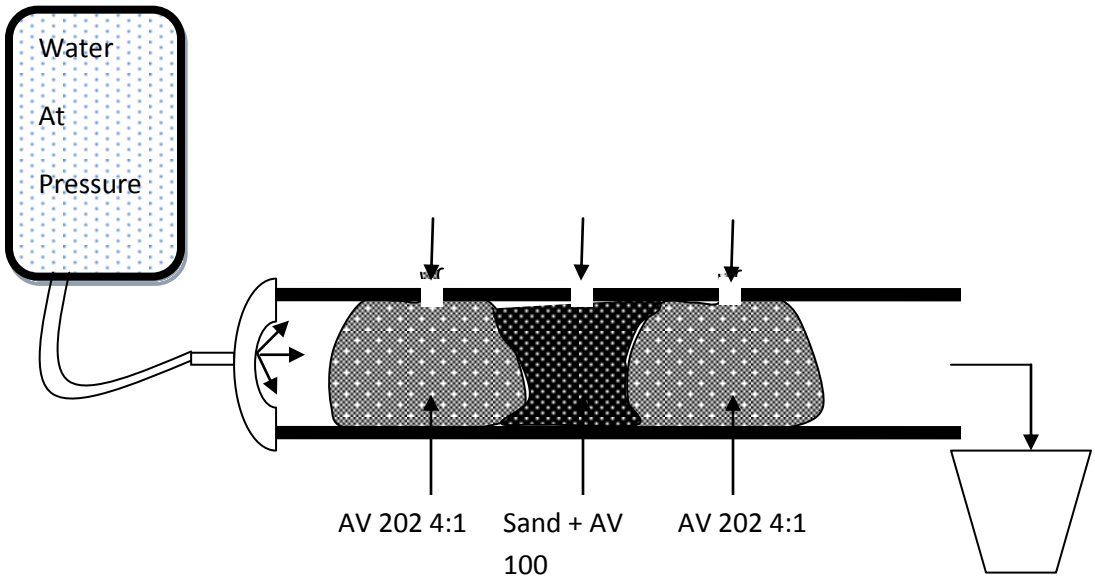

Figure 3-25. Case 4.

3.5 Cement Grout – Testing Methods

3.5.1 Mixing Procedure:

The grout mixes were prepared in batches varying from 200 g to 1000 g depending upon the number of samples to be prepared. A known quantity of cement was measured and clay was added to it. This solid composite was mixed well and following this, water was added and the mix was blended for 5 minutes using a shear mixer. It is to be noted that, the addition of clay was not by replacing the amount of cement in the grout. All the samples were prepared under room temperature and humidity. It is also to be noted that, the carbon fibers were added in parts to the grout mix during the process of mixing.

3.5.2 Test Methods to Evaluate the Working and Strength Properties

Setting Time: Setting time of the cement grout was measured using the Vicat's needle apparatus (ASTM C 191). The setting time of the cement grout is categorized into two stages, the initial setting time and final setting time. The initial setting time is when the Vicat's needle could no longer penetrate more than 25 mm into the grout sample. The final setting time was the time when the grout was fully hardened to a point where the Vicat's needle was not able to penetrate not more than 1 mm.

Bleeding: Bleeding tests were performed on the grout to check the stability of the various mix proportions. The volume of bleed water was noted by observing the solid-liquid interface. To measure the bleeding capacity, the grout mixes that were prepared were poured into 100 mL graduated cylinders and the readings were noted at regular intervals for a period of 2 hours. Bleeding was calculated by expressing the volume of water that separated out of the original volume of the grout sample.

Flowability: The time of efflux was measured using the Marsh funnel viscometer. The time taken for 950 mL (32 oz) of the freshly prepared cement grout to pass through the 5 mm diameter orifice of the funnel was measured. The time of efflux is an indication of the measure of flow-ability of the grout.

Pullout strength: The pullout strength of the cement grout was measured with the type of failure that occurred as a result of the test (Fig. 3-12). Cement grout specimens were prepared in Teflon molds with diameter of 1.5 in. and height of 4 in. Grooved anchor with a cross sectional radius of 0.24 in. (6.1 mm) was immersed into the cement grout to a depth of about 1 - 2 in. (25.4 – 50.8 mm). The samples were cured for a period of 14 days and then the pullout strength of the sample was measured using a

strength testing machine. A simple schematic set up of the pull-out strength is shown in Fig 3-12.

Compressive Strength: Compressive strength of the cement grout was measured using a 1.5 in. diameter and 4 in. high cylindrical sample. The strain rate was kept constant at 10%/hour. The test was conducted until the sample completely failed. The tests were performed after 7 days of air curing of the cement grout specimens.

Self sensing properties: The same approach as stated in section 3.2.2.6 was used to identify the dielectric constant of the cement grout and clay modified cement grout. Observations were conducted with and without application of load. It is to be noted that the effect of addition of clay to the cement grout has been investigated in detail. In addition to this, the effect of addition of carbon fiber is also briefly studied. The resistance of the cement grout sample was also noted on application of stress using the same circuit (parallel plate capacitor) however, resistance measurements were made only at high loads. In order to get accurate readings of the dielectric constant and resistance, the sides of the cement grout were smoothened and were painted with silver color paint. This enables good bonding between the material and the metal plates (parallel plates).

In addition to this, the typical variation of electrical resistivity with respect to time during the process of setting was also measured for some grout mixes. The resistance of the sample was measured using an ohm meter. The Resistivity was then calculated using the formula, $\rho = R.A/L$ where R is the resistance (kilo-ohm), A is the cross sectional area (sq.m) and L is the length of the specimen between which the resistance is measured (m). Similarly, the curing temperature was also measured using a thermocouple.

3.6 Summary

In order to characterize the grouts used in this study, several standard and new tests were developed and used. Based on the planned experiments, following observations are advanced.

1. Grouts were characterized based on the viscosity-time; and temperature time relationship.
2. Gelling time is an important factor to be studied for proper selection of the grout for different applications.
3. Permeability and extrusion tests are essential to designate the use of grouts for sealing pipelines.
4. Parallel plate capacitor method to determine the dielectric constant of the grout is an effective tool to evaluate the sensing capacity of the grout.

CHAPTER 4 MODIFIED CHEMICAL GROUTS

4.1 Introduction

In this chapter, the working, mechanical and sensing properties of modified acrylamide grout are presented. The role of surfactants on modifying the viscosity, gelling time, compressive strength and pullout strength was investigated. The behavior of acrylic grout as a lateral leaking joint sealant was investigated. Also the potential of using polyurethane grout for effectively sealing the pipelines for decommissioning was investigated.

4.2 Acrylamide Grout

4.2.1 Working Properties

(i) Viscosity: The viscosity of the aqueous solution of acrylamide resin was measured with varying amounts of cationic and anionic surfactant. The surfactant was added in different proportions to the aqueous solution made by dissolving 10% acrylamide resin. Addition of cationic or anionic surfactant did not have any noticeable effect on the viscosity of the grout as shown in Figure 4-1. The maximum change was observed with 4% addition of SDS where the increase was about 0.6 cP while 4% CTAB increased the viscosity by about 0.5 cP.

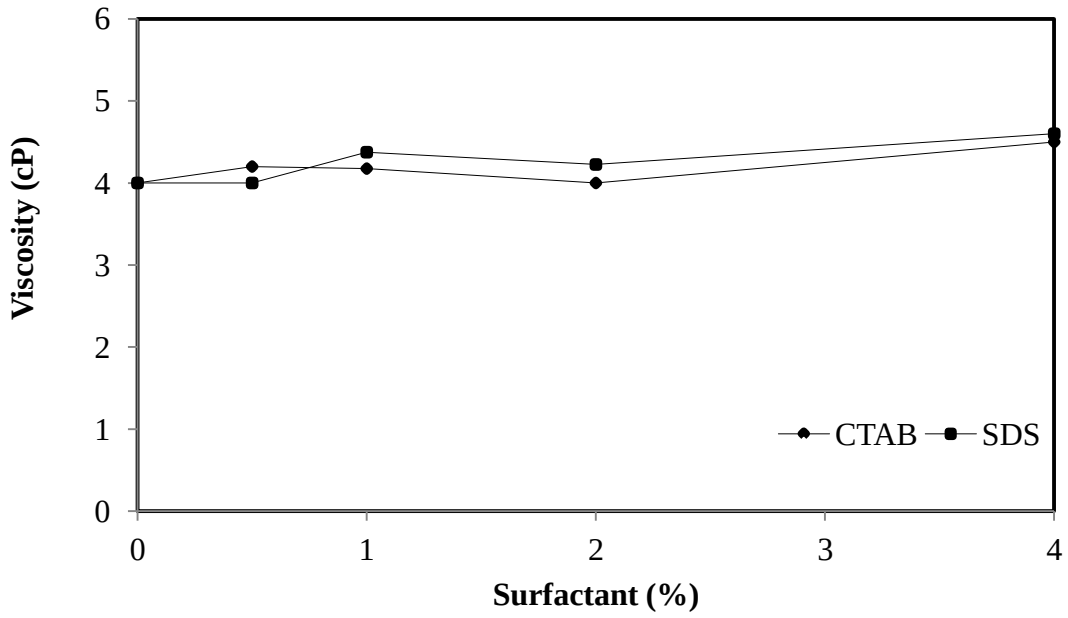

Figure 4-1 Variation of Viscosity of Acrylamide Grout on Addition of Surfactants (Vipulanandan and Sunder, 2011).

(ii) Gelling Time: The gelling time of the acrylamide grout was observed based on the procedure stated in section 3.2.2.3. It is to be noted that, the environmental conditions affect the gelling time of the grout. So, the setting time of the grout mix was observed at three different temperatures 40 ºF, 60 ºF and 80 ºF. The temperature was achieved by heating the two components of the grout individually to the desired temperature and then mixing them to initiate the polymerization reaction. Table 4-1 summarizes the gelling time and curing temperature of the grout solutions investigated in this study. Curing temperature is defined as the maximum temperature attained by the grout during the process of gelling. Curing temperature is also an important parameter to be investigated because lesser the curing time is, better the grout as the grout is often installed in subsurface applications. Figure 4-2, 4-2, 4-4, 4-5, 4-6, 4-7 show the gelling time curves of all the grout mixes studied. Curves corresponding to no surfactant are the

ones for the pure grout mix which had no surfactant addition. Addition of 0.5% SDS (2.5 times CMC) decreased the gelling time at 40^{o}F. The gelling time with 0.5% SDS increased with increase in initial temperature, relative to pure grout and the gelling time decreased by 15 sec at 40˚F while the gelling time increased by 60 sec and 15 sec when the initial temperature was 60˚F and 80˚F respectively. A similar trend was observed on addition of 4% SDS. Increasing the SDS content to 4% (20 times CMC) decreased the gelling time at 40^{o}F but increased it at other testing temperatures. The gelling time decreased by 135 sec at 40˚F but increased by 105 sec and 45 sec at 60˚F and 80˚F initial temperatures. Addition of 0.5% surfactant reduced the maximum curing temperature compared to the pure grout. Addition of 4% SDS increased the curing temperature at 40^{o}F, but the trend was reversed at other testing temperatures. Hence adding SDS affected the gelling time and maximum curing temperatures of the acrylamide grout. On Addition of 0.5% of CTAB, increased the gelling time of the grout at all three different initial temperatures, however, the least change was observed at 80˚F. An increase of gelling time by 60 sec, 75 sec and 15 sec for 40˚F, 60˚F and 80˚F was observed. Addition of 4% CTAB increased the gelling time by 16785 sec, 5715 sec, 1335 sec for initial temperatures of 40˚F, 60˚F and 80˚F respectively. Addition of surfactant reduced the maximum curing temperature of the grout, except at 40^{o}F with 0.5% CTAB. Also 4% CTAB had the largest reduction in the maximum curing temperature with the initial grout temperature of 40^{o}F.

Table 4-1: Gelling times and Curing Temperatures of Grout Mixes (Vipulanandan and Sunder, 2011).

Surfactant	Surfactant % by weight	40ºF		60ºF		80ºF	
		Gelling time (s)	Curing temperature (ºF)	Gelling time (s)	Curing temperature (ºF)	Gelling time (s)	Curing temperature (ºF)
None	0	615	95	165	114	45	134
CTAB	0.5	675	101	240	104	60	129
CTAB	4	17400	70	5880	104	1380	121
SDS	0.5	600	93	225	109	60	129
SDS	4	480	99	270	103	90	124

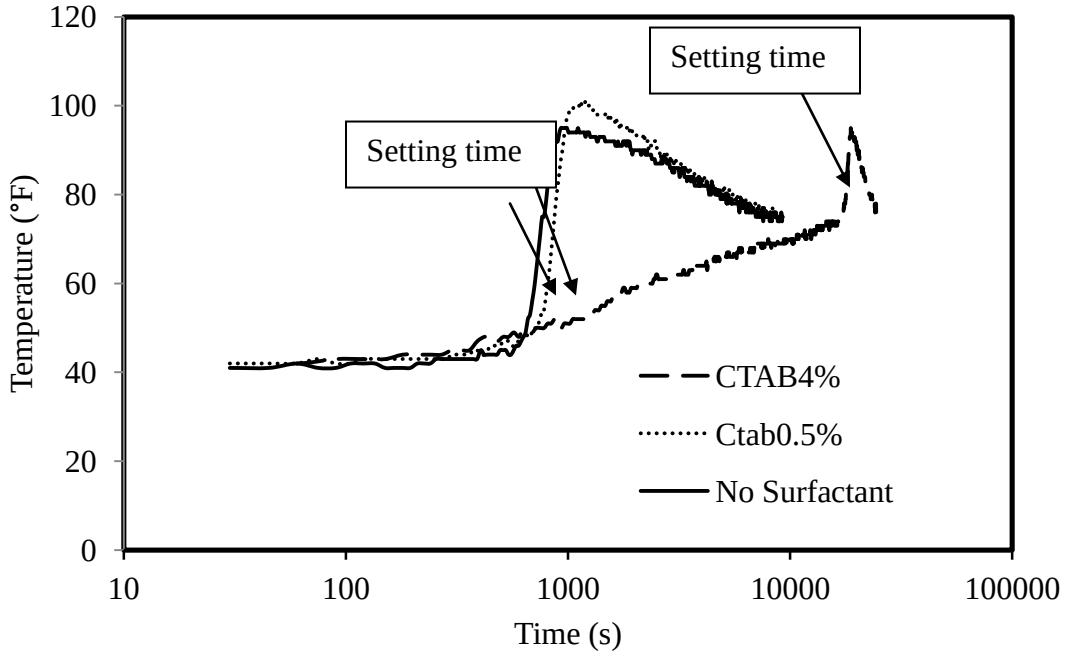

Figure 4-2: Gelling time curves of CTAB modified Grout mix at 40°F.

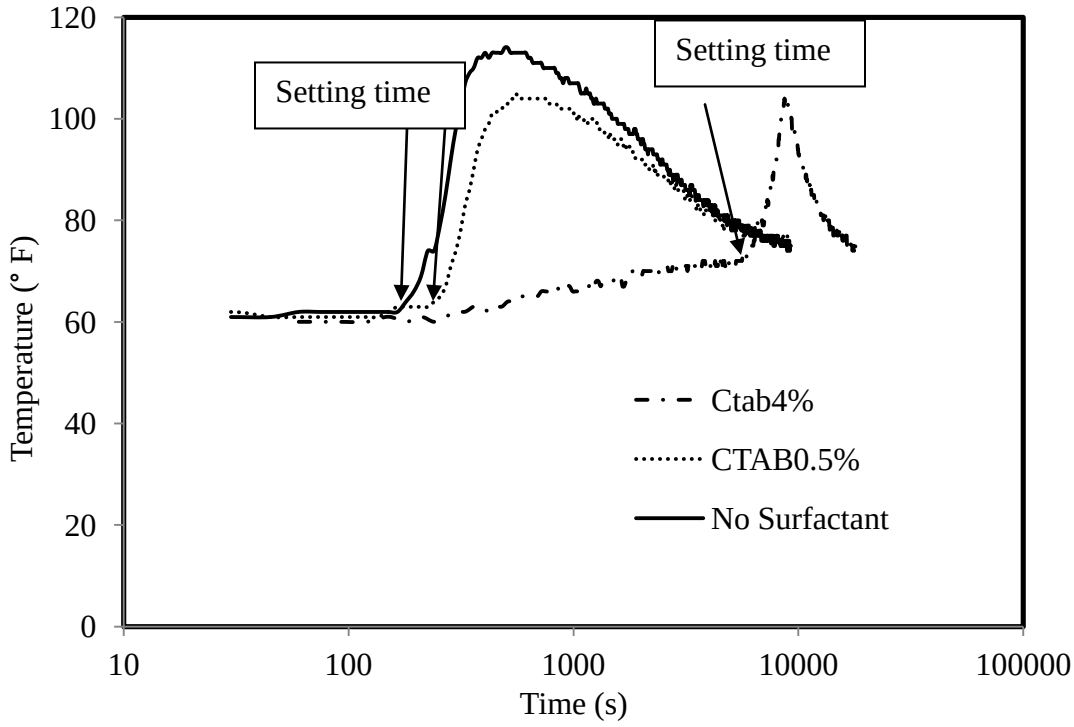

Figure 4-3: Gelling time curves of CTAB modified Grout mix at 60°F.

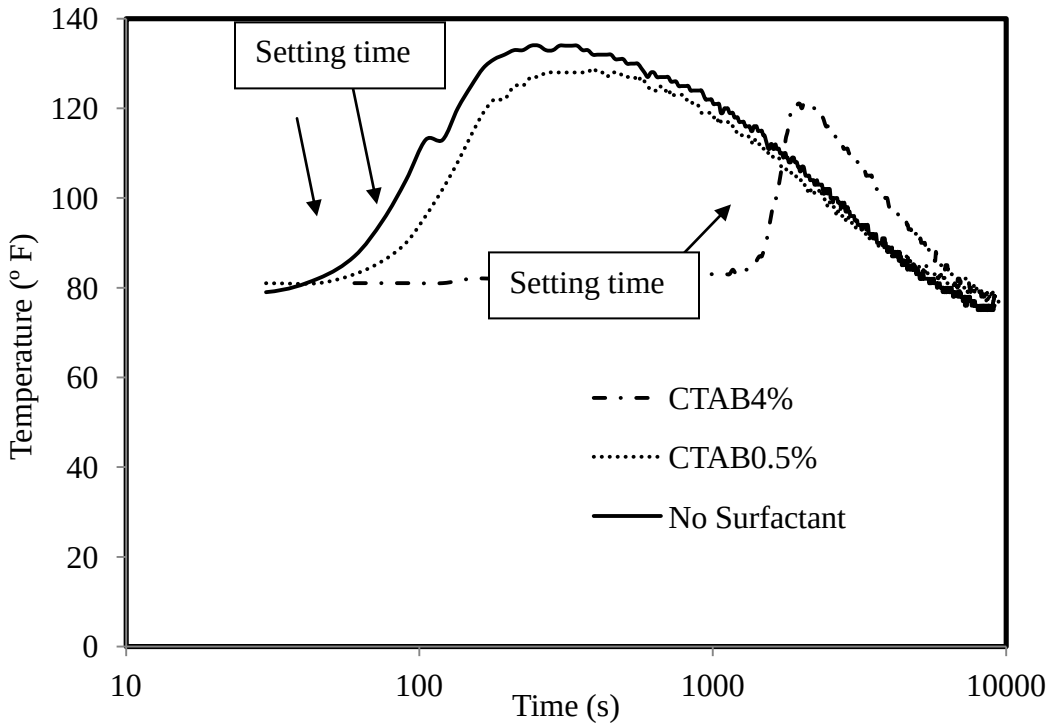

Figure 4-4: Gelling time curves of CTAB modified Grout mix at 80°F.

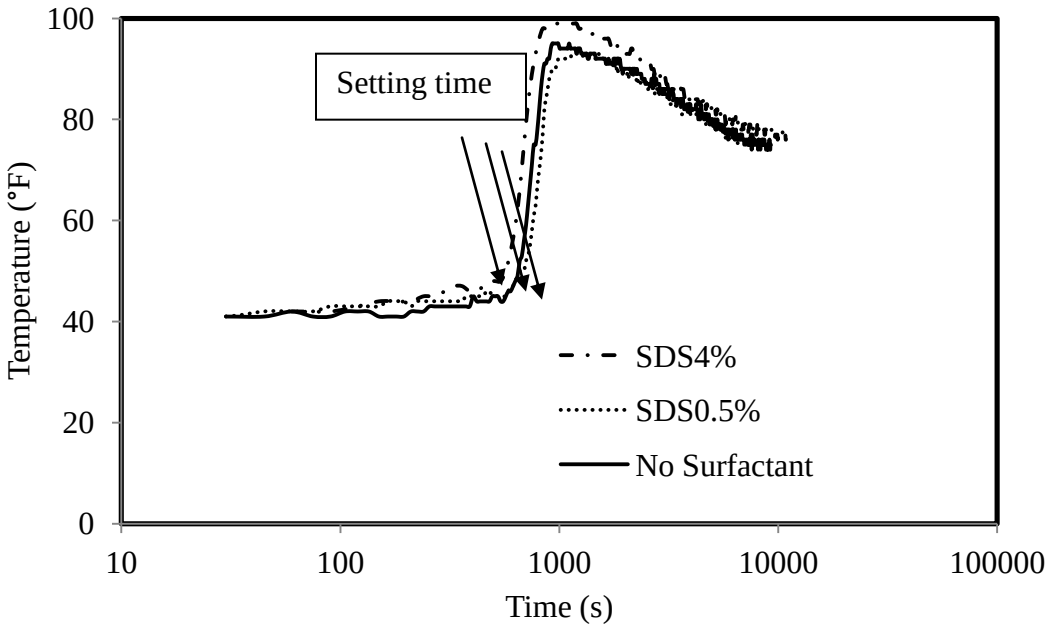

Figure 4-5: Gelling time curves of SDS modified Grout mix at 40°F.

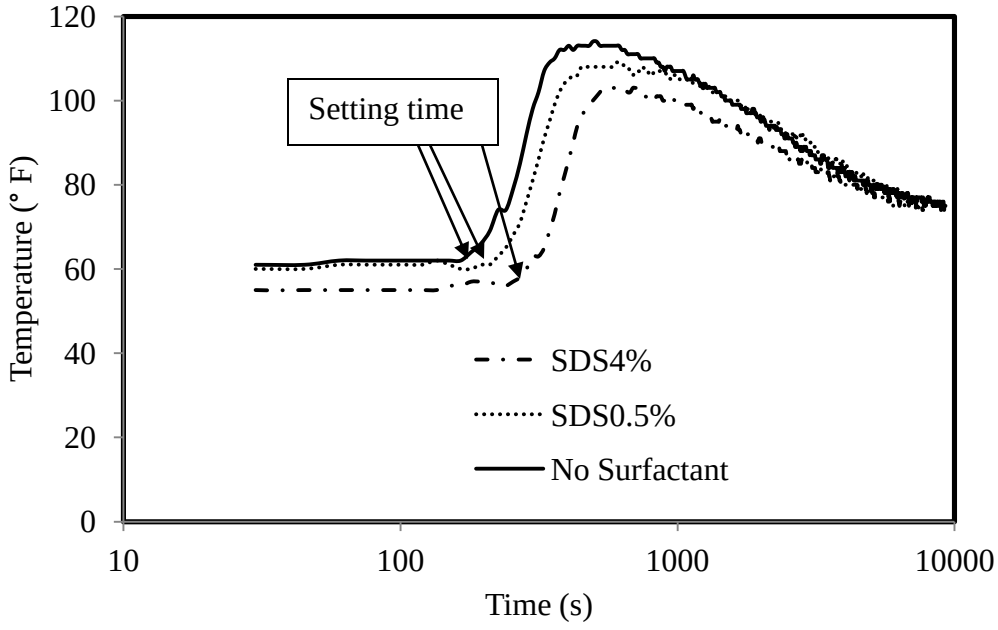

Figure 4-6: Gelling time curves of SDS modified Grout mix at 60°F.

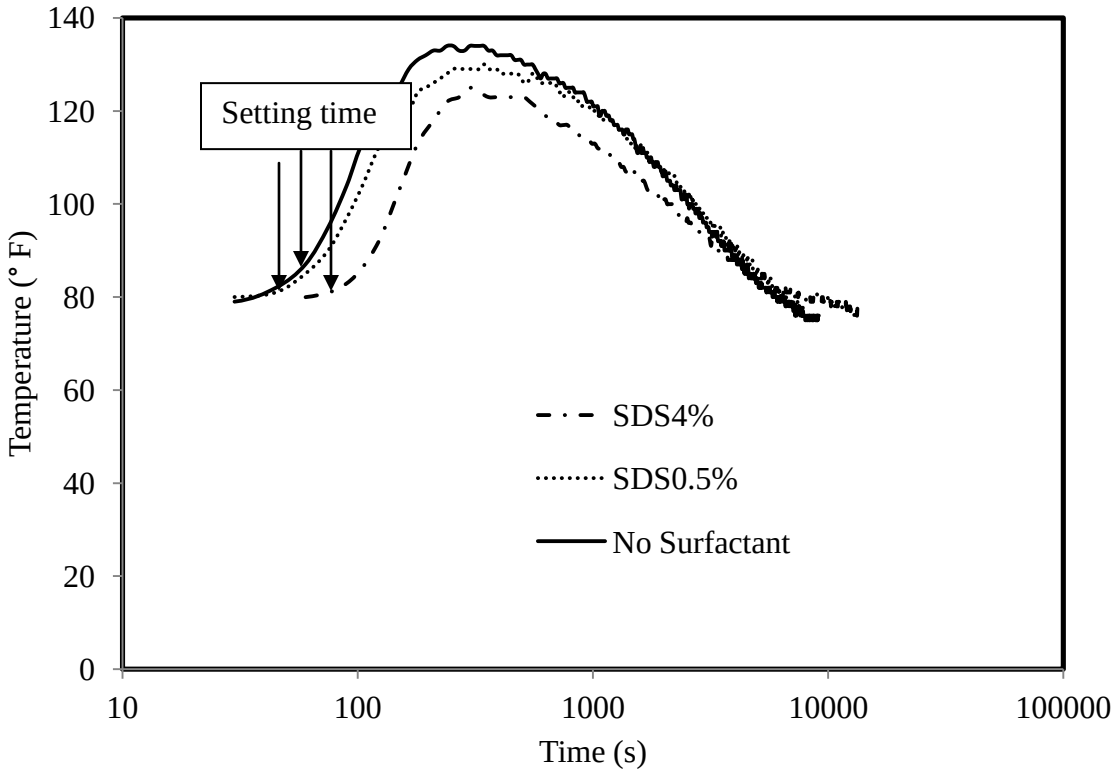

Figure 4-7: Gelling time curves of SDS modified Grout mix at 80°F.

4.2.2 Mechanical Behavior

(i) Pullout Strength: The pull-out strength of grout and grouted sand is shown in Figure 4-8 and Figure 4-9. The pull-out failure was by shearing at the anchor-grout and anchor-grouted sand interface. The pullout strength in the grout varied between 40 and 60 kPa with an average pull-out strength of 50 kPa. The pull-out strength for the grouted sand varied between 100 to 120 kPa with an average pull-out strength of 110 kPa. The pull-out strength in grout and grouted sand reduced with the addition of SDS. The pull-out strength in the grout reduced to about 30 kPa on addition of SDS. Also the pull-out strength of the grout was not affected by the concentration of the SDS surfactant. The pull-out strength with 0.5% SDS in grouted sand was in the range of 66 to 92 kPa with an

average of 79 kPa. The pull-out strength with 4% SDS in grouted sand varied between 45 to 72 kPa with an average of 58.5 kPa. Hence the addition of SDS reduced the pull-out strength of grouted sand and the reduction was also affected by the surfactant concentration. Also the pull-out test was sensitive to the changes in the grout and grouted sand.

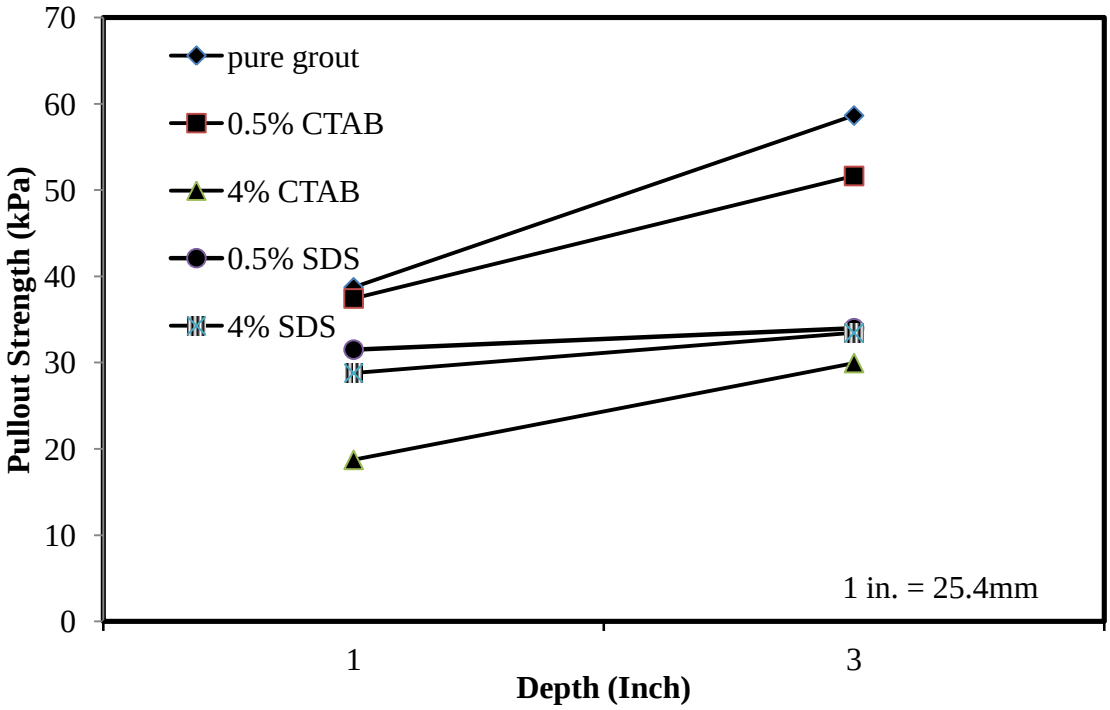

Figure 4-8: Pull-out Strengths of Grout mix solutions (Vipulanandan and Sunder, 2011).

The pull-out strength in the grout with 4% CTAB varied between 19 and 30 kPa with an average strength of 25.5 kPa. The pull-out strength in the grout with 0.5% CTAB varied between 37 and 52 kPa with an average strength of 44.5 kPa. Hence the pull-out strength in grout was affected by the concentration of the CTAB surfactant. The pull-out strength with 0.5% CTAB in grouted sand was in the range of 36 to 84 kPa with an

average of 60 kPa. The pull-out strength with 4% CTAB in grouted sand was 4 kPa. Hence the addition of CTAB reduced the pull-out strength of grouted sand and the reduction was also affected by the surfactant concentration. Thus pull-out test was sensitive to the addition of surfactant to the grout mix.

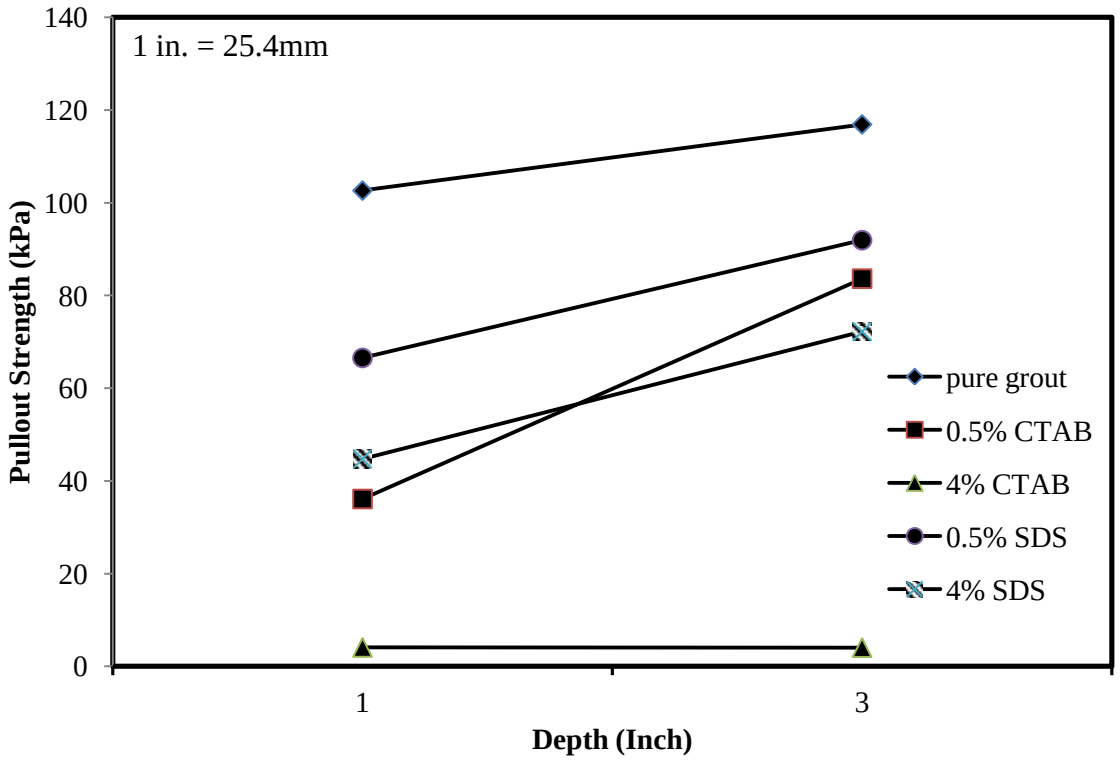

Fig 4-9: Pull-out Strengths of Grouted Sand Specimens (Vipulanandan and Sunder, 2011).

(ii) Compressive Strength: Addition of surfactants affected the compressive strength and the failure strain of the grouted sand. Figure 4-10 shows the variation in the compressive strength with strain on addition of surfactants. The grouted sand strength and strain without any surfactant was 174 kPa and 1.9% respectively. Addition of SDS increased the strength of grouted sand. The grouted sand strength with SDS was 240 kPa, over 30% increase in strength of the grouted sand without any surfactant. The increase in

compressive strength in grouted sand was opposite to what was observed in the pull-out test. Addition of SDS didn't influence the failure strain of grouted soil. Addition of CTAB increased the strength of grouted sand. The strength of the grouted sand increased by 51% and 37% with the addition of 0.5% and 4% of CTAB. The failure strain increased from 1.9% to 3.25% and 3.5% when 0.5% and 4% of CTAB was added to the grout mix. The increase in compressive strength in grouted sand was opposite to what was observed in the pull-out test.

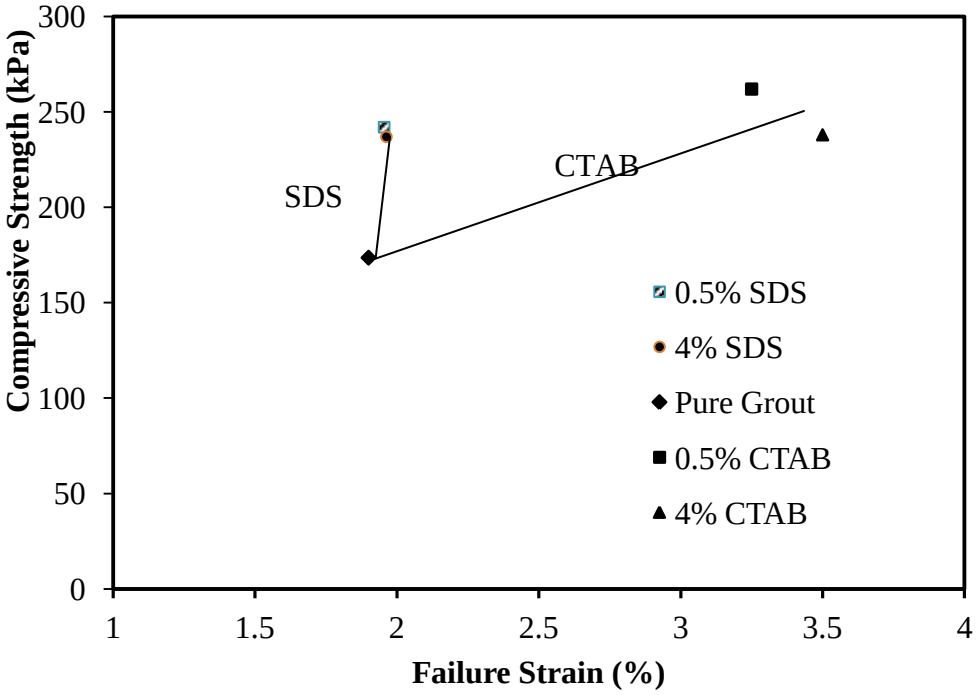

Fig 4-10: Compressive Strength of Grouted Sand (Vipulanandan and Sunder, 2011).

(iii) Extrusion Strength: The extrusion pressure needed to extrude the acrylamide grout from the copper tube is shown in figure 4-11. The methodology is an indicator to exhibit the efficiency of the grout to withstand high pressures when used in sealing applications (filling cracks in rocks and concrete). It is to be noted that, as the

colume of the grout increased the extrusion pressure of the grout increased. For a straight 0.25 in. diameter copper tube filled with grout to a length of 13.5 in. the pressure needed to extrude the grout was 37 psi and the pressure was sustained by the grout for 7 seconds. When the grout length increased to 19.5 in. the pressure needed to extrude the grout also increased to 50 psi. It must be noted that, the grout failed only at the end of 90th second after increasing the pressure in a step wise manner as indicated in Figure 4-11. When investigating the curl copper tubes, the pressure needed was even higher as the length of the grouted length was increased. The grout was not extruded even after 23 minutes on applying a pressure of 180 psi. This reveals the fact that acrylamide grout by itself is an excellent material which can be used for sealing purposes. Figure 4-12 shows the shear stress at the grout - tube interface, assume it was a constant along the total length (Equation 3.3)

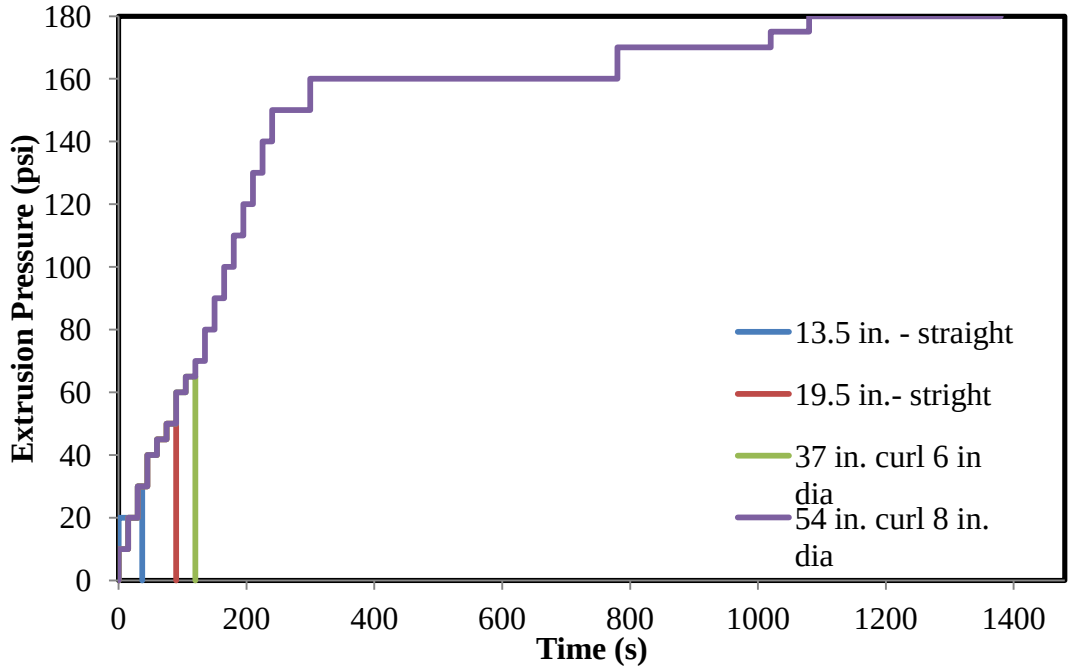

Figure 4-11: Extrusion pressure for acrylamide grout.

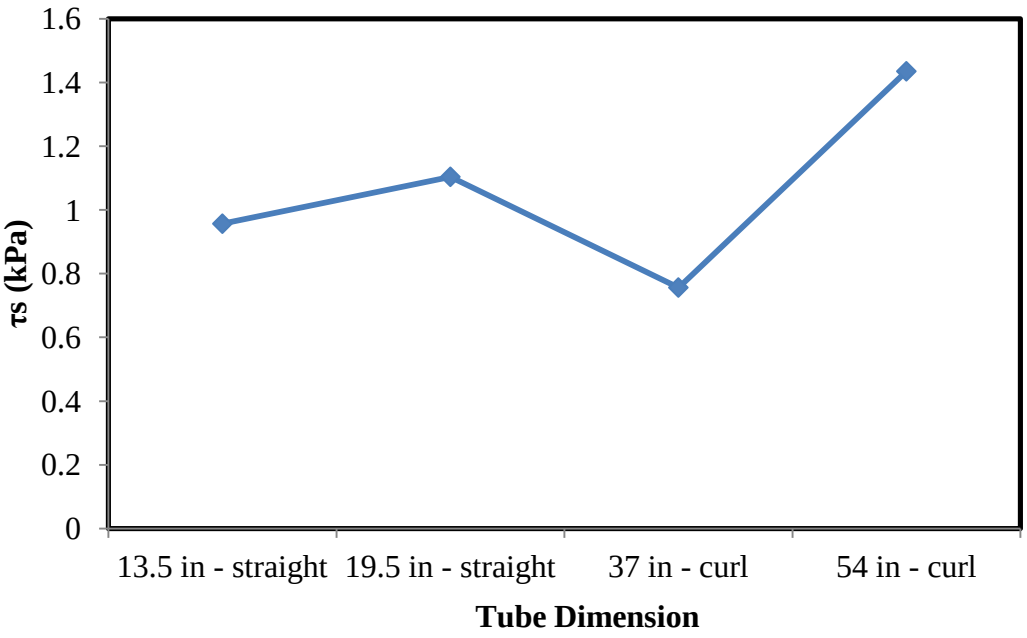

Figure 4-12: Interface Shear stress of Acrylamide Grout.

4.2.4 Self Sensing

The self sensing property of the grout was tested by preparing the grouted sand sample with and without the addition of carbon fiber and checking the variation in resistance and the dielectric constant of the grouted sand. The method of sample preparation and test setup is illustrated in section 3.2.2.6. Figure 4-13 shows the variation in the dielectric constant value of the grouted sand on adding Carbon Fiber. It is to be noted that without the addition of carbon fiber (density of the sample = 99 pcf), the dielectric constant value was 4.3, but on adding 2% Carbon fiber by weight of sand (density of the sample = 86 pcf), the value increased to as high as 1230. Figure 4-14 shows the variation of dielectric constant with the application of load on the six inch thick grouted sand sample. The dielectric constant varied from 4.3 to 5.8 when the load

applied vaied from 0 to 80 lbs. the change in dielectric constant value was noted to be 35%, A similar trend was observed in the grouted sand sample with carbon fiber which is shown in Figure 4-15. The initial value of the dielectric constant was 1200. It was observed that, the value increased from 1200 to 4200 which was a 250% increase.

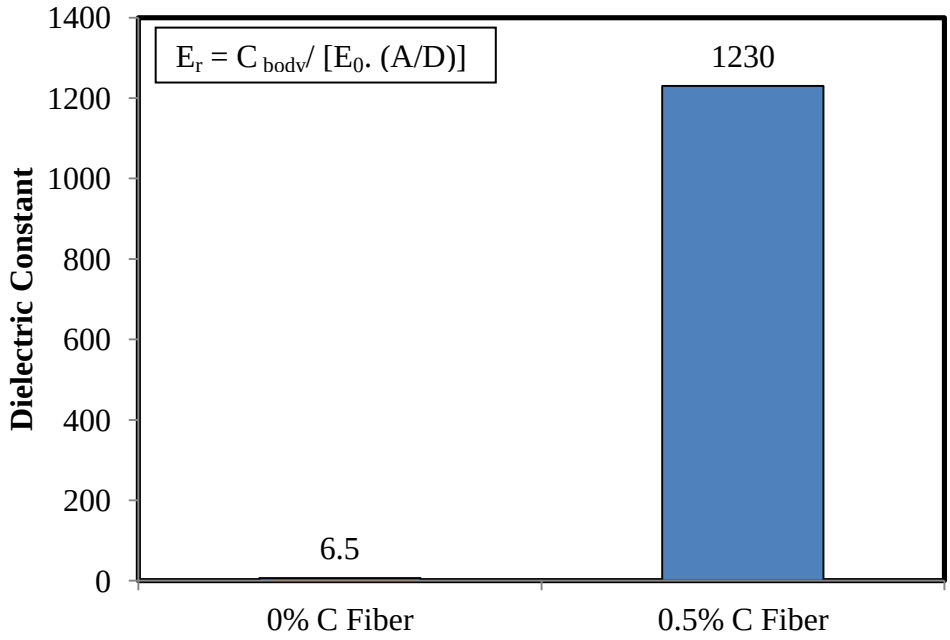

Figure 4-13: Effect of C-Fiber on Dielectric Constant.

Figure 4-16 shows the change in resistance value of the grouted sand with C-fiber with the change in dielectric constant value. This figure shows that, the grout also possesses a piezo-resistive behavior in addition to change in dielectric constant on application of stress on addition of Carbon fiber as opposed to the grouted sand with no C-fiber which does not show the piezo resistive behavior since the resistance value was too high to measure.

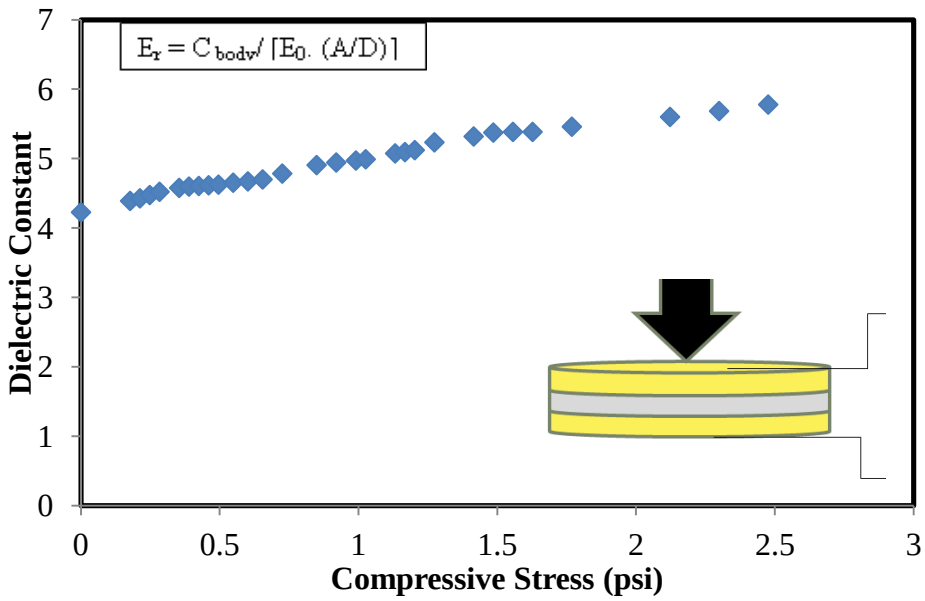

Figure 4-14: Variation in Dielectric Constant with applied Load for Grouted Sand without C- Fiber.

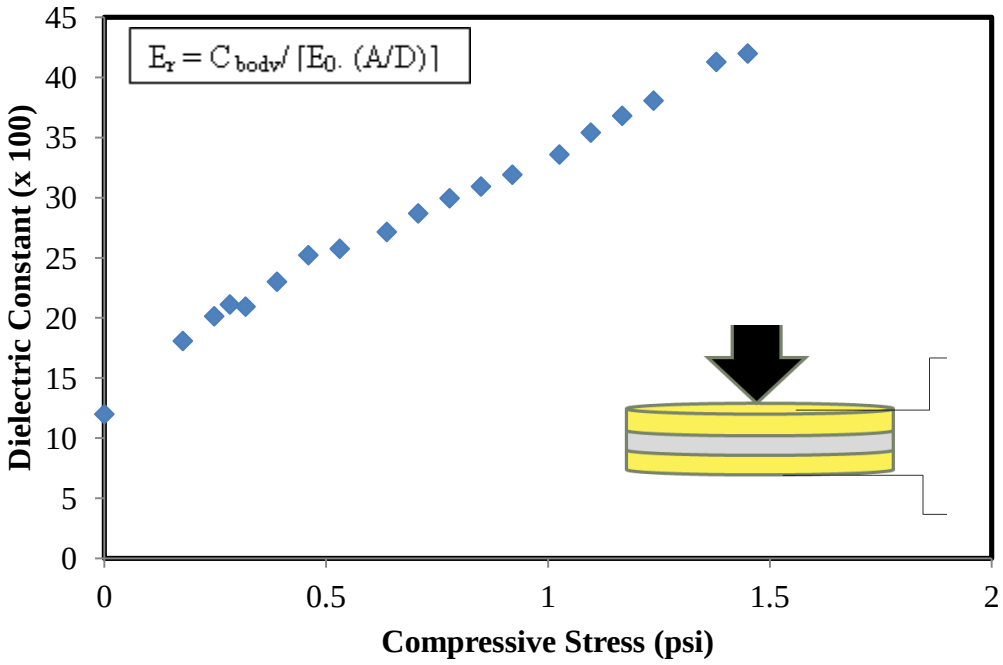

Figure 4-15: Variation in Dielectric Constant with Load for Grouted Sand with C-Fiber.

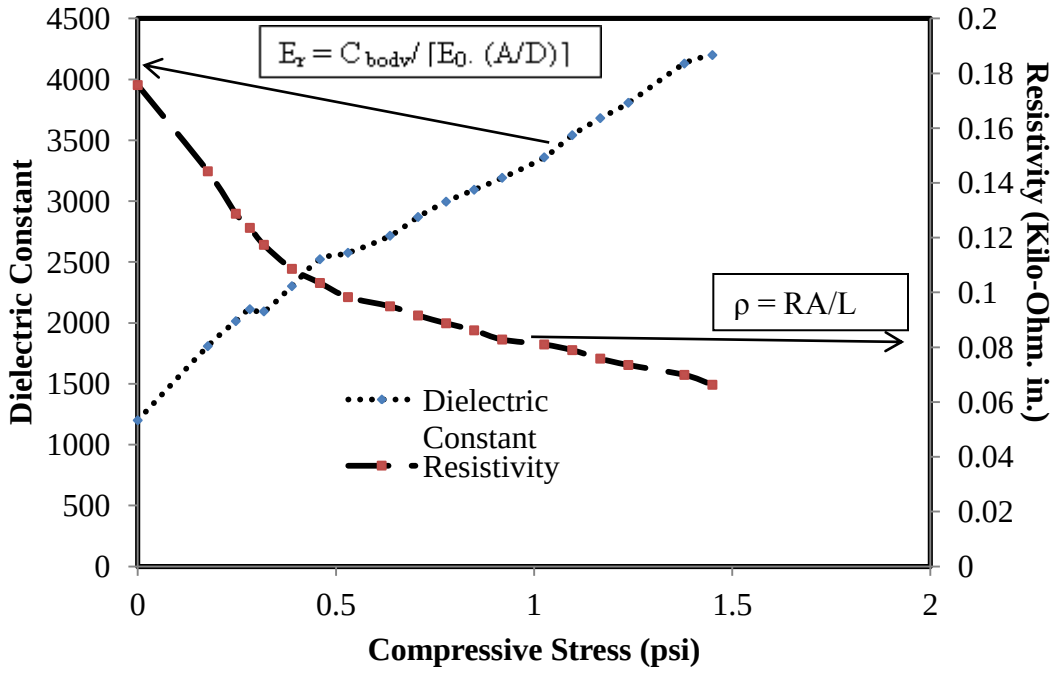

Figure 4-16: Variation in Resistivity and Dielectric Constant with Load for Grouted Sand with C- Fiber.

4.3 Acrylic Grout

4.3.1 Working Properties

(i) Viscosity: The grout viscosity was evaluated using the procedure outlined in CIGMAT GR 6 – 04. Three samples were tested for viscosity. The tests were performed at three speeds (12, 30 and 60 rpm) are summarized in Table 4-2.

Table 4-2: Viscosity of Acrylic Chemical Grout.

Spindle	Speed	Sample 1		Sample 2		Sample 3	
		Reading	Viscosity	Reading	Viscosity	Reading	Viscosity
Units	Rpm		cP				cP
1	60	6.00	6.00	6.00	6.00	5.75	5.75
1	30	2.40	4.80	2.25	4.50	2.40	4.80
1	12	1.00	5.00	1.00	5.00	1.00	5.00
Average Viscosity			5.27		5.17		5.18
			Average Viscosity (cP) = **5.2**				

It was concluded that the viscosity was independent of the rate of shearing. The average viscosity for the three samples varied from 5.17 to 5.27 cP.

Table 4-3: Statistical Analysis of the Viscosity.

Sample	Average Viscosity (cP)	Standard Deviation (σ)	Coefficient of Variance (COV)
1	5.27	0.5	0.10
2	5.17	0.7	0.14
3	5.18	0.4	0.08
Average	5.21	0.53	0.11

The average viscosity of the acrylic resin solution was 5.21 cP with a standard deviation of 0.53 and coefficient of variation of 0.11. The viscosity was independent of the rate of strain (spindle speed).

(ii) Gelling Time: The gelling (setting) time for the grout mix was evaluated as outlined in CIGMAT standard GR 8 – 09. Gelling time is defined as the time taken by the grout mix to transform itself from liquid state to solid state from the time of mixing. The gelling time testing was performed at room temperature and room humidity. Total of 6 samples (100 mL) of grout were prepared and the test was performed.

Table 4-4: Gelling Time of the Samples.

Sample #	1	2	3	4	5	6	Mean
Gelling time (sec)	25	23	23	25	30	21	**24.5**
Standard Deviation: (sec)		**2.81**	Coefficient of Variance (COV):			**0.115**	

The gelling time varied from 21 to 30 seconds and an average gelling time was 24.5 seconds with a standard deviation of 2.8 sec and the coefficient of 0.12.

4.3.2 Compressive Strength:

Unconfined compression tests were performed according to CIGMAT GR 2-02 standard. Compression tests were performed using screw-type machine with capacity of 5,000 lbs. Specimens were loaded at a strain rate of 1%/min. Grouted sand specimens were approximately 1.5 in. (38 mm) in diameter and 2.6 to 3.5 in. (65 to 90 mm) in height. The specimens were trimmed and capped (using a sulfur compound commonly used for capping cement concrete) to ensure smooth and parallel surfaces. Specimens were tested in triplicate after 3, 7 and 28 days of curing. The test results are

summarized in Table 4-5. The modulus was determined from the initial slope of the stress/strain curve and the failure strain is the maximum loading point before the specimen failed.

Table 4-5: Summary of Compressive strength of Grouts.

Sample	**Time**	**Stress**	**Strain**	**Modulus**
#	day	psi	%	Psi
1	3	23.09	4.8	667
2	3	21.84	7.1	500
3	3	35.07	3.4	1500
Average	**3**	**26.7**	**5.1**	**888**
1	7	21.97	5.4	556
2	7	16.81	9.9	286
3	7	23.39	4.4	667
Average	**7**	**20.72**	**6.6**	**502**
1	28	25.69	2.9	929
2	28	32.25	3.8	1250
3	28	31.28	4.1	1000
Average	**28**	**29.74**	**3.6**	**1060**

Based on the test results, the compressive strength and modulus increased with curing time. The failure strain decreased with curing time. The average compressive strength after 3 days of curing was 26.7 psi and it increased to 29.7 psi after 28 days of curing time. The average compressive modulus after 3 days of curing was 888 psi and it increased to 1060 psi after 28 days of curing time.

4.3.3 Durability Properties

(i) Environmental Test – Leaching Test: Three solidified grout specimens were placed in equal volume of water and the leachates were analyzed to determine the TOC. The grout (60 mL) samples were placed in the water for 7 days before

sampling and testing the water. Also blank water sample was used as a control. The test results are summarized in Table 4-6.

Based on three specimens, the TOC in the water varied from 5.346 to 5.500 mg/mL with an average of 5.399 mg/mL standard deviation of 0.07 mg/mL and the coefficient of variation was 1.33%

Table 4-6: Summary of TOC in the Water.

Specimen #	Description	Wt. (g)	Volume of Grout (mL)	Volume of Tap water (mL)	Measured TOC (mg/L)	Dilution Factor (mg/l)	corrected TOC (mg/mL)	TOC (/g grout)
1	7 day old Tap water		-	100	0.026	1x	0.01	
2	AV-118	54.2	50	50	5.884	100x	5.500	0.101
3	AV-118	55.5	50	50	5.686	1000x	5.346	0.096
4	AV-118	54.5	50	50	5.692	1000x	5.350	0.098

(ii) Water Absorption: Water absorption was evaluated for grouted sand specimens as outlined in the standard procedure CIGMAT GR 3-00. Three grouted sand specimens were immersed in tap water (initial pH in the range of 7 to 8) and changes in weight and volume (determined by measuring specimen diameter and height) of the specimens were recorded until the changes in weight or volume become negligible (less than 0.5 percent of the previous weight and volume), or for one week, whichever occurred first.

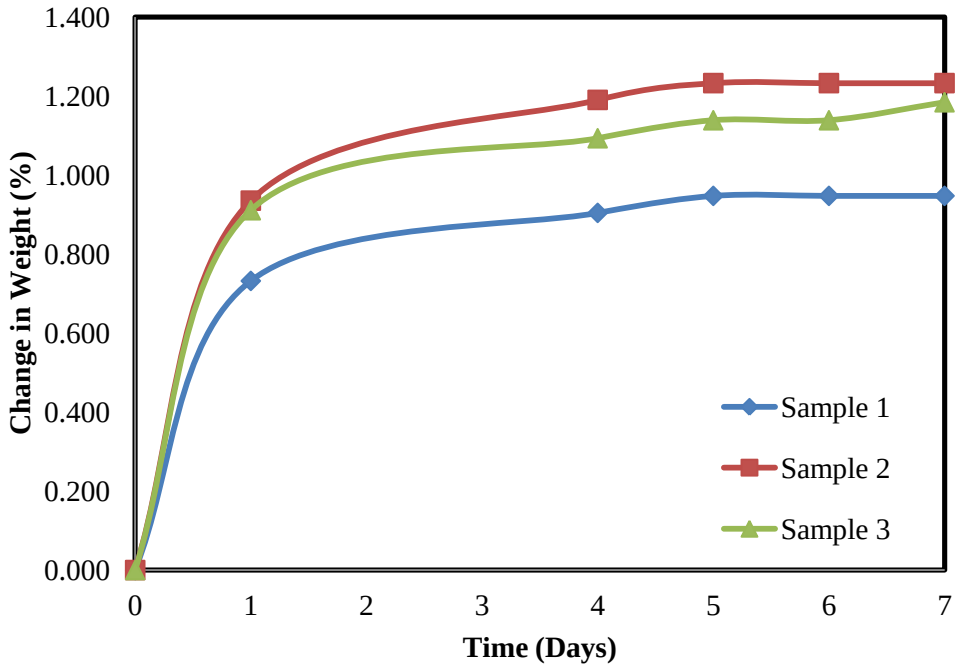

Figure 4-17: Change in weight with respect to time during the water absorption test.

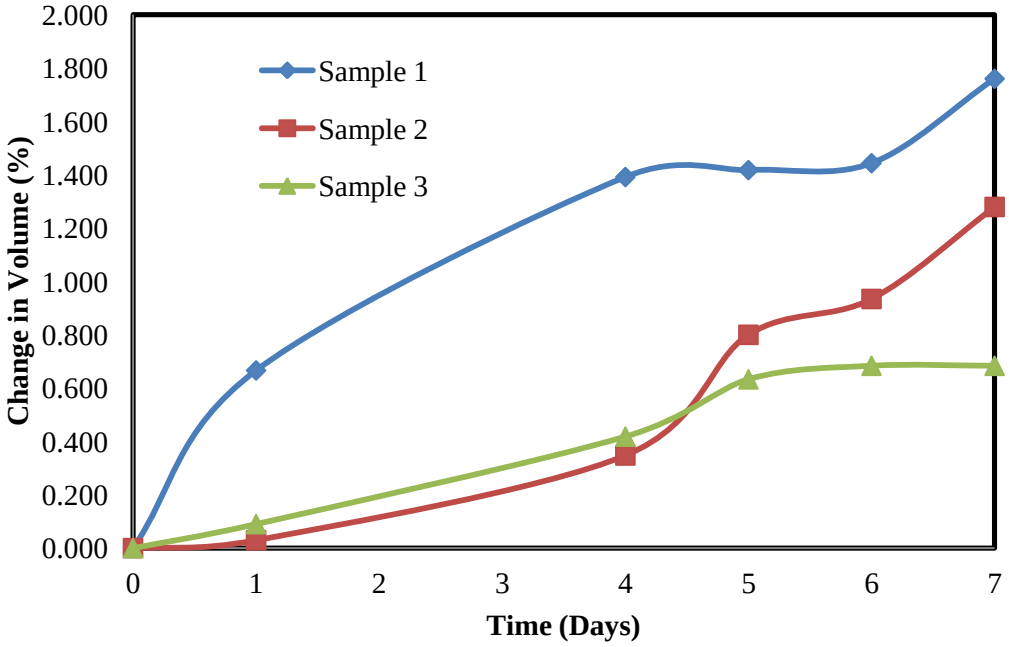

Figure 4-18: Change in volume with respect to time during the water absorption test.

Variation in sample weight and volume over a period of one week is shown in Figures 4-17 and 4-18. The maximum weight gained varied from 0.947 to 1.139 %. The measured maximum volume change varied from 0.684 to 1.76% with a standard deviation of 0.1% and coefficient of variation of 10.8%. This result signifies that the change in weight and volume when exposed to saturated conditions were negligible which signifies the use of grout in saturated conditions.

(iii) Shrinkage: Based on the test results from three specimens, the weight loss varied from 0.042 to 0.045%. The average weight loss was 0.043% with a standard deviation of 0.0012% and coefficient of variation of 2.9%. The volume change measured for the three specimens varied from 0.201 to 1.036 %. The average volume reduction was 0.613% with a standard deviation of 0.341% and coefficient of variation of 55.7%. The shrinkage results are shown in Table 4-7.

Table 4-7: Summary of Shrinkage Test Results.

S.No	Time	Temp	Humidity	Weight	Diameter	Height	Volume	vol. change	Wt.change
	days	C	%	g	mm	mm	cu.cm	%	%
1	1	22	89	236.9	38.20	100.91	115.61		
	28	22.8	92	236.8	38.00	100.94	114.41	-1.036	-0.042
2	1	22	89	233	37.90	101.07	113.94		
	28	22.8	92	232.9	37.90	100.86	113.71	-0.201	-0.043
3	1	22	89	221.6	36.80	102.54	109.04		
	28	22.8	92	221.5	36.70	102.49	108.38	-0.601	-0.045

(iv) Permeability Test: Three grouted sand specimens were used to determine the permeability. Specimens were prepared in Plexiglas/glass cylinders and permeated with water under a hydraulic gradient of 100 as specified in CIGMAT GR 7-02. Tests were performed at room temperature and humidity.

In Table 4-8 permeability test result are summarized. The permeability of the grouted sand was zero and hence characterized as impermeable.

Table 4-8: Permeability of Grouted Sand.

	Effluent (mL)	Permeability (cm/s)
Specimen 1	0	0
Specimen 2	0	0
Specimen 3	0	0
Average	0	0

Based on the three test results, the permeability of the grouted sand was zero under the testing conditions adopted in this study. This lab test signifies that the grout is efficient as a sealant for water leaks.

(v) Chemical Resistance : Total of 9 specimens were tested for a period of 6 months. Total of 3 specimens were tested in pH=2, 7 & 10 solutions. The test results are summarized in Table 4-9.

pH= 2 solution: After one month the average change in weight, volume and unit weight were 2.57%, 0.31% and 1.53% respectively After six months the average change in weight, volume and unit weight were 2.65%, 0.92% and 1.35% respectively. The weight and volume increased over period of 6 months. The average compressive strength was found to be 18.25 psi.

pH= 7-water: After one month the average change in weight, volume and unit weight were 0.00%,1.03% and 0.86% respectively. After six months, the average change in weight, volume and unit weight were -0.03%, 1.47% and 0.48% respectively. The change in weight was negligible and volume increased over period of 6 months. The average compressive strength was found to be 17.5 psi.

pH= 10 solution: After one month the average change in weight, volume and unit weight were 1.61%, 1.00% and 0.75% respectively After six months the average change in weight, volume and unit weight were 1.66%, 0.72% and 0.99% respectively. The change in weight was negligible and volume marginally decreased over period of 6 months. The average compressive strength was found to be 21.24 psi.

Table 4-9 – Chemical resistance test results.

Specimen #		Weight (g)	Length (in)	Diameter (in)	Volume (in^3)	Density (pcf)
Original (pH=2)	1	231.00	3.96	1.49	7.02	125.45
	2	240.90	4.09	1.50	7.18	127.84
	3	178.90	3.07	1.50	5.38	126.61
	Average	216.63	3.71	1.50	6.53	126.63
30 days (pH=2)	1	234.70	3.97	1.50	6.98	128.09
	2	244.90	4.12	1.49	7.23	129.03
	3	184.00	3.09	1.50	5.45	128.61
	Average	222.20	3.73	1.50	6.55	128.57
	% Change	2.57	0.54	0	0.31	1.53
3 months (pH=2)	1	236.2	3.96	1.50	7.01	128.32
	2	247.2	4.13	1.49	7.24	130.0
	3	184.5	3.08	1.50	5.44	129.29
	Average	222.63	3.72	1.50	6.56	129.20
	% Change	2.77	0.27	0.00	0.46	2.03
6 months (pH=2)	1	236.2	3.98	1.50	7.00	128.53
	2	246.8	4.13	1.50	7.27	129.39
	3	183.8	3.1	1.50	5.51	127.10
	Average	222.27	3.74	1.50	6.59	128.34
	% Change	2.60	0.81	0.00	0.92	1.35

Table 4-9 – Chemical resistance test results (Continued).

Specimen #		Weight (g)	Length (in)	Diameter (in)	Volume (in^3)	Density (pcf)
Original (pH=7)	1	231.1	3.97	1.5	7.02	125.50
	2	237.2	4.01	1.49	7.02	128.79
	3	214.7	3.94	1.44	6.43	127.17
	Average	231.93	3.97	1.48	6.82	127.15
30 days (pH=7)	1	235.90	3.97	1.50	7.00	128.41
	2	241.30	4.02	1.51	7.16	128.34
	3	218.60	3.96	1.45	6.51	127.98
	Average	231.93	3.98	1.49	6.89	128.24
	% Change	0.00	0.25	0.68	1.03	0.86
3 months (pH=7)	1	237	3.96	1.5	6.99	129.13
	2	241.3	4.03	1.503	7.14	128.66
	3	218.6	3.98	1.444	6.52	127.80
	Average	232.3	3.99	1.48	6.88	128.53
	% Change	0.16	0.50	0.00	0.88	1.09
6 months (pH=7)	1	236.3	4.03	1.5	7.12	126.44
	2	240.5	4.03	1.51	7.17	127.79
	3	218.8	3.95	1.45	6.48	128.65
	Average	231.87	4.00	1.49	6.92	127.63
	% Change	-0.03	0.76	0.68	1.47	0.48

Specimen #		Weight (g)	Length (in)	Diameter (in)	Volume (in^3)	Density (pcf)
Original (pH=10)	1	232.7	3.94	1.49	7.02	126.37
	2	233.3	3.96	1.49	6.93	128.25
	3	235.1	3.98	1.49	6.97	128.43
	Average	233.7	3.96	1.49	6.97	127.68
30 Days (pH=10)	1	236.20	3.97	1.50	7.02	128.22
	2	237.9	3.97	1.50	7.00	129.47
	3	238.60	4.01	1.50	7.09	128.24
	Average	237.47	3.98	1.50	7.04	128.64
	% Change	1.61	0.51	0.67	1.00	0.75
3 months (pH=10)	1	236.3	3.97	1.50	6.96	129.36
	2	238.1	3.98	1.50	7.00	129.60
	3	238.6	4.00	1.49	6.99	129.98
	Average	237.67	3.98	1.50	6.98	129.65
	% Change	1.70	0.51	0.67	0.14	1.54
6 months (pH=10)	1	236.2	3.96	1.50	6.99	128.81
	2	237.9	3.96	1.51	7.06	128.45
	3	238.6	3.96	1.50	7.02	129.57
	Average	237.57	3.96	1.50	7.02	128.94
	% Change	1.66	0.00	0.67	0.72	0.99

Table 4-10– Compressive Strength after Chemical resistance tests.

Sample	pH	Stress	Strain	Modulus
#		psi	%	psi
1	2	17.32	6.12	516
2	2	20.52	6.63	361
3	2	16.92	6.87	374
average		**18.25**	**6.54**	**417**
1	7	14.35	5.89	313
2	7	22.35	5.13	530
3	7	15.79	4.94	421
average		**17.50**	**5.32**	**476**
1	10	22.15	4.53	749
2	10	20.35	5.38	506
3	10	21.22	4.73	471
average		**21.24**	**4.88**	**575**

4.3.4 Lateral Leak Control Model

The main aim of this study was to verify the performance of acrylic grout in controlling leak at a lateral joint using a 3-Dimensional model. This was done by determining the infiltration/inflow (I&I) before and after grouting the joint to determine the effectiveness of grouting used in controlling the leak at a lateral joint. Approximately 950 pounds of sand was used for the model test. The average dry unit weight of the sand was 94.5 pcf.

The top of the chamber had an air outlet valve to de-air during the saturation process. The water inlet valve was used to deliver water into the chamber and the pressure gage was attached to the water inlet valve to measure the pressure at which the water was entering the chamber. Water outlet valve was installed at the bottom of the chamber to drain the water from the chamber.

Once the sand was placed inside the chamber, the chamber was sealed with plexiglass top plate and water was injected to saturate the sand inside the chamber. Once the sand was saturated, the water pressure was maintained at 3 psi for a period of 5 minutes and the water leaking through the lateral joint was collected to determine the water leak. Same procedure was used for the pressures 4 psi and 5 psi. Water leak in model 3A and model 3B are shown in Figure 4-20. It is to be noted that the leak rates at the pressures of 3, 4 and 5 psi in Model A were 1227 gallons per day (gpd), 1274 gpd and 1324 gpd respectively. Water leak rate in Model B at 3, 4 and 5 psi were 1223 gpd, 1322 gpd and 1364 gpd respectively. Figure 4-19 shows the water leaks at a pressure of 3-5 psi in the Model 3 before grouting.

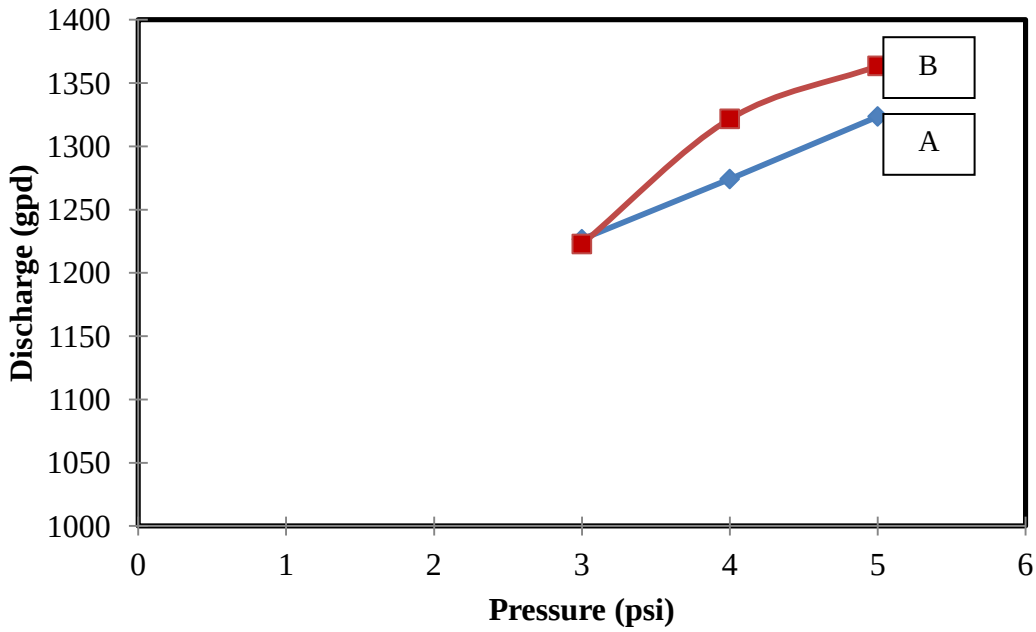

Figure 4-19: I&I Leak Flow Discharge vs Applied Pressure before Grouting.

The two models were grouted by the Grouting Company. The grouting truck was brought to the CIGMAT Laboratory and the grouting of the models was done.

About 2 - 6 gallons of grout was injected in the models. The entire process of preparing the setup and grouting each leak joint took about 10 min. The room temperature at the time of grouting process varied from 22.7 to 23.6˚C and room humidity varied from 45% to 57%. The day after grouting, the lateral joints were tested for leaks at 3, 4 and 5 psi.

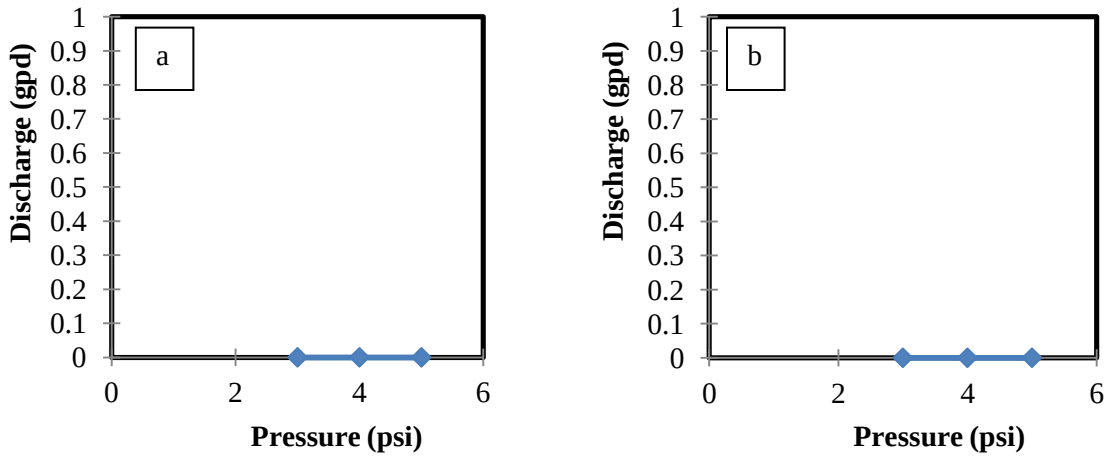

Figure 4-20: Leak Rate Test, day after grouting a) Model A, b) Model B.

The joints were tested for leaks at 3, 4 and 5 psi, a day after grouting. As shown in Figure 4-20, it was observed that there was no water leak at 3, 4 and 5 psi pressures in Model A and Model B after the day of grouting. This indicated that the grout that was injected formed the grouted sand around the lateral joint which stopped water infiltration at the lateral joint. The grouted joint was subjected to wet-dry cycles before testing the leak at the joints again. For the first week the chamber was kept saturated by sealing the ends of the horizontal pipe. After 7 days the water was drained and the model was maintained in this condition for 7 days. The chamber was saturated again for a week and then water was drained for another week before testing for leak

at the joint. The leak rate at the joints was tested at 3, 4 and 5 psi pressures. The results are shown in Figure 4-21. Both models had no leaks (zero) after the wet-dry cycles. Hence the grouting was effective in completely eliminating the leak at the lateral joint.

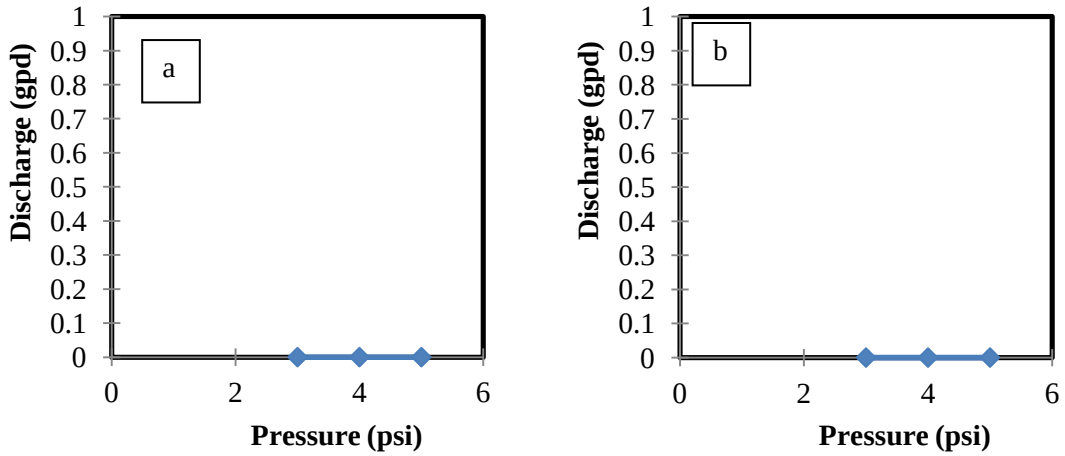

Figure 4-21: Leak Rate Test, after 2 wet-dry cycles a) Model A and b) Model B.

4.4 Polyurethane Grout for Decommissioning

4.4.1 Gelling and expansive Behavior

(i) Setting time: Figure 4-22 shows the gelling time of AV-202 grout at different environments. It is to be noted that the gelling time of AV-202 is not significantly altered in oil environment. The geltime of the grout at resin:solution ratio 1:1 was 82 seconds in the case of water and 84 seconds in the case of oil solution. Similarly at higher resin:solution ratios also, the difference between the setting times of the grout in water and oil environment is negligible. It is to be noted that the addition of surfactants has a significant impact of the gelling time.

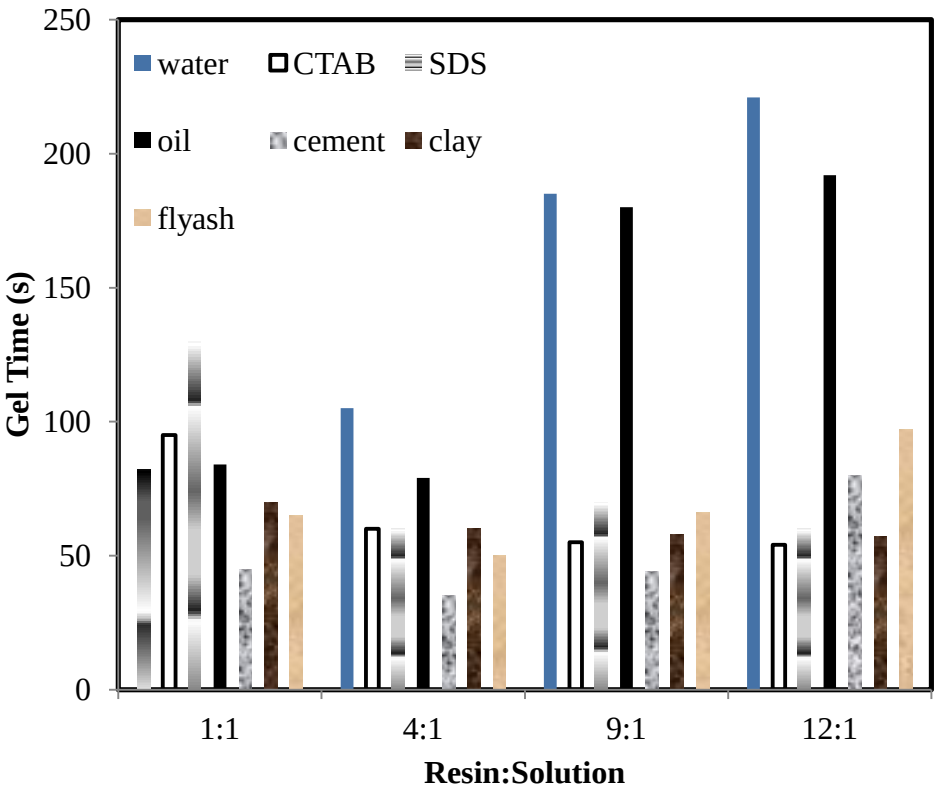

Figure 4-22: Gelling time of the Grout Mixes.

(ii) Pressure – Controlled Volume Test: Figure 4-23 shows the variation in pressure vs time of polyurethane grout. It is to be noted that addition of oil increases the pressure for both mixes (1:1 and 4:1) compared to water environment. The pressure peaks at around 10^{th} minute for all mixes and then decreases however it is to be noted that even after a period of one day, the pressure does not drop all the way to the initial pressure.

(iii) Temperature – Controlled Volume Test: Figure 4-24 shows the variation in temperature vs time of polyurethane grout. It is to be noted that rise in temperature is associated with the setting of the grout as the process of polymerization of polyurethane grout is an exothermic reaction. But from the figure it is evident that, the addition of oil is

decreased the peak setting temperature for the grout mixes (1:1 and also 4:1) compared to water environment. Upon observation, the temperature of the grout mix comes back to room temperature much sooner than the pressure drops down to initial pressure.

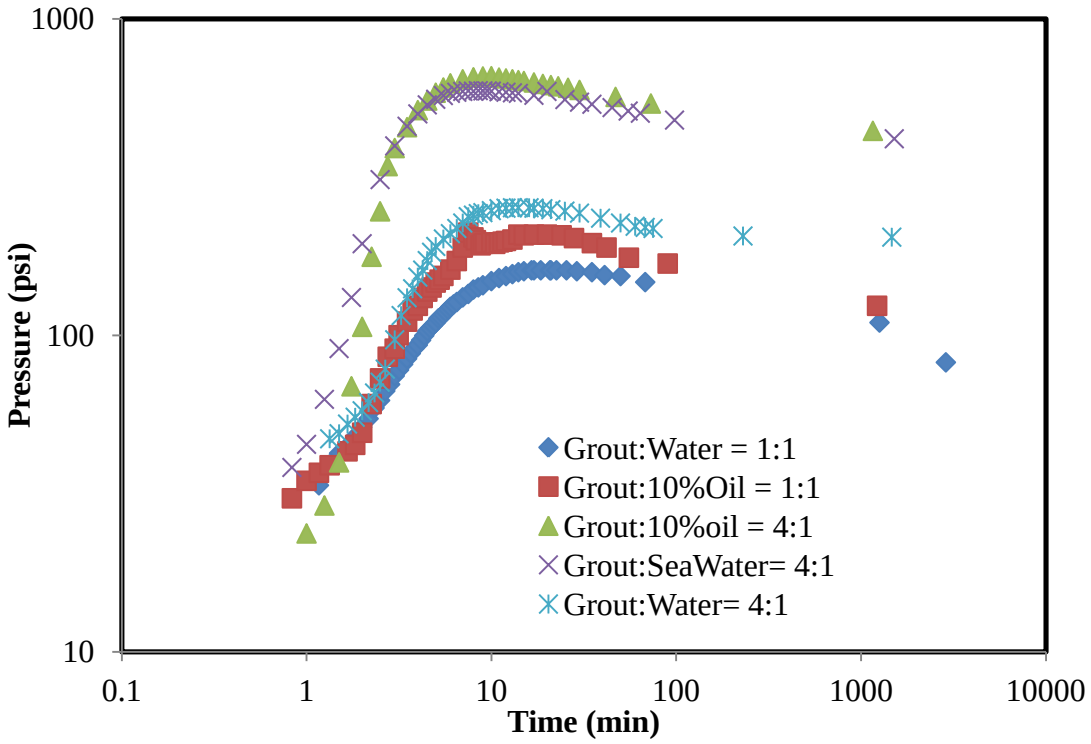

Figure 4-23: Pressure vs Time for Polyurethane Grout.

Figure 4-25 – Figure 4-29 shows the variation of pressure and temperature with respect to time for different grout mixes that were allowed to expand at a control volume of 20% of the total mold space. It is to be noted that for all the mixes of grout: solution = 4:1 the peak pressure is extremely high when compared to that for grout: solution of 1:1. It is also to be noted that the peak temperature for grout: solution mixes 4:1 was very high when compared to grout: solution of 1:1. The peak pressure and the temperature for each grout mix is given in table 4-11.

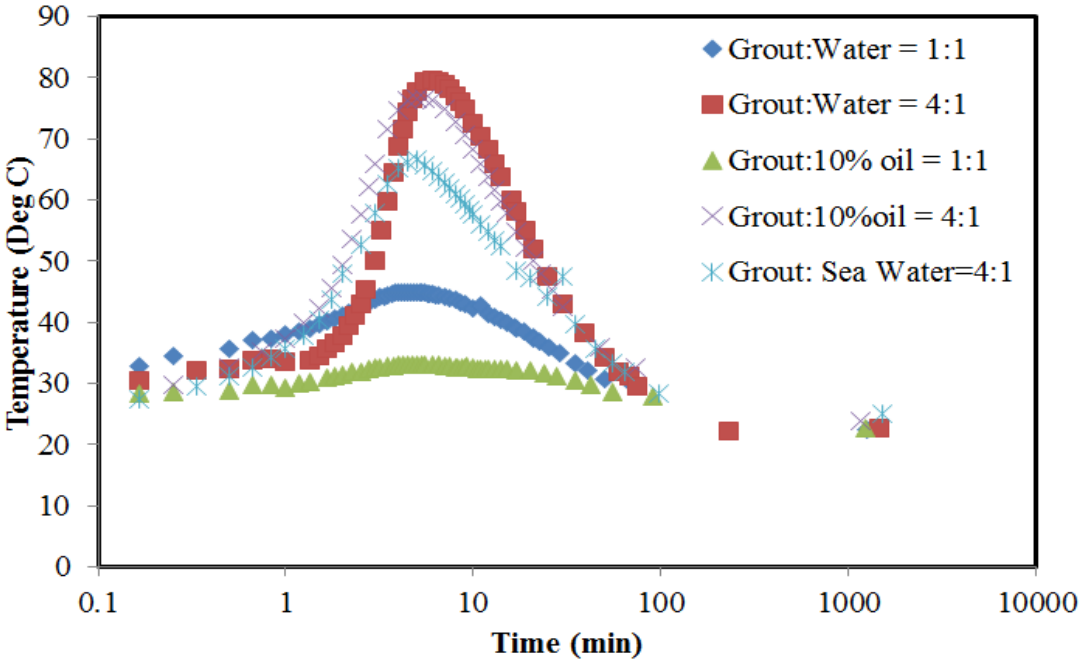

Figure 4-24: Temperature vs Time for Polyurethane Grouts.

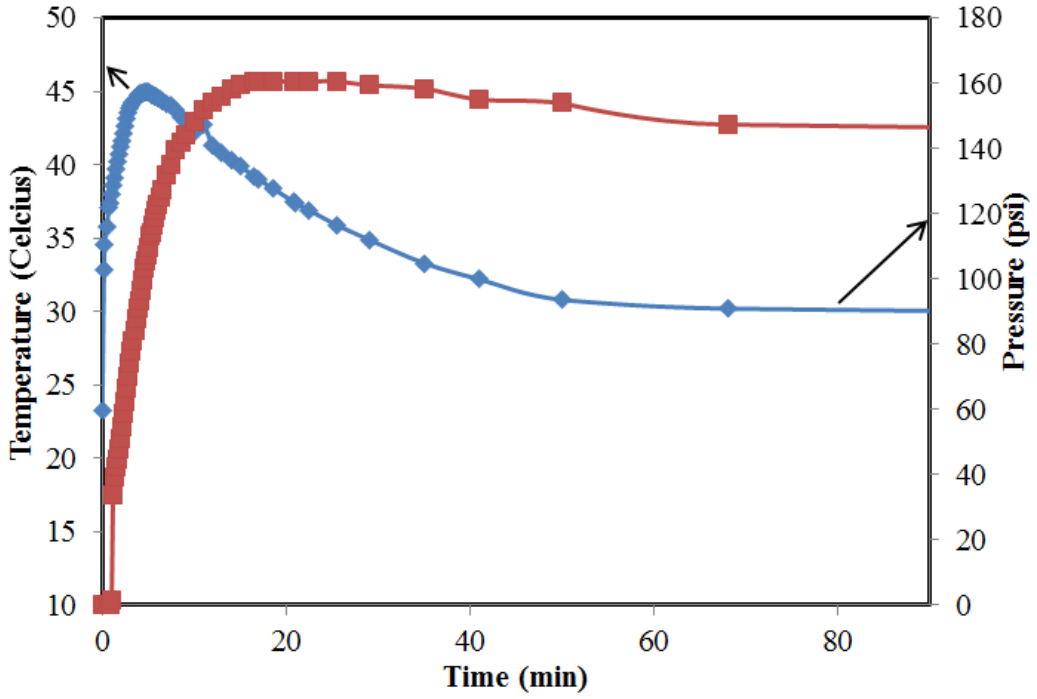

Figure 4-25: Variation of Pressure and Temperature with Time Grout:Water = 1:1.

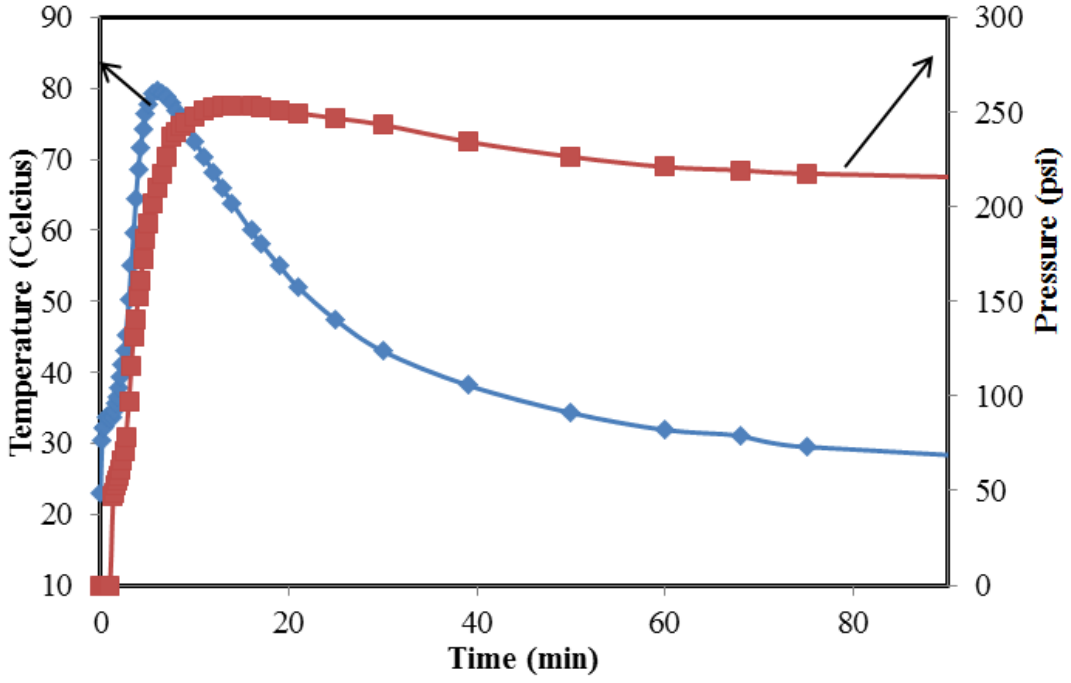

Figure 4-26: Variation of Pressure and Temperature with Time Grout:Water = 4:1.

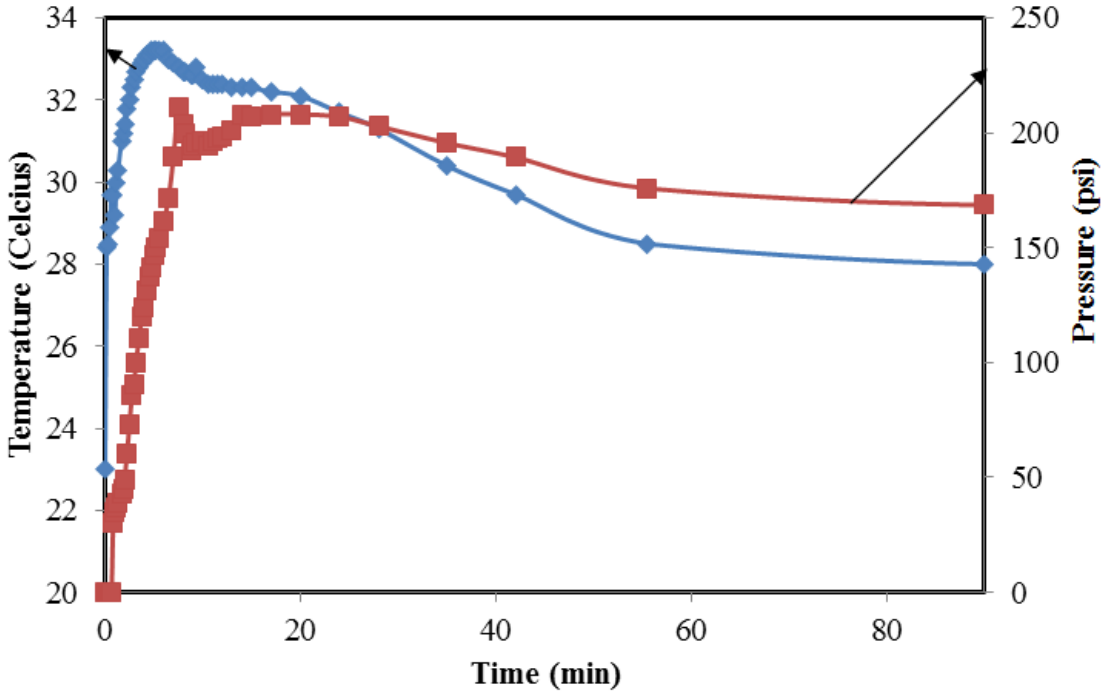

Figure 4-27: Variation of Pressure and Temperature with Time Grout:10%oil solution=1:1.

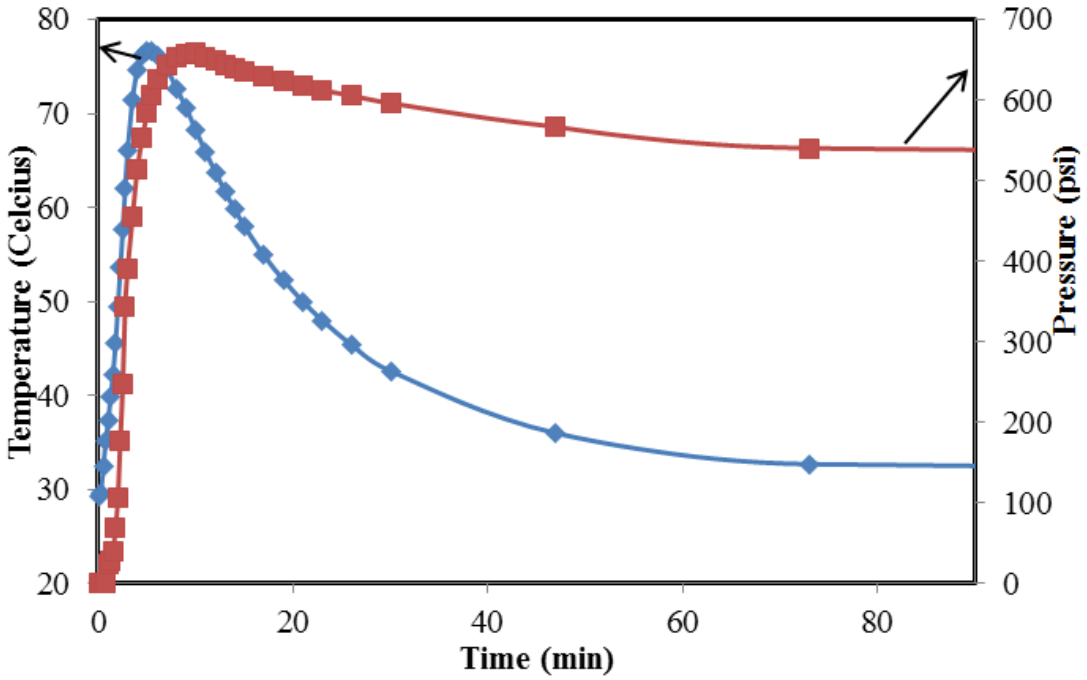

Figure 4-28: Variation of Pressure and Temperature with Time Grout:10%oil solution=4:1.

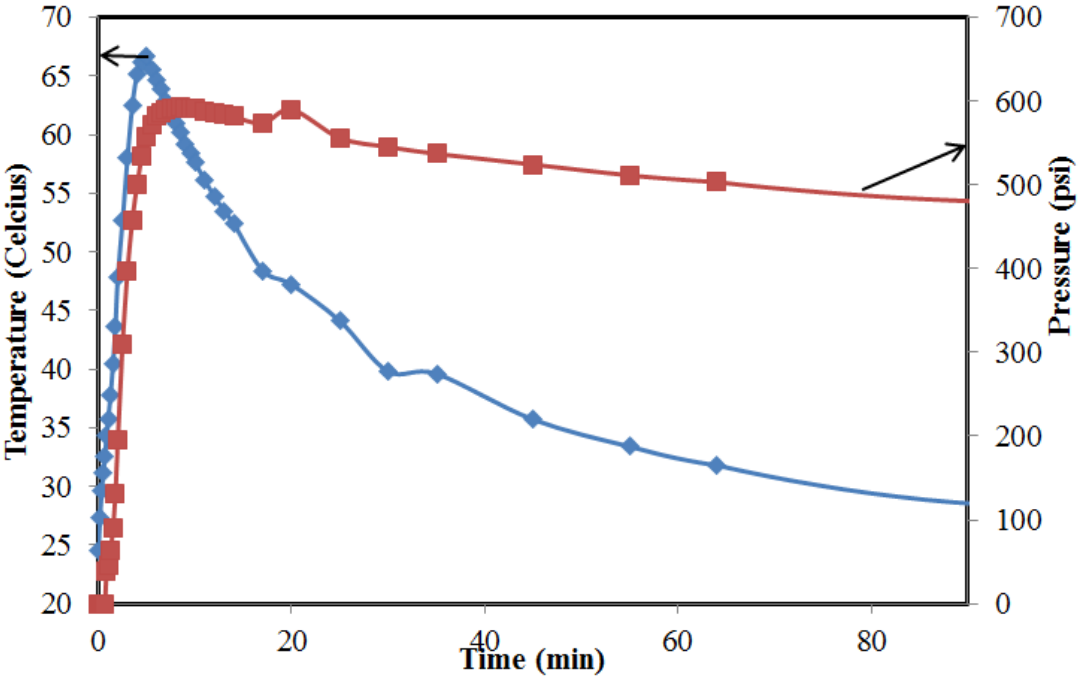

Figure 4-29: Variation of Pressure and Temperature with Time Grout: Sea Water = 4:1.

Table 4-11: Summary of Peak Pressure and Peak Temperature for Grout Mixes.

Grout	Ratio	Peak Pressure	Peak Temperature
		psi	*Celcius*
Resin:Water	1:1	161	45
Resin:Water	4:1	253	79.7
Resin:10% oil solution	1:1	211	33.2
Resin:10% oil solution	4:1	659	51.2
Resin: Sea Water	4:1	592	52.6

4.4.2 Mechanical and Durability Properties

(i) Permeability Test: Based on the test results, the permeability of the grout specimen that were prepared subjecting the grout mix to a controlled volume expansion of about 34.5% was zero under the testing conditions adopted in this study. On applying a water pressure of 14.5 psi (hydraulic gradient of 100), for a time of 4 hours and 1 day, both the samples were impervious to water. The samples prepared with grout:water ratio of 1:1 were impervious to water even after 3 months. Figure 4-30 gives the change in confined stress values with incremental strain values. It is to be noted that the peak stress of the specimen subject to permeability is way more than that of the specimen not subjected to permeability. This indicates that, even after fully set, the grout attains strength on interaction with water.

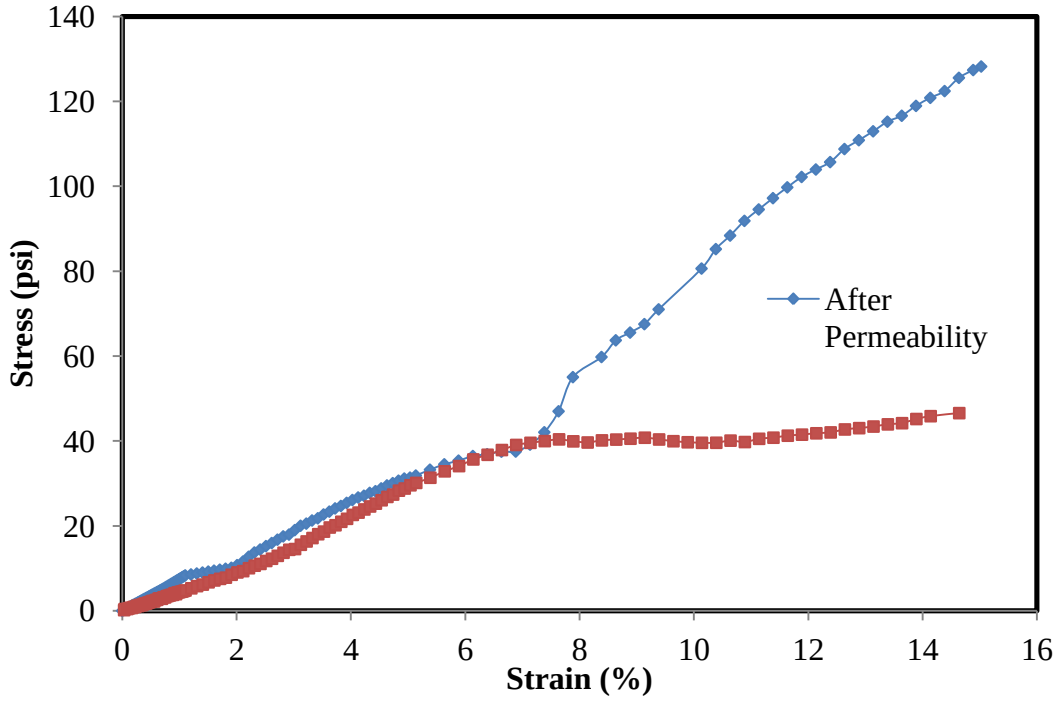

Figure 4-30: Stress-Strain Curve for Polyurethane grout (Grout:Water = 1:1).

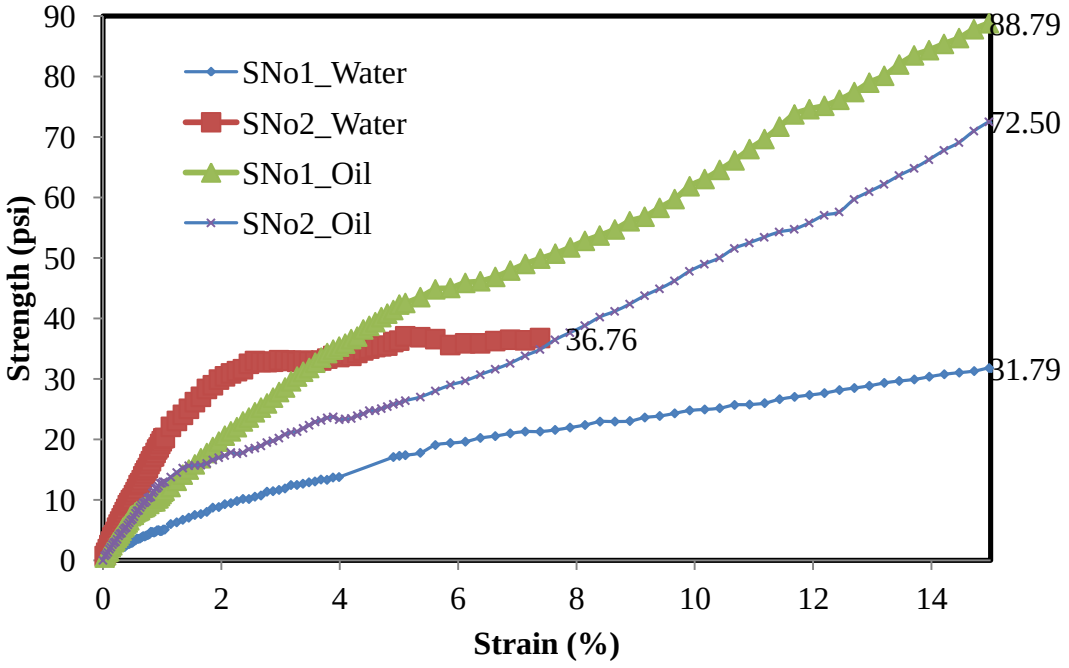

Figure 4-31: Stress-Strain Curve for Polyurethane grout (Grout:Water/Oil Soln. = 1:1).

Confined Compressive strength Test: Figure 4-31 shows the stress-strain curve of the samples prepared with water and with 10% oil solution. The oil environment, the strength of the grout increases to almost doube from about to 36 psi to over 72 psi.

Extrusion test: Figure 4-32 gives the change in Stress-strain curve of the extrusion test performed on the grout samples that were prepared with W/G = 1/1. The heights of the samples were 1 in., 2 in. and 3 in. respectively. It is to be noted that, as the height of the sample increases, the extrusion strength also increases. The peak extrusion strength increases from 13 psi for 1 in sample to 35 psi for 2 in. sample to a further increase to 48 psi for 3 in. sample. This result shows that the bonding between the grout and the PVC is good and that more the contact surface area of the grout with the pipe wall, better the extrusion strength. Figure 4-33 shows the extrusion strength comparison of 3 in. long sample prepared with water and oil solution. It is to be noted that the average extrusion strength of the grout prepared with water (W/G = 1/1) was 32 psi but the average extrusion strength test of the grout prepared under oil environment (10% oil solution) was 42 psi. This indicates that the selected grout performs well under the oil environment with respect to its bonding with the pipe wall.

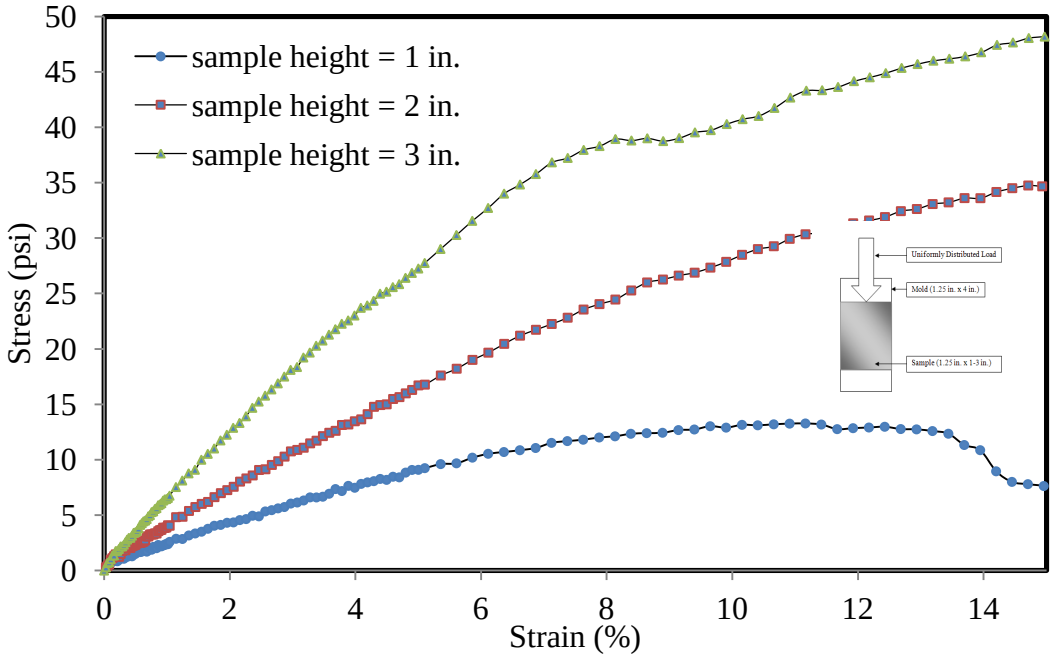

Figure 4-32: Extrusion Stress-Strain Curve for Polyurethane grout (Grout:Water = 1:1).

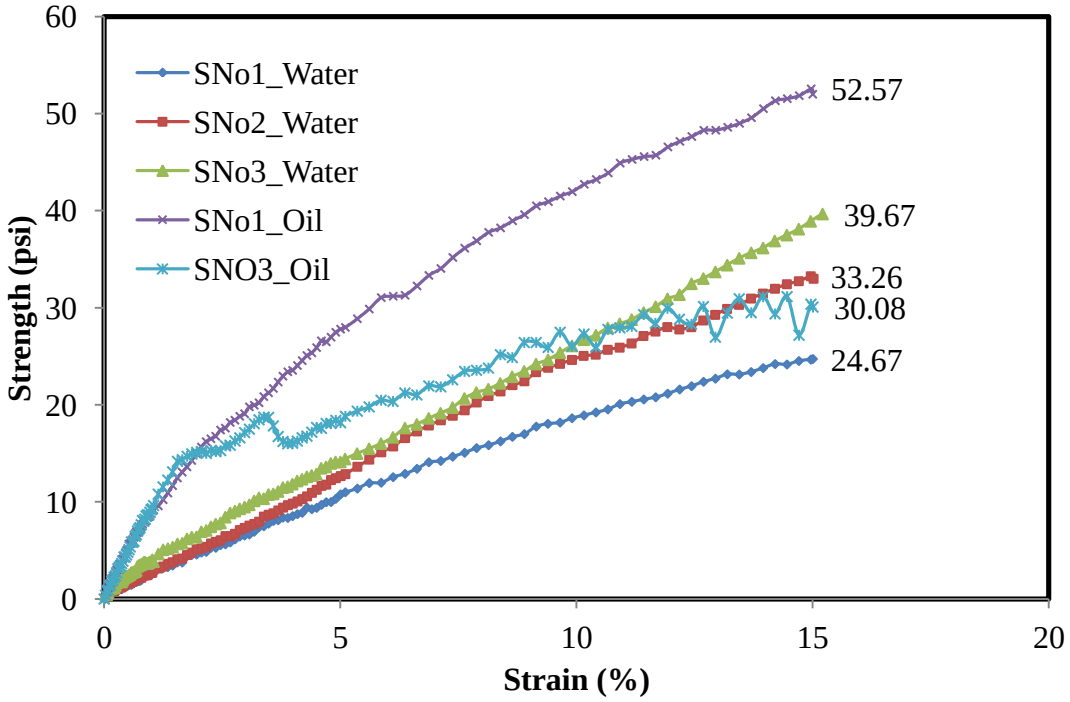

Figure 4-33: Extrusion Stress-Strain Curve for 3 in. Polyurethane grout (Grout:Water/oil soln = 1:1).

4.4.3: Large Scale Model for Decommissioning

Figure 4-34 and 4-35 shows the variation of discharge (Q) and coefficient of permeability (k) with applied pressure. It is to be noted that of all the cases, the proposed case 4 best reduces the permeability even at high hydraulic gradients of over 100. Case 2 gives high discharge values and so the k value also is very high and so, it is the least recommended of all the cases. The discharge arising in case 4 was only due to the lack of grout filling on the top of the pipe interface and the grouted sand. So, if this method could be more perfected with filling the barrier with 100% grouted sand, the leak could be minimized to a negligible value. The k value is the least in case 4 which is less than 0.1 cm/s and the maximum in case 2 varying between 0.25 to 0.6 cm/s.

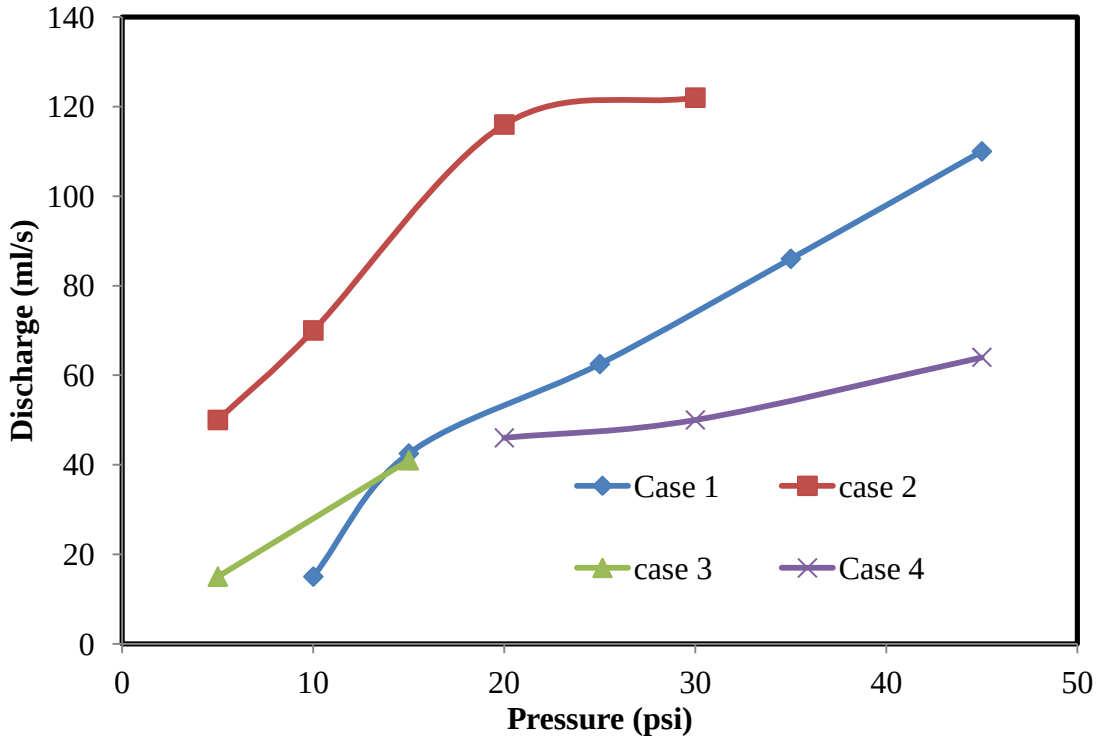

Figure 4-34: Pressure vs Discharge (Q) for all 4 case.

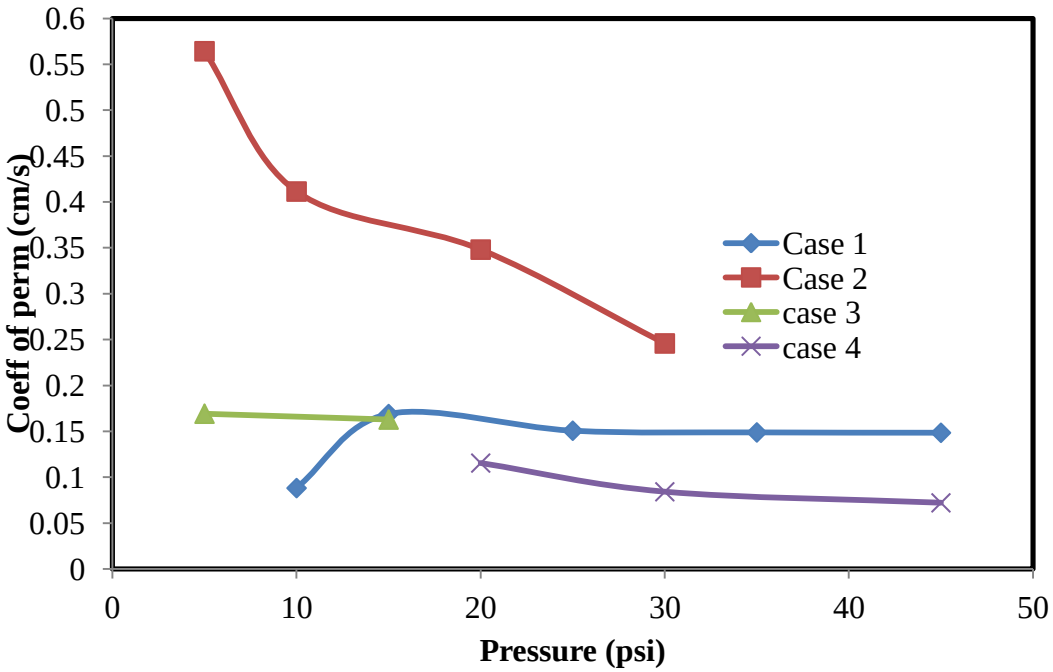

Figure 4-35: Pressure vs hydraulic conductivity (k) for all 4 cases.

4.5 Analyzing the Working Properties of Acrylic and Acrylamide Grout.

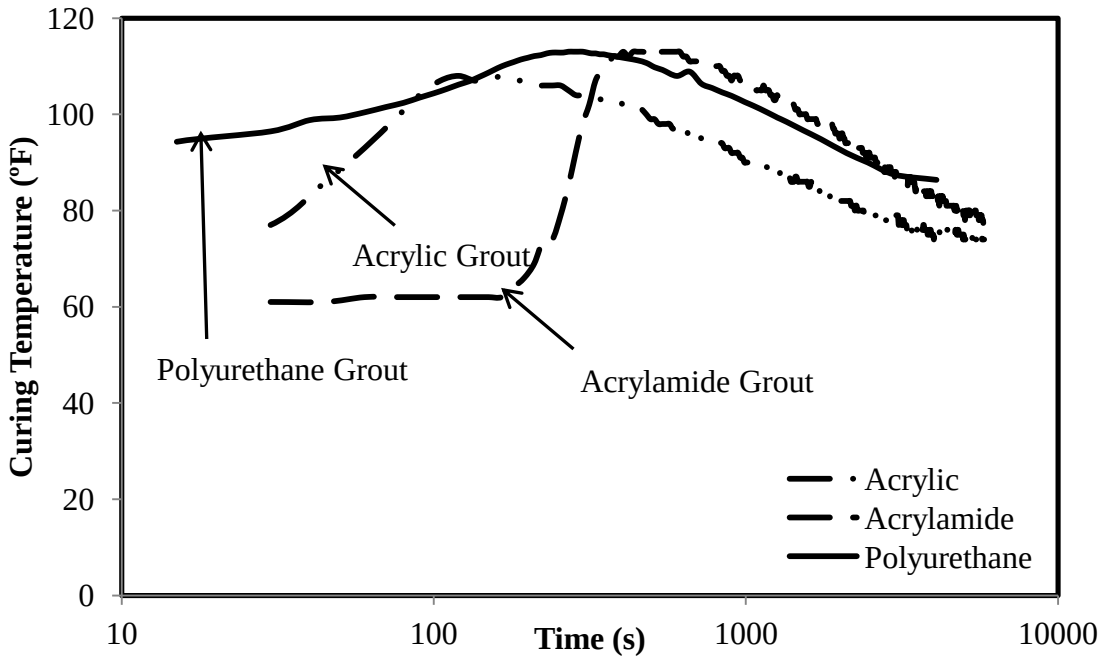

Figure 4-36: Comparison of Curing Temperatures of Acrylic, Acrylamide and Polyurethane Grout.

It is interesting to note that the trend in the rise in curing temperature is very similar for all three types of grouts. The acrylamide grout reaches a maximum curing temperature of 114ºF in 8.25 minutes even though the initial temperature of the grout was only 60ºF. The acrylic grout reached a maximum of 107ºF in 2.5 minutes and polyurethane grout reached a maximum of 113ºF in 4.5 minutes. Thus the initial temperature of the grout is a vital factor to be considered as the time at which the curing temperature of the grout reaches the peak depends on the initial temperature. The higher the initial temperature of the grout, the more quicker the curing temperature will be reached.

When analyzing the gelling time of acrylic and acrylamide grout mixes, the following equations were assumed to predict the behavior of the grout.

Addition of SDS:

$$T_g = A_0 + A_1*\%S + A_2*T, \quad (4\text{-}1)$$

Addition of CTAB:

Acrylic: $$T_g = A_0 + A_1*\%S + A_2*Tr, \quad (4\text{-}2)$$

Acrylamide: $$T_g = e^{(A1*\%S)}*A_2*Tr. \quad (4\text{-}3)$$

Where T_g, T_r and \$S are gelling time, % surfactant added and initial temperature of the grout respectively. $A_0 - A_2$ values for different surfactants and different initial temperatures are shown in Table 4-12.

It can be seen that addition of surfactant increases the gelling time of the acrylic grout which is evident from a positive value of 1.579 and 6.263 for CTAb and SDS respectively. for A2. It is also to be noted when the material is at room temperature (72

˚F), the role of surfactants dominates the gelling time of acrylic grout then the initial temperature of the grout.Addition of SDS at 40˚F to acrylamide grout reduces the gelling time of the grout which is indicated by A1 value of -33.947. addition of CTAB to acrylamide grout changes the trend of gelling time to an exponential increase rate as opposed to a linear rate of increase with the addition of SDS to the acrylamide grout (however, at 40˚F SDS addition decreases the gelling time). Figures 4-37 – 4-40 show the model vs experimental gelling times of the acrylic and acrylamide grout with the addition of surfactants.

Table 4-12: Model Parameters to Predict the Gelling Time of the Grout.

Surfactant	**Grout**	**A_0**	**A_1**	**A_2**	**Initial Temperature (Tr)**
				1/˚F	**˚F**
CTAB	Acrylic	**0.004**	**1.579**	**0.291**	72
SDS	Acrylic	**0.004**	**6.263**	**0.263**	72
CTAB	Acrylamide		**0.892**	**12.262**	40
SDS	Acrylamide	**0.382**	**-33.947**	**15.388**	40
CTAB	Acrylamide		**0.907**	**2.608**	60
SDS	Acrylamide	**0.178**	**21.316**	**3.131**	60
CTAB	Acrylamide		**0.881**	**0.508**	80
SDS	Acrylamide	**0.197**	**10.263**	**0.618**	80

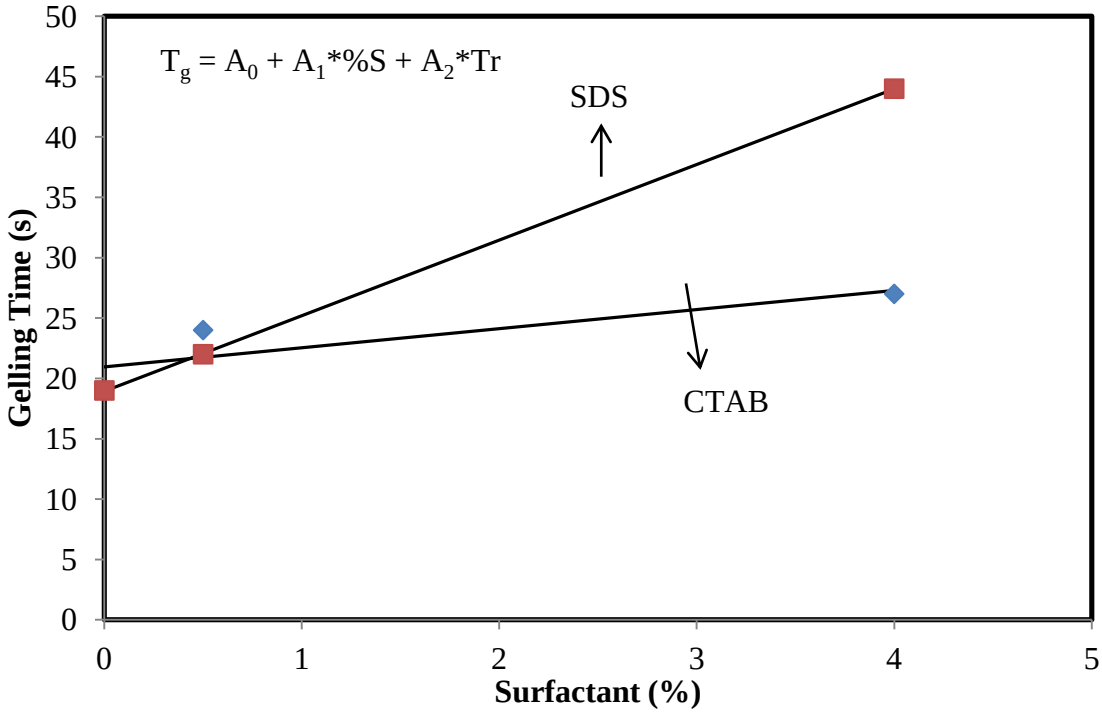

Figure 4-37: Predicted Gelling time with Experimental Gelling Time for Acrylic Grout (Tr = 72˚F).

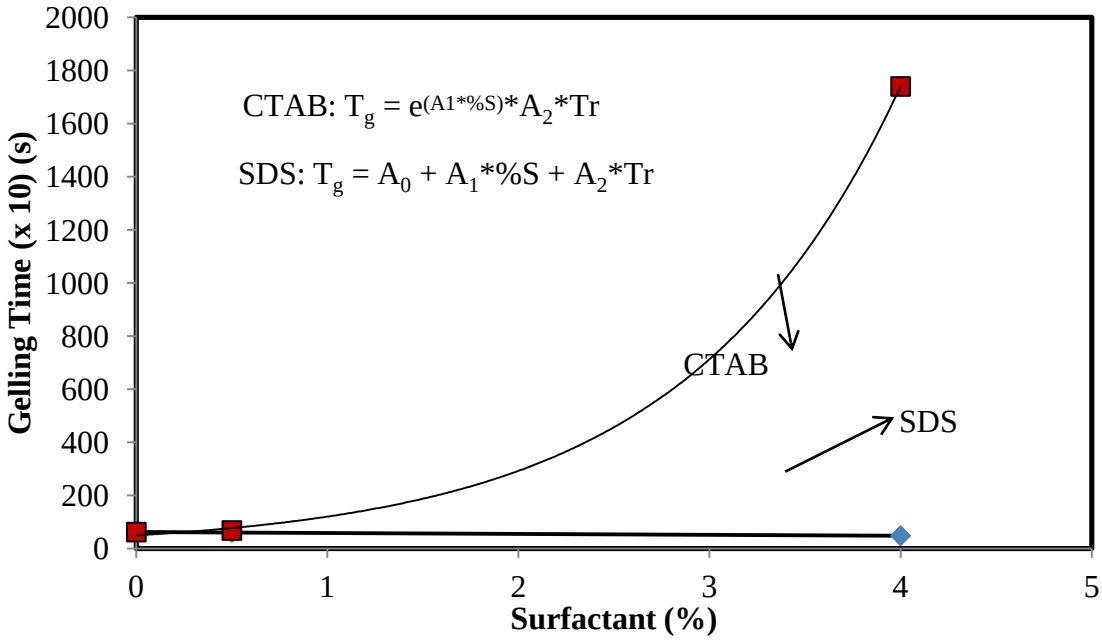

Figure 4-38: Predicted Gelling time with Experimental Gelling Time for Acrylamide Grout (Tr = 40˚F).

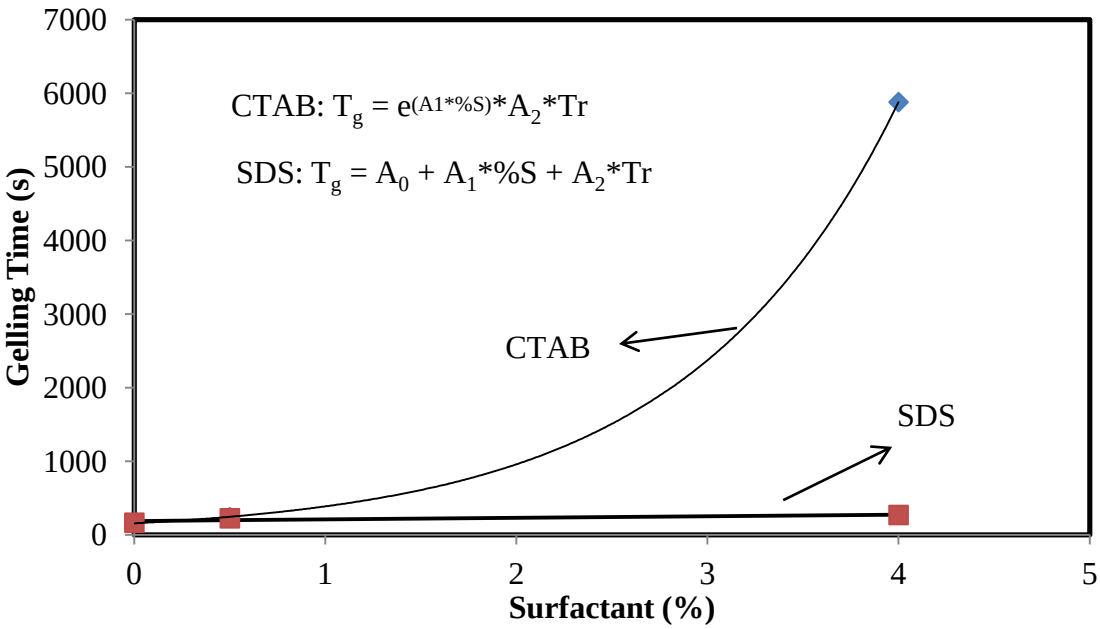

Figure 4-39: Predicted Gelling time with Experimental Gelling Time for Acrylamide Grout (Tr = 60˚F).

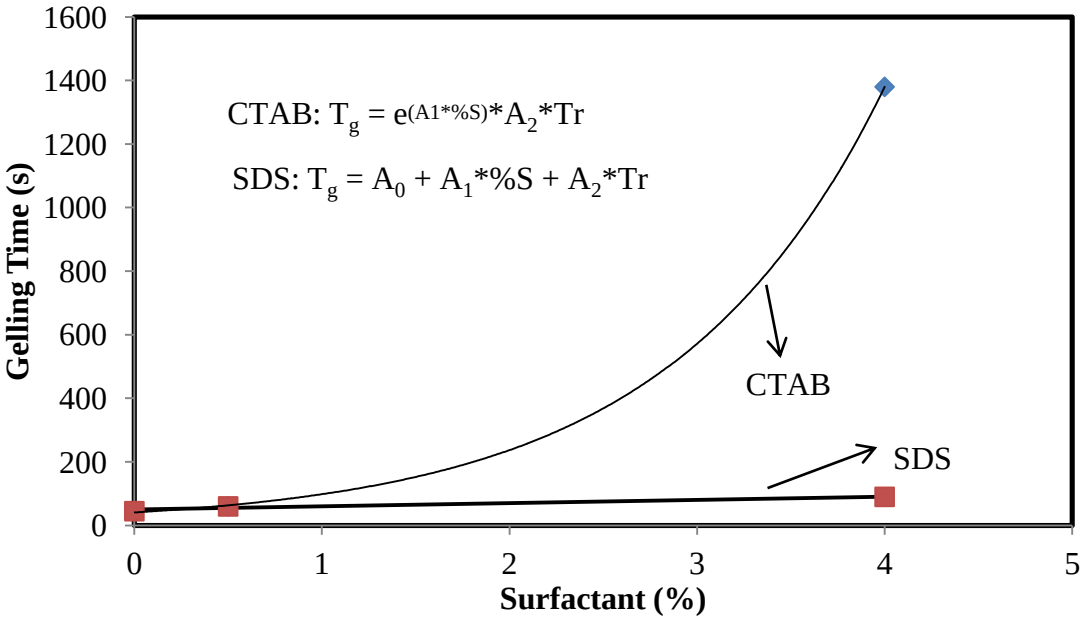

Figure 4-40: Predicted Gelling time with Experimental Gelling Time for Acrylamide Grout (Tr = 80˚F).

When analyzing the Viscosity of acrylic and acrylamide grout mixes, the following equations were assumed to predict the behavior of the grout,

$$\mu = A_0 + A_1 * T_r + A_2 * \%S. \quad (4\text{-}4)$$

Where T_g, T_r and %S are gelling time, % surfactant added and initial temperature of the grout respectively. $A_0 - A_2$ values for different surfactants are shown in Table 4-13. It is observed that in all the cases the magnitude of A1 parameter is more than that of A2 indicating the fact that the temperature of the grout has a greater influence than the quantity of surfactant added which highlights the necessity to study the gelling property of the grout at different temperatures. Variation in Modeled vs Experimental viscosity values can be seeen in Figure 4-41 and 4-42. It is also observed that one of the model parameters in negative when CTAB is added to acrylic grout indicating the fact that when CTAB is added to the acrylic grout, the viscosity decreases.

Table 4-13: Model Parameters to Predict the Viscosity of the Grout.

Grout	Surfactant	A_0	A_1	A_2
			1/˚F	
Acrylic	CTAB	0.0009	-0.2500	0.0625
Acrylamide	CTAB	0.0006	0.0963	0.0560
Acrylic	SDS	0.0010	0.1250	0.0750
Acrylamide	SDS	0.0006	0.1425	0.0559

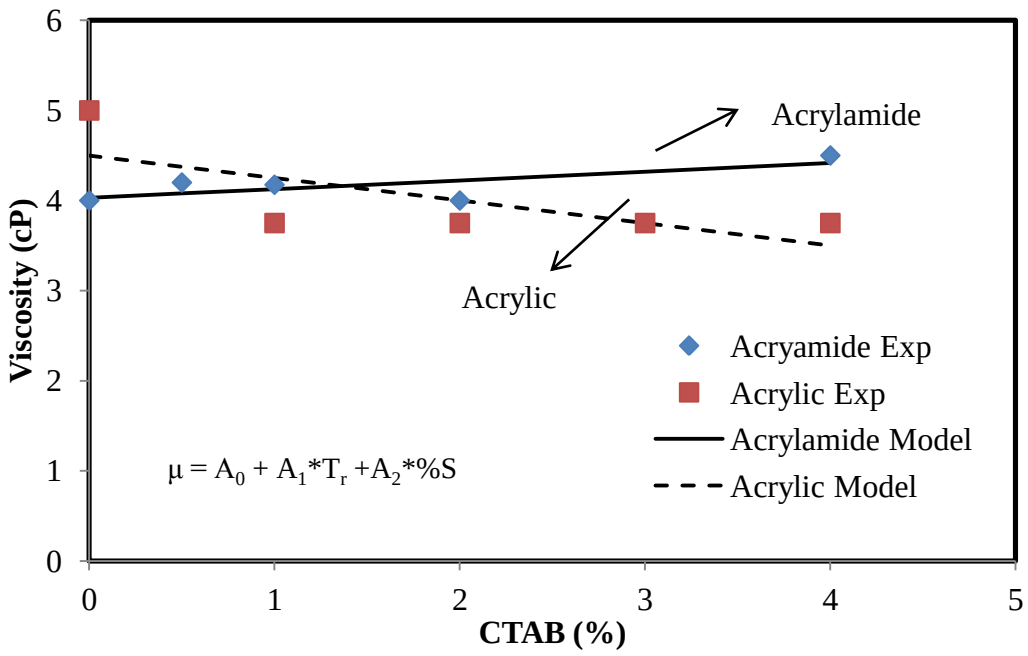

Figure 4-41: Predicted Viscosity with Experimental Viscosity With the addition of CTAB.

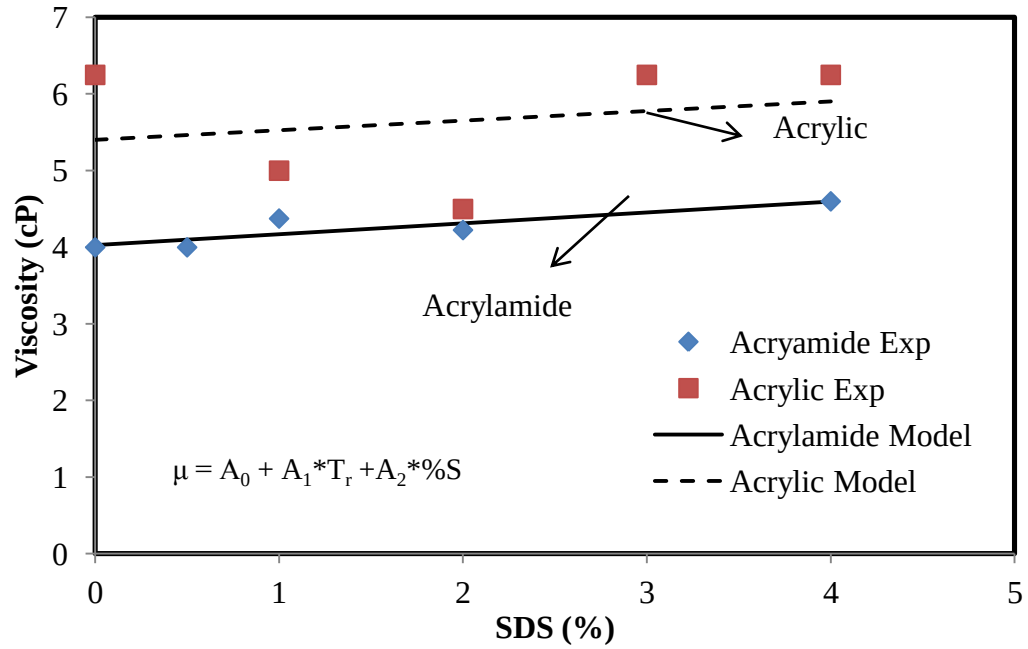

Figure 4-42: Predicted Viscosity with Experimental Viscosity with the addition of SDS.

4.6 SUMMARY

The effect of adding anionic and cationic surfactants to enhance the behavior of an acrylamide grout was investigated. Based on the Experimental study, following conclusions are advanced:

1. The addition of CTAB and SDS up to 4% by weight of the grout solution did not affect the viscosity of the grout solution.
2. The gelling time of the grout was increased with the addition of CTAB at all initial temperatures investigated in this study. Addition of SDS increased the gelling time at higher temperatures but reduced the gelling time when the test was conducted at an initial temperature of 40ºF. Addition of CTAB increased the gelling time to 17400, 5880 and 1380 seconds at initial grout temperatures of 4 F respectively. Maximum curing temperature decreased with the addition of surfactants for most cases investigated.
3. The pullout strength of the grout and grouted sand decreased with the addition of surfactants. The pullout strengths in the grouted sand were higher than the grout. The failures in the grout and grouted sand were at the interface, shear failure.
4. The addition of surfactants increased the compressive strength of the grouted sand by about 50%, but however the failure strain was increased when CTAB was added to the grout.

5. The addition of carbon fiber caused a significant change in the dielectric constant value of the chemically grouted sand. The value increased from 4 to 1199 and the effect of uniaxial loading caused a significant variation in the sample containing the carbon fibers. Grouted sand with carbon fiber exhibits both piezo-resistive as well as dielectric variation behavior on stress application.

The use of acrylic grout as an effective sealing grout for resolving lateral leaking pipeline joints was investigated by evaluating the material properties and with a large scale model:

1. The average weight change of grouted sand due to water absorption in 7 days was negligible. The shrinkage, change in length, at 90% humidity was zero. The permeability of the grouted sand was zero, impermeable under a hydraulic gradient of 100. The compressive strength increased with curing time. The average compressive strength after 28 days of curing was 19 psi;
2. The average change in weight in pH 2, 7 and 10 after six months was less than 3%.
3. The average leak rate at the 4-inch diameter lateral pipe joint was 1300 gallons/day before grouting. Model tests showed that grouting with acrylic grout was effective in eliminating the leak at the lateral joint (zero water leak at 5 psi water pressure) immediately after grouting and after two wet and dry cycles over period of one month.

Polyurethane grout as an effective foam grout for sealing of offshore pipeline for decommissioning has been studied:

1. The gelling time of the grout was not altered when subjected to oil environment. The surfactants and cement had a significant effect in altering the gelling time of the grout.

2. The pressure was more in oil environment indicating greater expansion of the grout whereas, the peak temperature was low in oil environment compared to water.

3. The polyurethane grout was totally impervious to water at a hydraulic pressure as high as 14.5 (hydraulic gradient, I = 100). The strength of the grout increased on subjecting the ample to permeability (interaction with water).

4. The coefficient of permeability was zero for a hydraulic gradient of 100 even after three months.

5. The confined compressive strength of the grout increased when it was exposed to the oil environment. The strength after permeability is more than the strength before permeability indicating the continued chemical reaction of the grout with water.

6. The polyurethane grout had good bonding with the PVC pipe which is evident from the extrusion test results. It is to be noted that the larger the contact area of the grout with the pipe wall, more the extrusion strength.

7. Four possible cases have been studied as large scale testing method for the pressure-leak rate test. It was observed that enclosing an impermeable barrier of grouted sand in-between grouted balloons gave best results however sealing and eliminating the interface leak at high pressures are still a challenge.

CHAPTER 5 MODIFIED CEMENT GROUTS

5.1 Introduction

In this chapter, the effect of selected modifiers on the cement grout working, mechanical and sensing properties were investigated. The effect of water/cement (W/C) ratio on the cement grout and the effect of metakaolin clay in modifying the flow-ability, setting time and the strength properties of the cement grout were investigated. The performance of cement and modified cement grout as a self sensor was also investigated. W/C ratio of 1 and 0.6 were chosen for this study. The testing methodologies to get the results have been discussed in chapter 3. The grout mixes used in this study are summarized in Table 5-1.

Table 5-1: Cement Grout Mixes Used.

Mix	W/C Ratio	% Clay Added	Remarks
GR-1	1:1	0%	Control Medium (1:1); no clay
GR-2	1:1	3%	Varying clay content
GR-3	1:1	5%	
GR-4	1:1	10%	Maximum clay content
GR-5	0.6:1	0%	Control Medium (0.6:1); no clay
GR-6	0.6:1	3%	Varying clay content
GR-7	0.6:1	5%	
GR-8	0.6:1	10%	Maximum clay content

When testing the sensing behavior of the grout, GR-1, GR-3 and GR-5 and GR 7 grout mixes were selected and 0.5% C-fiber was added to the mixes. It is to be noted that sand was also added at a ratio of S/C = 2 in order to test the impact of sand addition on dielectric variation.

5.2 Cement Grouts

5.2.1 Setting

The Vicat needle test results are shown in Fig 5-1. Initial and final setting times of all the grout mixes are summarized in Table 5-2. It was noted that the grout mixes with w/c ratio of 1 had longer initial and final setting times than the grout mixes with w/c ratio of 0.6. From the setting times of GR-5, GR-6, GR-7 and GR-8 it can be observed that as the clay content increased in the grout mix with w/c ratio of 0.6, the setting time decreased. Addition of clay not only affected, generally reduced the initial and final setting time but also affected the time difference in setting.

Table 5-2: Setting Time of Grout Mixes.

Grout mix	Initial setting time (min)	Final setting time (min)	Difference (min)
GR-1	598	978	380
GR-2	646	1000	354
GR-3	611	833	222
GR-4	580	885	305
GR-5	500	586	86
GR-6	407	520	113
GR-7	360	517	157
GR-8	280	485	205

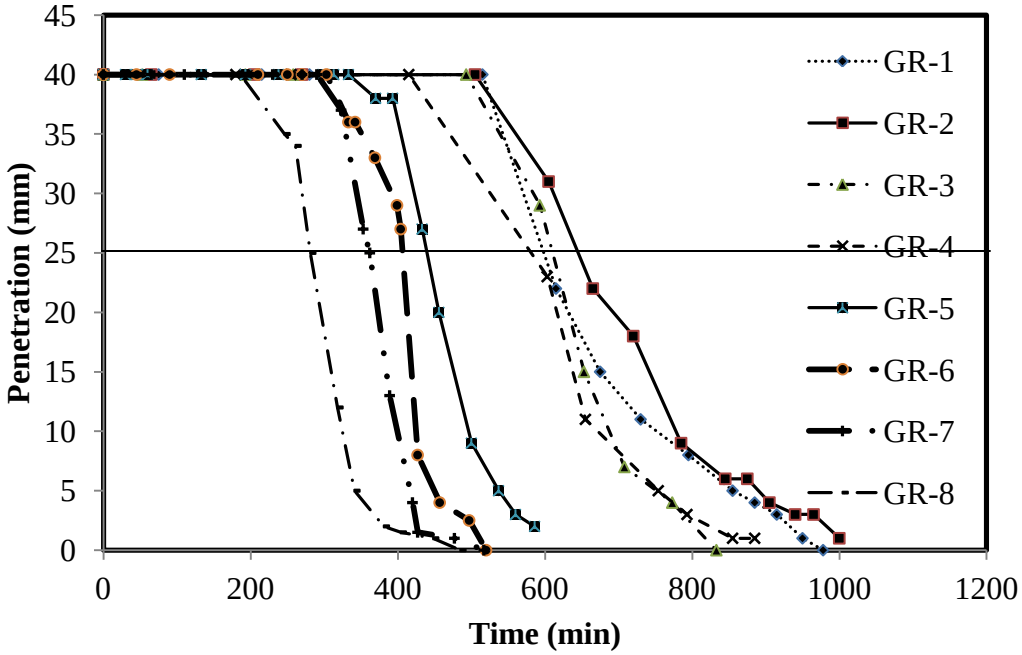

Fig 5-1: Setting Time Curves of the Grout Mix.

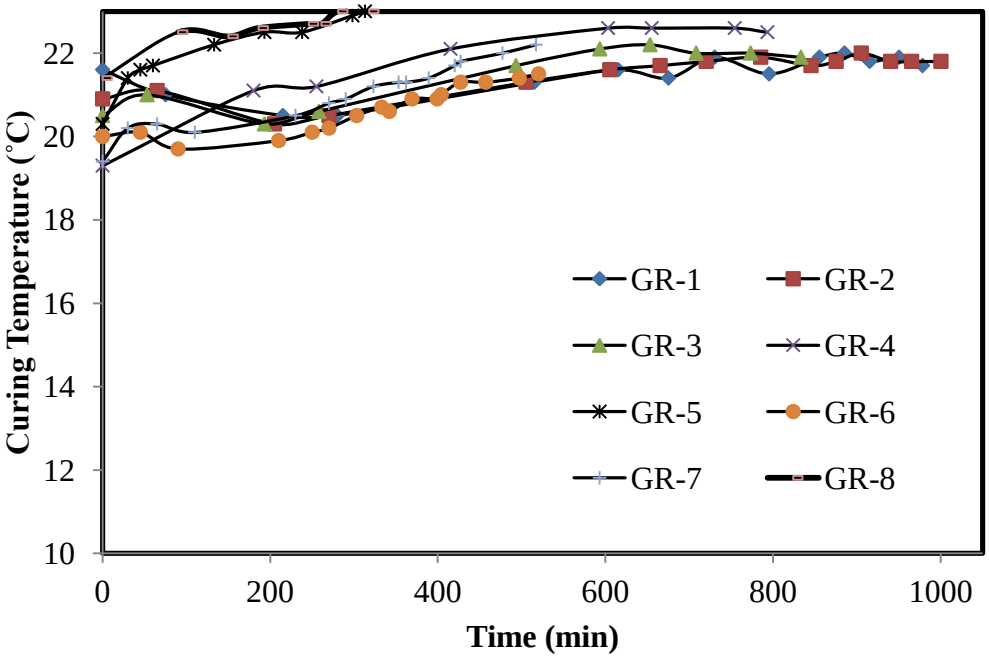

Fig 5-2: Curing Temperature Curve of the grout mixes.

Temperature versus setting time: Variation of curing temperature with time for various grout mixes are shown in Fig 5-2. The maximum change in temperature during the process of curing varied from 1˚C to 3.3˚C. The maximum difference was observed during the setting of GR-5 and GR-8 grout mixes which was 3.3˚C and the minimum change of 1.1˚C was observed in GR-2 grout.

5.2.2 Flowability

(i) Bleeding Capacity: Bleeding capacity of the grout indicates the flowability of the grout. Flowability is an important property especially for a suspension grout like cementitious grout as the suspension grouts are supposed to be viscous than the solution grouts. It was observed that addition of clay reduced the bleeding in the cement grout for w/c ratios investigated. It can be seen in Fig 5-3a that GR-1 had a bleeding as high as 20% which was reduced to 11%, 5% and 1% with the addition of 3%, 5% and 10% of the clay (GR-2, GR-3 and GR-4 mixes) respectively. Reducing the w/c ratio from 1 to 0.6 reduced the bleeding from 20% to 3%. Addition of 3%, 5% and 10% clay further reduced the bleeding in the grout. GR-5 had a bleeding capacity of 3% but with the addition of 3% clay (GR-6), the bleeding was reduced to 0.5% which further was reduced to 0.2% and 0% with the addition of 5% and 10% clay (GR-7 and GR-8) respectively.

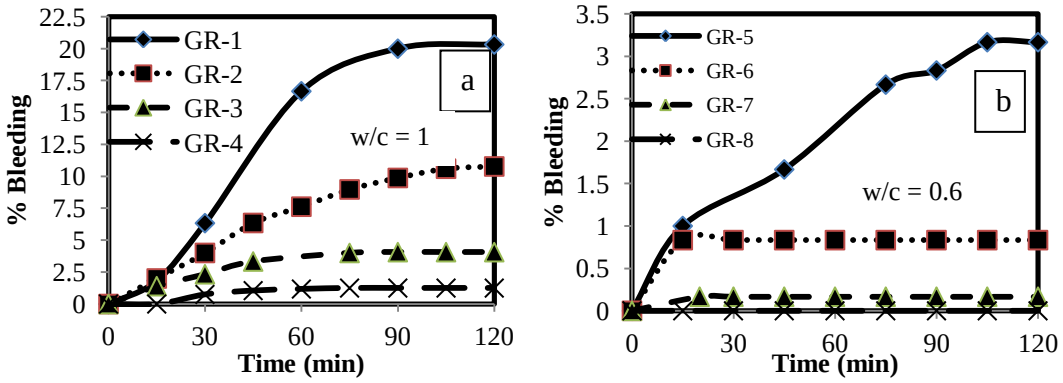

Fig 5-3: Variation of Bleeding Capacity of Cement-clay grout mixes with a) w/c ratio of 1 b) w/c ratio 0.6.

(ii) Flowability: Variation in the flowability with the addition of clay is shown in Fig 5.4. It was observed that the grout mixes with w/c ratio of 1 have a very low time of efflux than the grout mixes with w/c ratio of 0.6. The time of efflux increased with addition of the amount of clay in the grout mixes with w/c ratio of 0.6. However, there was no significant change in the case of mixes with w/c ratio of 1. GR-1 and GR-4 had a time of efflux of 35 seconds and GR-2 had a time of efflux of 36 seconds. GR-3 had a slightly higher value of 43 seconds. Cement grout with w/c ratio of 0.6 and with no clay content (GR-5) had a time of efflux of 80 seconds which was more than double the time of GR-1. GR-7 which had a w/c ratio of 0.6 had a very high time of efflux value of 253 seconds with 5% clay. GR-6 with 3% clay content had a time of efflux of 130 seconds.

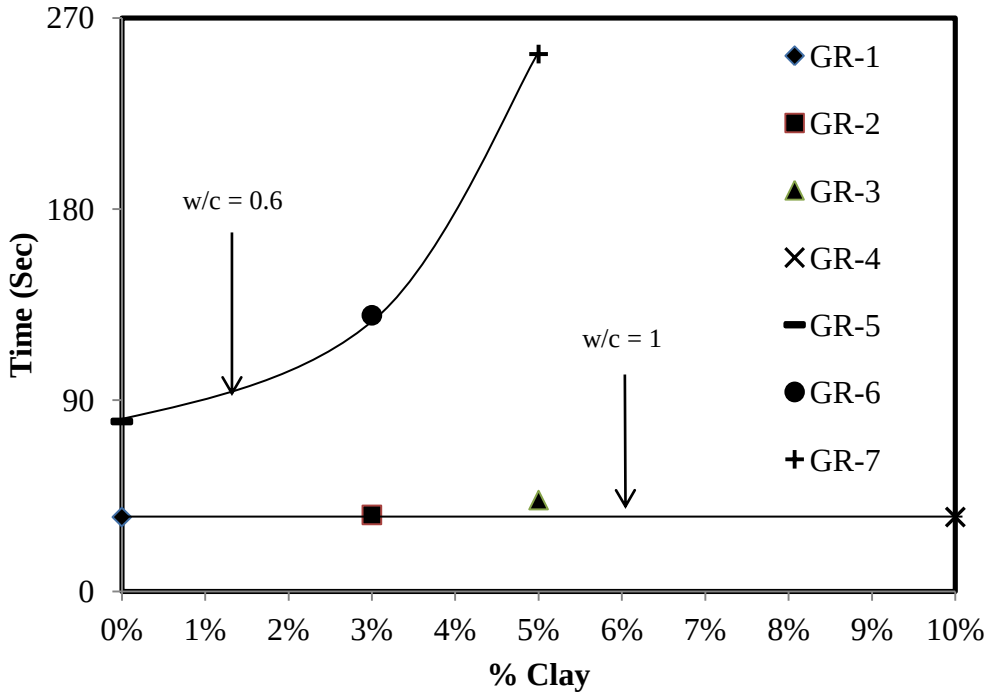

Fig 5-4: Effect of Clay Content on Time of Efflux of the cement grout.

5.2.3 Mechanical Behavior

(i) Pullout strength: The variation of pull-out strength after 14 days of curing for various grout mixes are shown in Figure 5-5. The dominant failure was interface shear. For the grout with w/c ratio of 1, the pullout strength reduced with the addition of clay. The pull-out strength was 2.53 and 2.54 MPa for both grout mixes GR-1 and GR-5 respectively. The pull-out strength was not influenced by the clay content in the grout mixes with w/c ratio of 0.6. The average pull-out strength for cement grouts with w/c ratio of 1 (GR-1 to GR-4) varied from 0.9 MPa to 2.53 MPa.

(ii) Compressive Strength The variation of Compressive strength of the cement grout with the addition of clay is shown in Fig 5-6. It was observed that up to an addition

of 5% clay, the compressive strength of GR-1 increased to 6.9 MPa and then became stable on further addition of clay. However, the strength of GR-5 which was 8.8 MPa increased with the addition of 3% clay to 12.2 MPa and on further addition of clay the strength was reduced to the 8.2 MPa. The strength of grout mixes with w/c ratio of 0.6 had a higher strength than those with w/c ratio of 1.

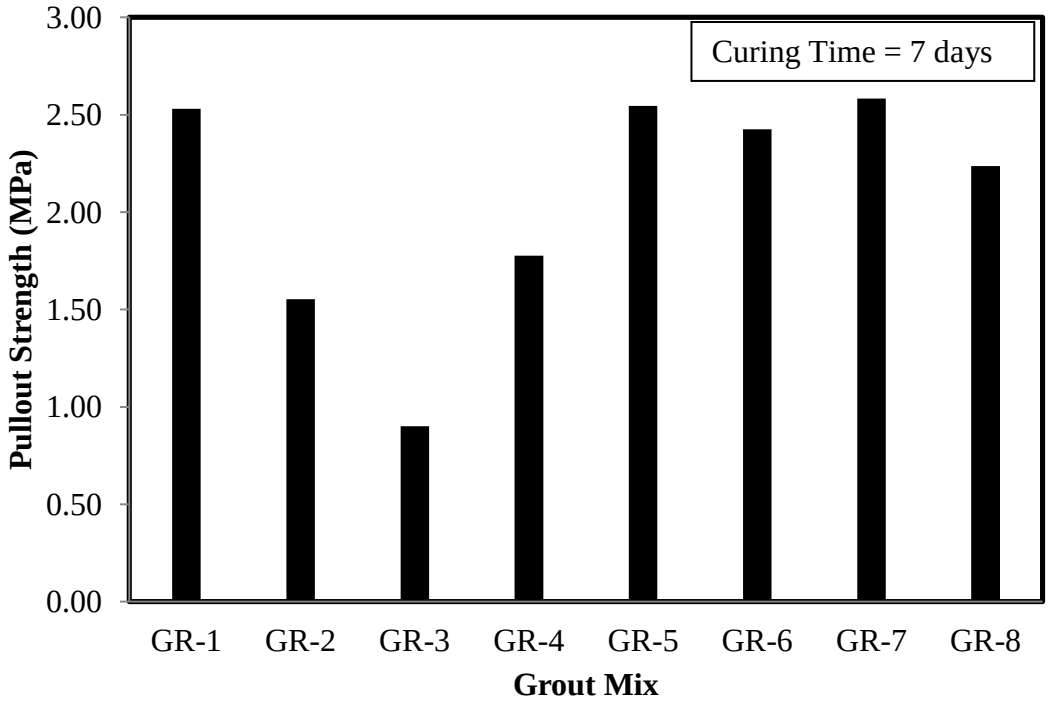

Fig 5-5: Variation of Pull-out strength of the cement-clay grout mixes.

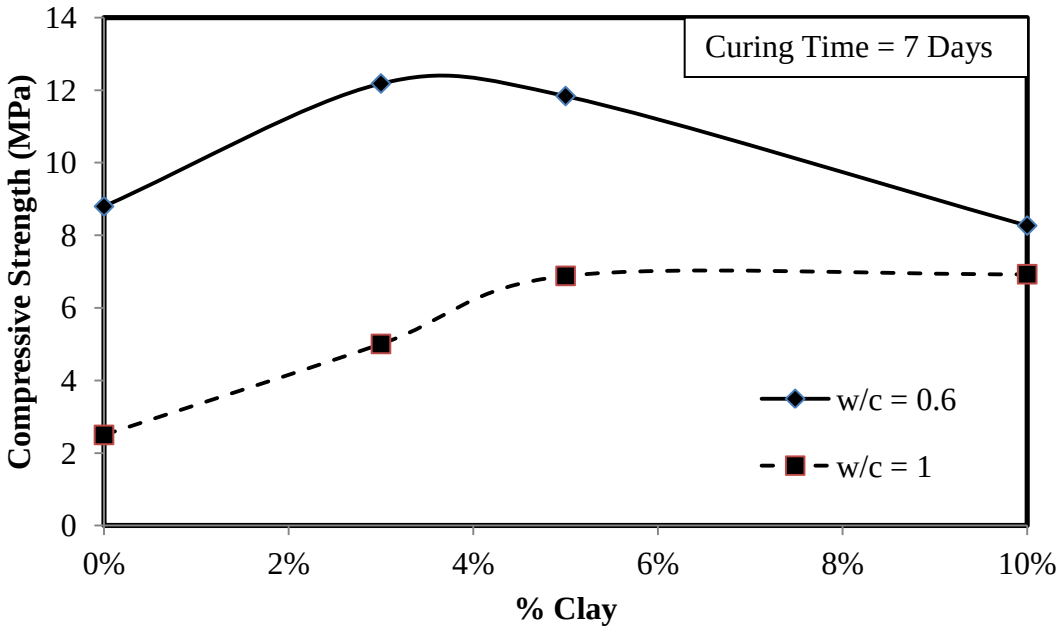

Fig 5-6: Variation of Compressive Strength of the Cement-Clay Grout Mixes.

5.2.4 Application as a Self Sensor

(i) During Curing: The variation of electrical resistivity with time is shown in Figure 5-7. For all the mixes studied the resistivity peaked before the initial setting time. Addition of clay increases the electrical resistivity and the increase was influences by w/c ratio. The resistivity values of GR-3 and GR-4 were around 11 kilo ohm-m and 20-23 kilo ohm-m respectively consistently which made it hard to identify the initial setting time. Hence resistivity measurement was not a good indicator for the initial setting time of the cement grout with w/c ratio of 0.6 and 1.

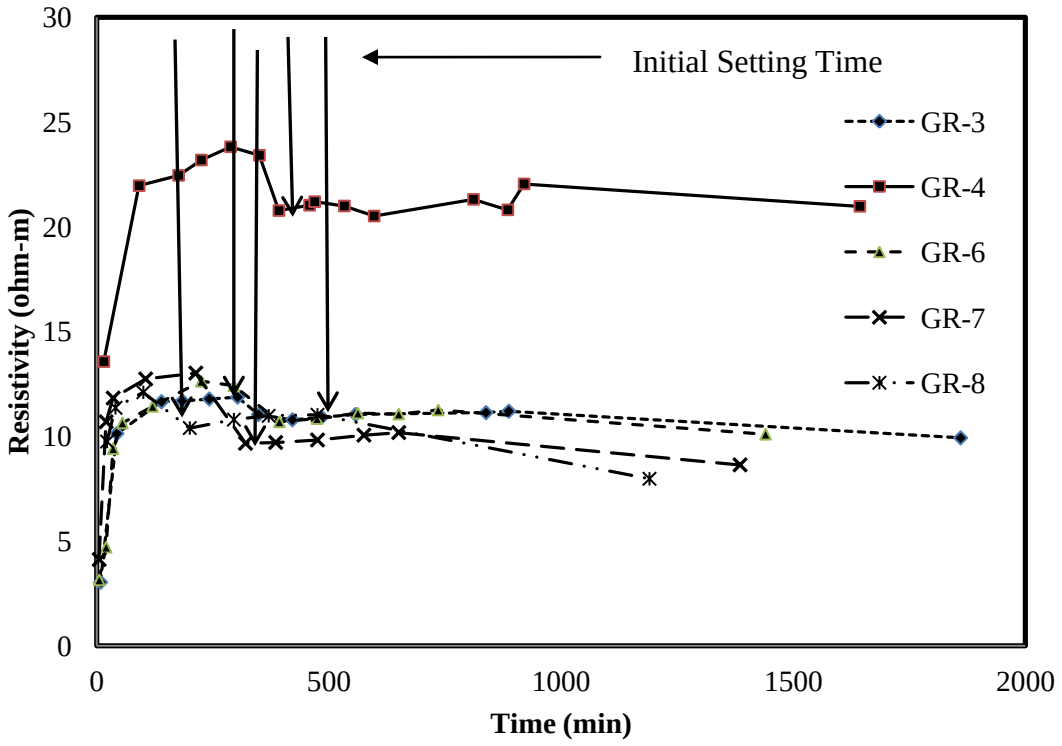

Fig 5-7: Variation of Electrical Resistivity of the Cement-Clay Grouts.

(ii) After Curing:

(a) Effect of Meta-Kaolin: the Er (Dielectric constant) values were measured for the circular disc shaped samples kept under the parallel plate capacitor setup. The sample height varied from 0.4 to 0.8 in. and the diameters of the samples were 6 in. Figure 5-8 shows the effect of metakaolin addition on cement grout.

It is to be noted that the addition of metakaolin clay increases the Er irrespective of the W/C ratio in the grout mix. For the cement grout of W/C 0.6 the mean Er increased by 6.4% from 21.9 to 23.3 on adding 5% clay. This increase was even more significant in the case of cement grout with W/C = 1. The Er value increased by about 18% from 38.2 to 45 when the W/C was 1. It is to be noted that, the density of the sample is related to the

dielectric constant of the sample because, as the density of the sample increases, the void content in the sample decreases which results in the increase in the dielectric constant of the sample. It is to be noted that the mean density of the cement grout without clay at W/C of 1 and 0.6 were, 76.2 and 92.2 pcf respectively. The mean density of the clay modified cement grout was at W/C 1 and 0.6 were 79.6 and 95.5 respectively. Thus, it can be concluded that, increase of mean density by 4.5% on adding clay to cement grout with W/C =1 increased Er by 18%. Also, increase in the mean density of the cement grout with W/C 0.6 on adding clay by 5%, increased the Er value by 6.4%.

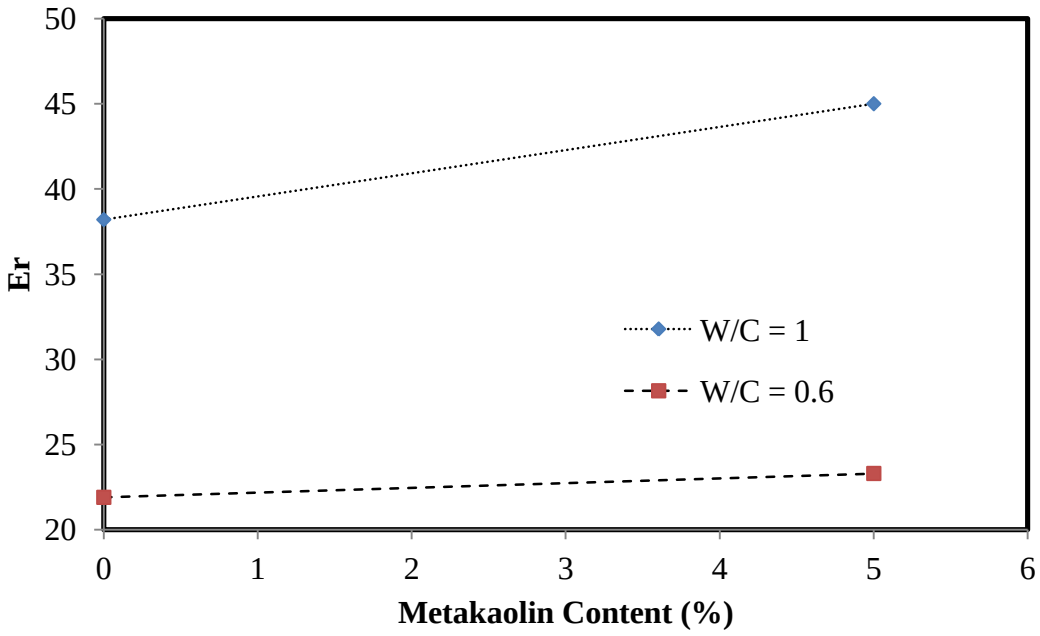

Figure 5-8: Effect of Metakaolin addition on Er of Cement Grout.

(b) Effect of C-Fiber: Figure 5-9 shows the effect of addition of 0.5% C-fiber on the cement grout and also clay modified cement grout at W/C ratio of 0.6 and 1. It can be observed that, the mean Er of the cement grout with W/C = 1 decreases by only 2.2 which is a 5.7% decrease when compared to a 24% decrease in the case of cement grout

modified with 5% clay. A similar effect can be observed when the W/C was 0.6 where the change in the mean Er value was close to 0% when no clay was added and on adding 0.5% carbon fiber. The Er value however, changed from 23.3 to 16.2 which is a 28.7% decrease. The density changes noted in the cement grouts with and without the addition of 0.5% carbon fiber in W/C = 1 mixes were 77.7 pcf and 76.24 pcf respectively, which accounts to only 1.9% change. Thus it is to be noted that, the addition of clay nullifies the effect of addition of carbon fiber on Er and hence the changes in the Er values can be attributed to the density and the void content parameters.

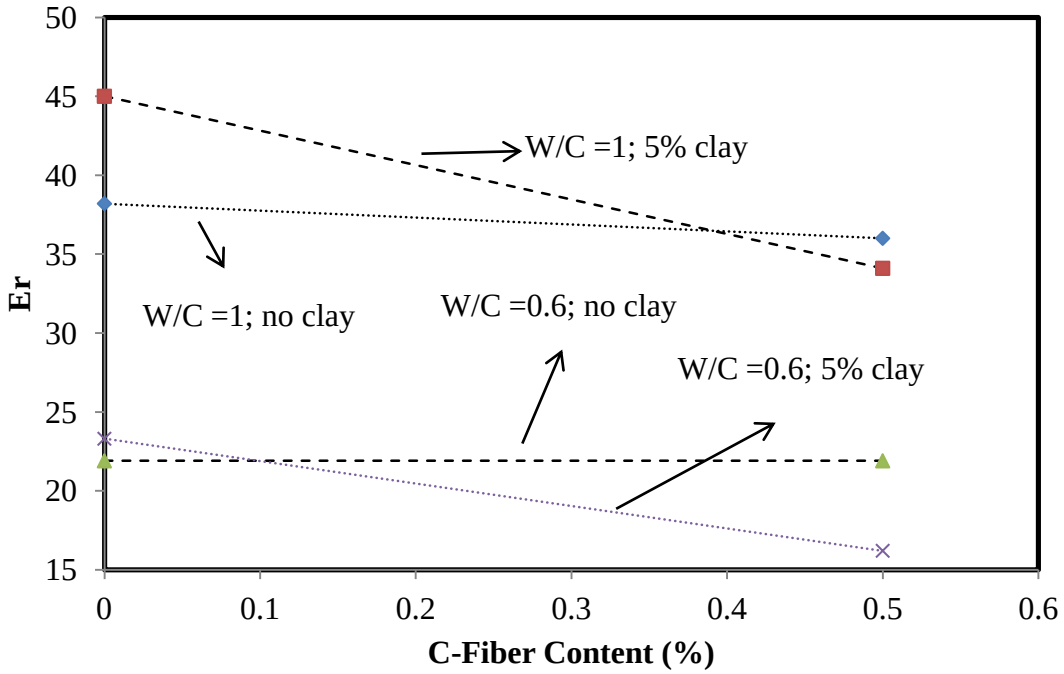

Figure 5-9: Effect of C-Fiber addition on Er of Cement Grout.

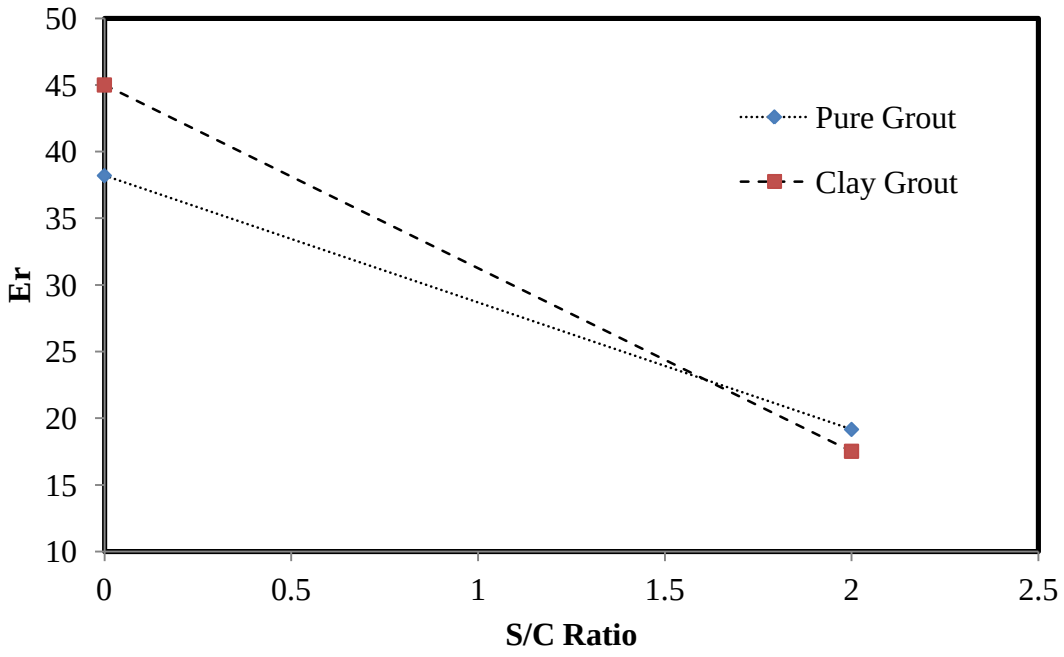

Figure 5-10: Effect of Sand addition on Er of Cement Grout (W/C = 1).

(c) Effect of Sand (S): Figure 5-10 shows the effect of sand addition on Er of the cement grout. The sand used in the study was the blasting sand 3-4 mix whose properties are detailed in chapter 3. Similar effect on Er values of the grout mix was observed on adding sand. The sand was added to the grout at S/C = 2. It is to be noted that on adding sand, the Er values of cement grout and also modified cement grout decreases significantly, at W/C = 1 because of the density of the cement grout and clay modified cement grout increased by 36% and 29.4% respectively on adding sand.

(d) Loading-Unloading Cycle: A dielectric material sensitive to the application of load would behave in one of the following ways.

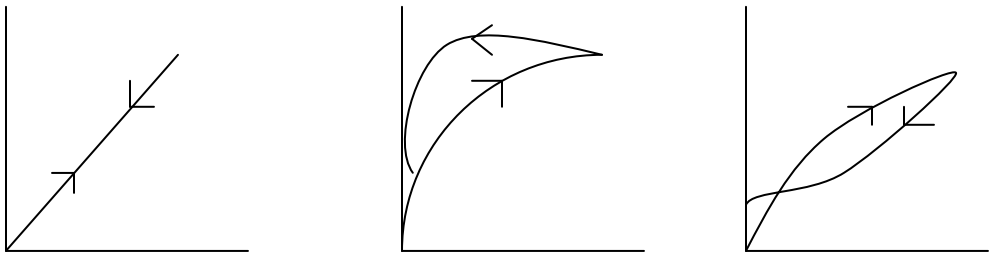

Figure 5-11: Typical trends in variation of dielectric constant on stress application.

Figure 5-12, 5-13, 5-14, 5-15, 5-16 and 5-17 show the change in the dielectric constant of the grout samples on loading and unloading. It also shows the change in resistance values on stress application.

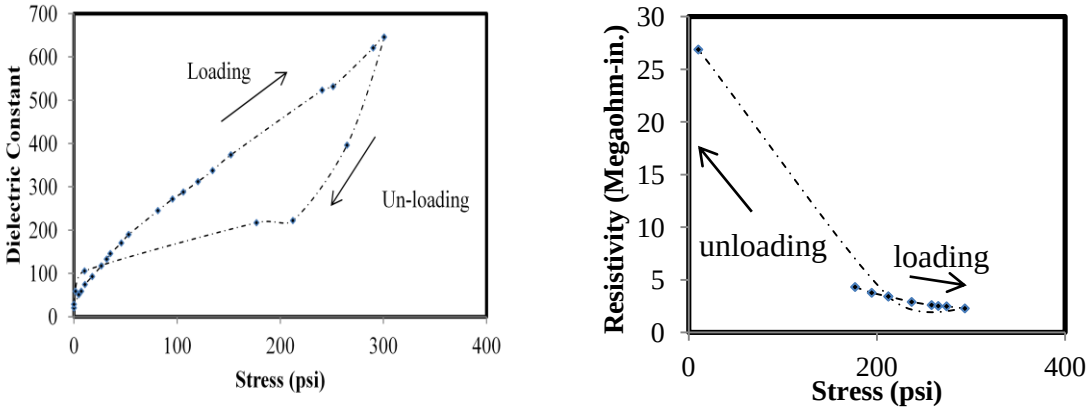

Figure 5-12: Er and Resistivity variation on loading and un-loading cycle (W/C = 0.6, No clay, No C-Fiber).

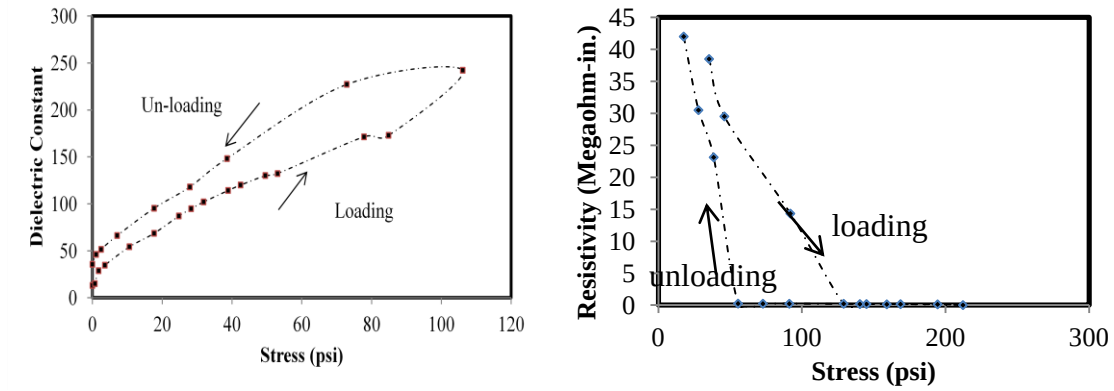

Figure 5-13: Er and Resistivity variation on loading and un-loading cycle (W/C = 0.6, No clay, 0.5% C-Fiber).

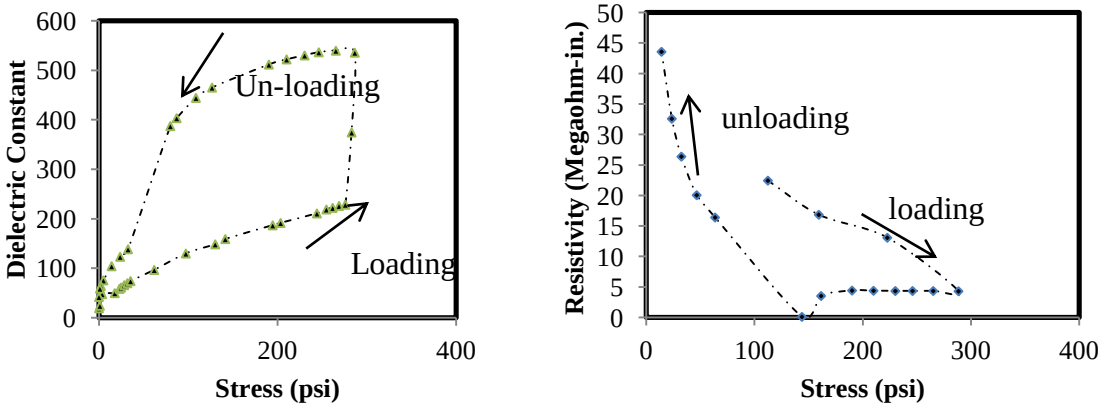

Figure 5-14: Er and Resistivity variation on loading and un-loading cycle (W/C = 0.6, 5% clay, 0.5% C-Fiber).

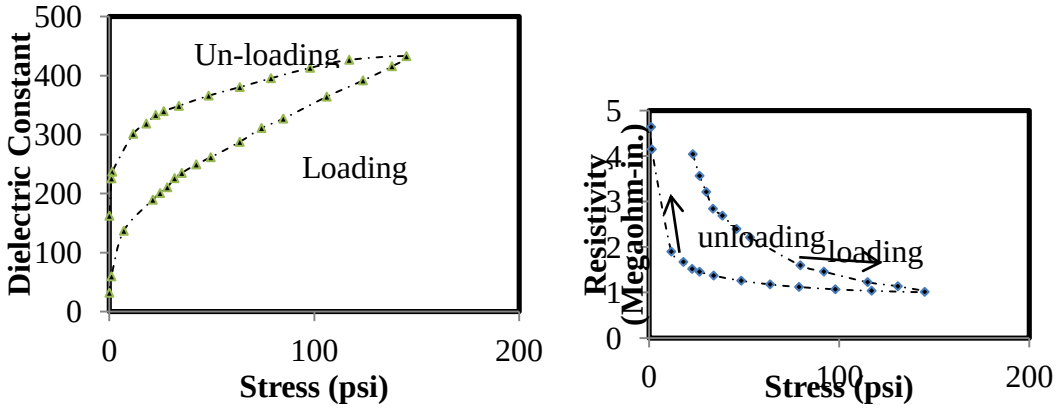

Figure 5-15: Er and Resistivity variation on loading and un-loading cycle (W/C = 0.6, 5% clay, no C-Fiber).

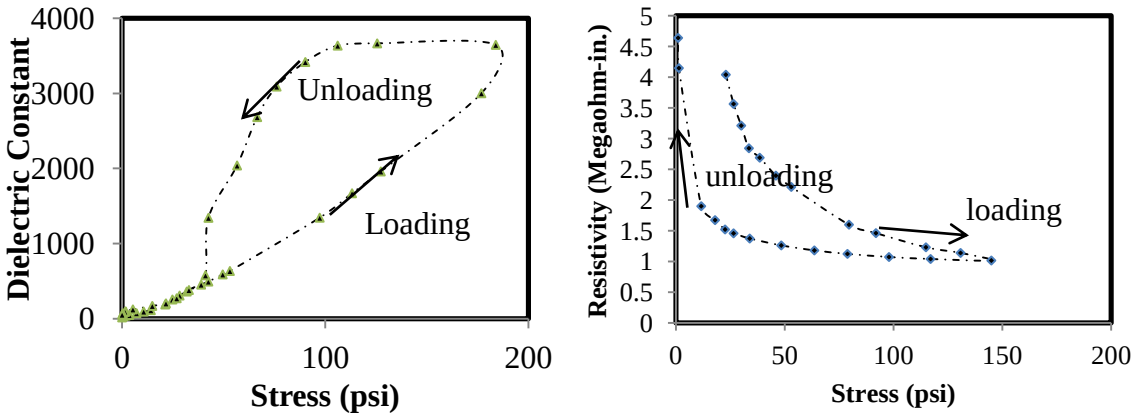

Figure 5-16: Er and Resistivity variation on loading and un-loading cycle (W/C = 1, 5% clay, 0.5% C-Fiber).

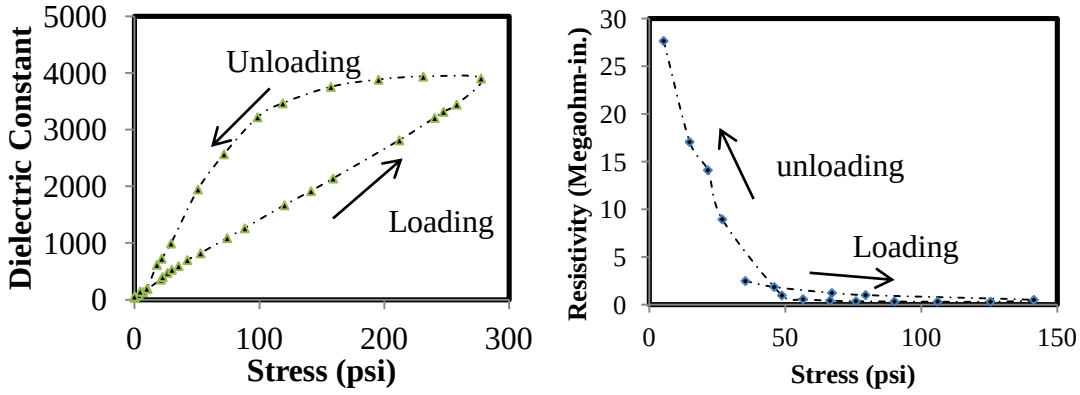

Figure 5-17: Er and Resistivity variation on loading and un-loading cycle (W/C = 1, no clay, 0.5% C-Fiber).

It can be seen that, the Er value before loading was not the same as the Er of the sample after one full loading and unloading cycle in all the cases. This indicates that on subjecting the material to stress, there is a accountable loss in the Er value of the sample. On investigating further, it was noted that, the % change in Er value before and after one full cycle was 40% for cement grout with W/C 0.6, 167% for cement grout with W/C = 0.6 and C-fiber 0.5%, was 410% for cemen grout with 5% clay and W/C = 0.6 and was 119% for cement grout with 5% clay and 0.5% C-fiber at W/C = 0.6. Similar trend was also observed in the case of the samples that had W/C 1. It is to be noted that, even

though, the addition of carbon fiber affects the change in the Er value before and after the cycle, addition of clay significantly affects the change in the dielectric constant Which means that the recovery of Er was not 100%. It is also to be noted that, in most of the cases, the Er value of a sample during loading is always less than the Er values of the corresponding stress during the unloading cycle. The residtivity values were very high during the early stages of loading but as the stresses acting on the samples increased, the resistivity decreased indicating the ideal piezo resistive behavior which is contributed by the addition of clay and C-fiber. It is also to be noted that exact opposite trend was observed in the case of resistivity change as compared to the dielectric constant variation. Resistivity for stress values during loading cycle was more than the resistance values corresponding the the same stresses during the unloading cycle as opposed to the dielectric constant variation. One interesting observation is that, the samples having C-fiber content of 0.5% reaced very low values of resistivities in the order of 1 – 10 kilo-ohm-in. as opposed to the resistivities exhibitted by the samples which did not possess C-fiber.

(e) Heat Impact: the impact of increase in the temperature of the sample on the Er variation was investigated in this study. The samples were placed in the oven at a constant temperature of 200˚F for a period of 3 hours and were subjected to compression test. The results were compared to the samples not subjected to heat treatment. The ressults show that, the trend in the Er variation of samples subjected to heat treatment were similar to that of those not subjected to the heat treatment. However, the values reduced considerably at all stresses for the heated samples. Figures 5-18, 5-19, 5-20 and 5-21 show the impact of heat treatment on the different grout samples.

From Figure 5-18 it is evident that as the stress levels get higher, the difference between the dielectric constant increases rapidly. For example, when the compressive stress of 28 psi was applied to the sample at room temperature, the Er observed was 51 but for the heated sample at the same stress level the Er value was 71 which attributed to 28% decrease. But, when the stress level was 320 psi, the value of Er decreased from 436 to 177 attributing to 59% on subjecting the grout to heat treatment. Same effect can be observed in all the samples. But the addition of clay has a greater impact on the Er difference which can be observed in Figure 5-21 and Figure 5-19. It can be seen from figure 5-20 that sample possessing 5% clay content significantly shows a greater difference in the Er values when subjected to heat treatment on incremental stress levels. The Er value at 25 psi and 290 psi compressive stresss on the Cement grout sample at W/C = 1 with 5% clay and 0.5% C-Fiber was 93 and 1697 respectively which accounts to 1720% increase in the value of Er. When the identical sample was subjected to heat treatment the Er value increased from 48 to 422 attributing to an increase of 780%. It is to be noted that, at 25 psi, the Er value was almost halved when the sample of heated and was ¼ of the original value at 320 psi when the sample was heated. Thus it is interesting to note the the reduction in the Er value is also accompanied by the reduction in the slope of the curve of Er vs stress.

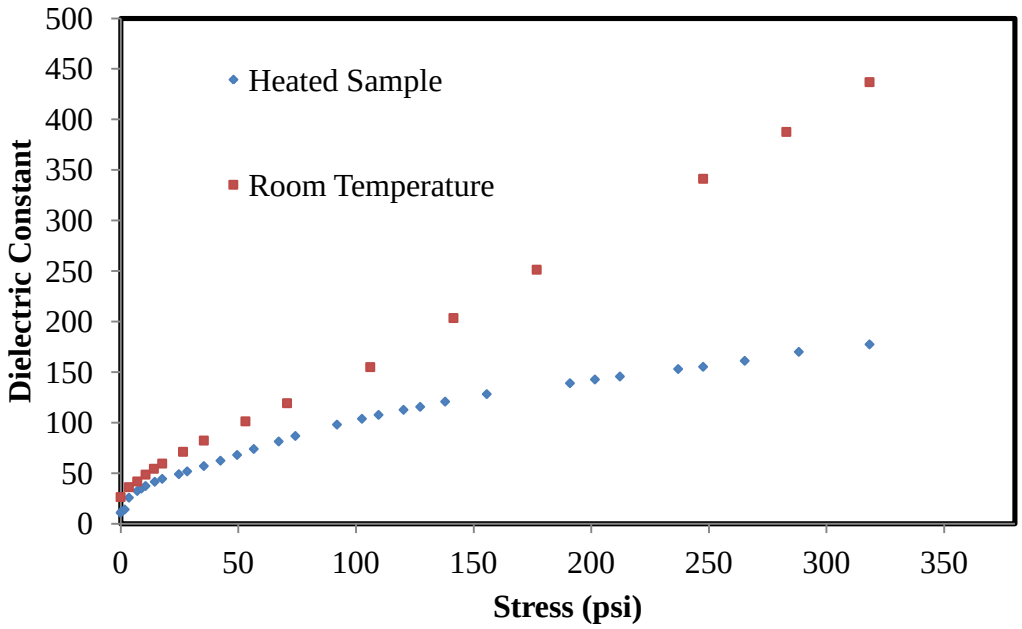

Figure 5-18: Comparison of Dielectric Variation of Cement grout at W/C = 0.6; 0.5% Fiber.

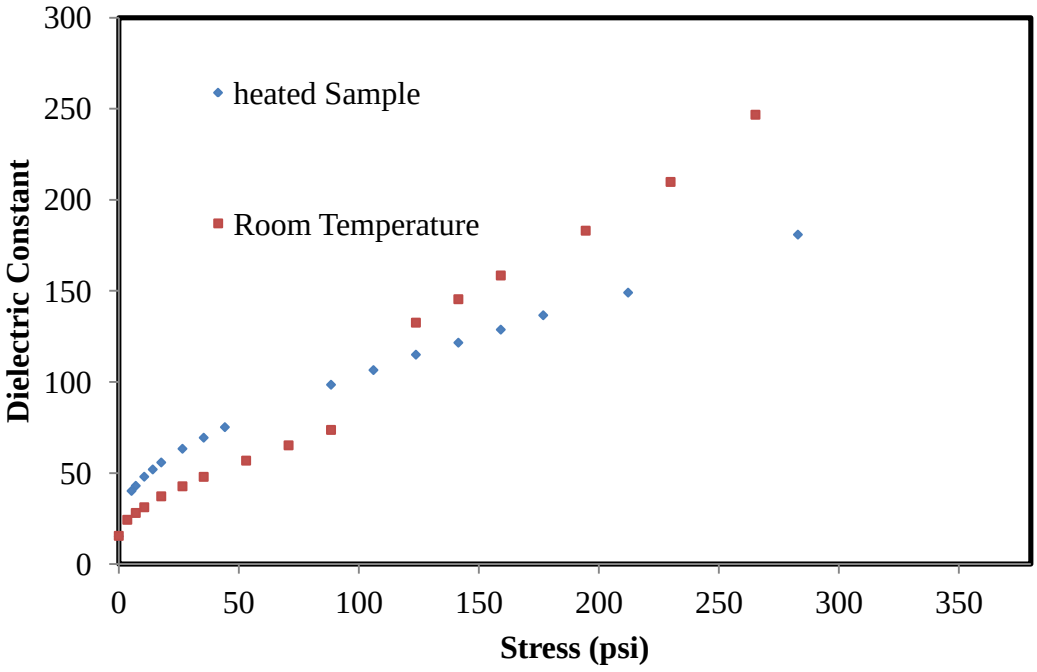

Figure 5-19: Comparison of Dielectric Variation of Cement grout at W/C = 0.6; 0.5% Fiber; 5% clay.

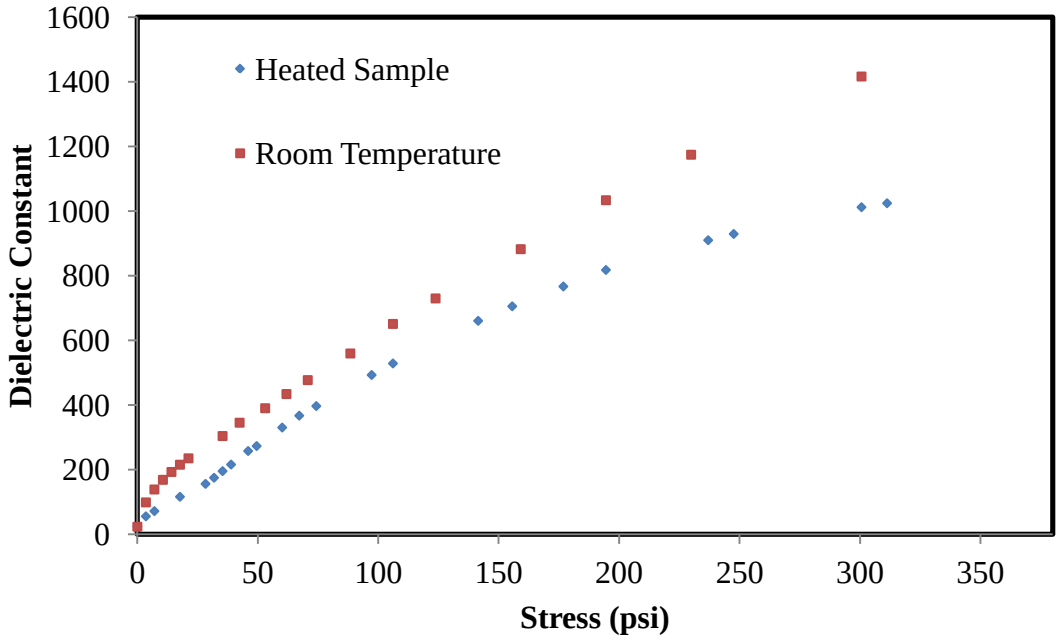

Figure 5-20: Comparison of Dielectric Variation of Cement grout at W/C = 1; 0.5% Fiber.

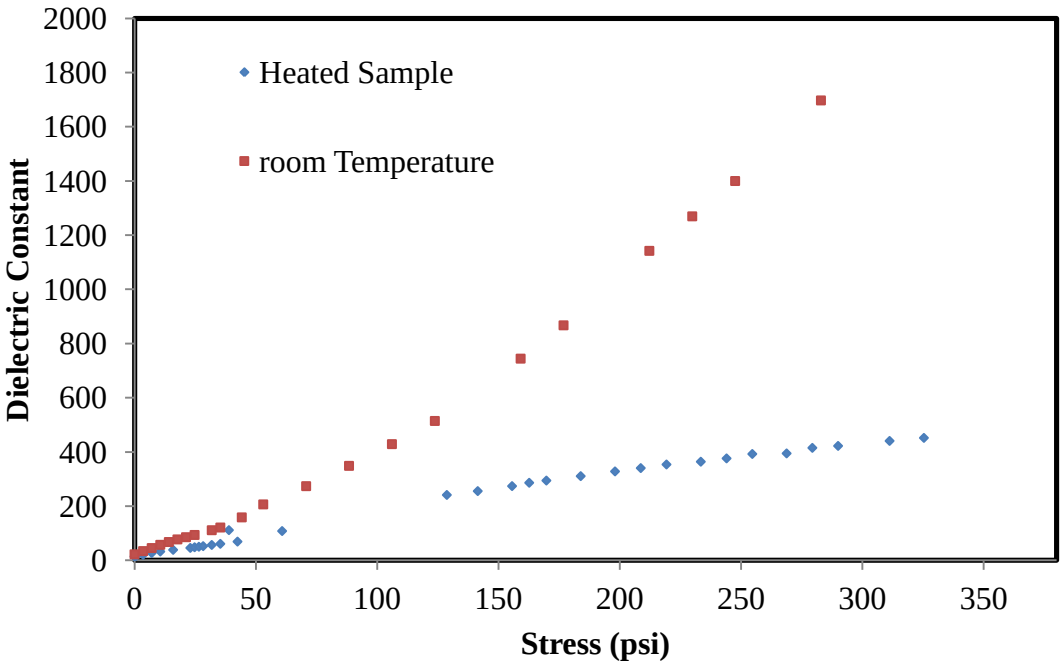

Figure 5-21: Comparison of Dielectric Variation of Cement grout at W/C = 1; 0.5% Fiber; 5% Clay.

(f) Piezo Resistive Behavior: Figure 5-22 and 5-23 Give the comparison of change in the piezo resistive behavior of Cement grout with and without the addition of clay at W/C = 1 and 0.6 respectively. Addition of clay changes the resistivity of the cement grout significantly. However the % decrease in the resistivity is more when the W/C = 1 as opposed to the case where W/C = 0.6. at a stress level of 630 psi, the % decrease as 94% when no clay was added but the % decrease was 99.8% when 5% clay was added. It was noted that, the resistivity change attained peak sooner when clay was added. However, contrasting trend was observed when W/C was 0.6. it can be seen from figure 5-23 that, the % decrease in the resistivity value was less on adding 5% clay as compared to cement grout without clay. At a stress level of around 1100 psi, the % decrease in resistivity was 61% when no clay was added to the grout as opposed to only a 50% when 5% clay was added. These observations shw that, in addition to metakaolin clay, water to cement ratio also has a significant impact on the piezo resistive behavior of the grout.

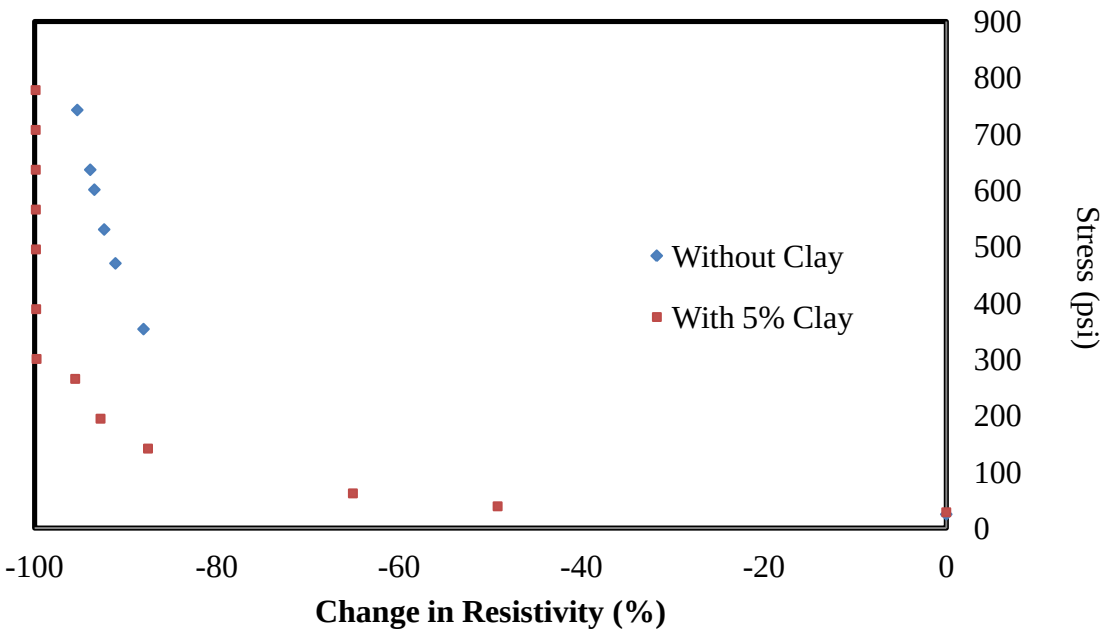

Figure 5-22: Piezo-resistive behavior of cement grout at W/C =1; Fiber content = 0.5%.

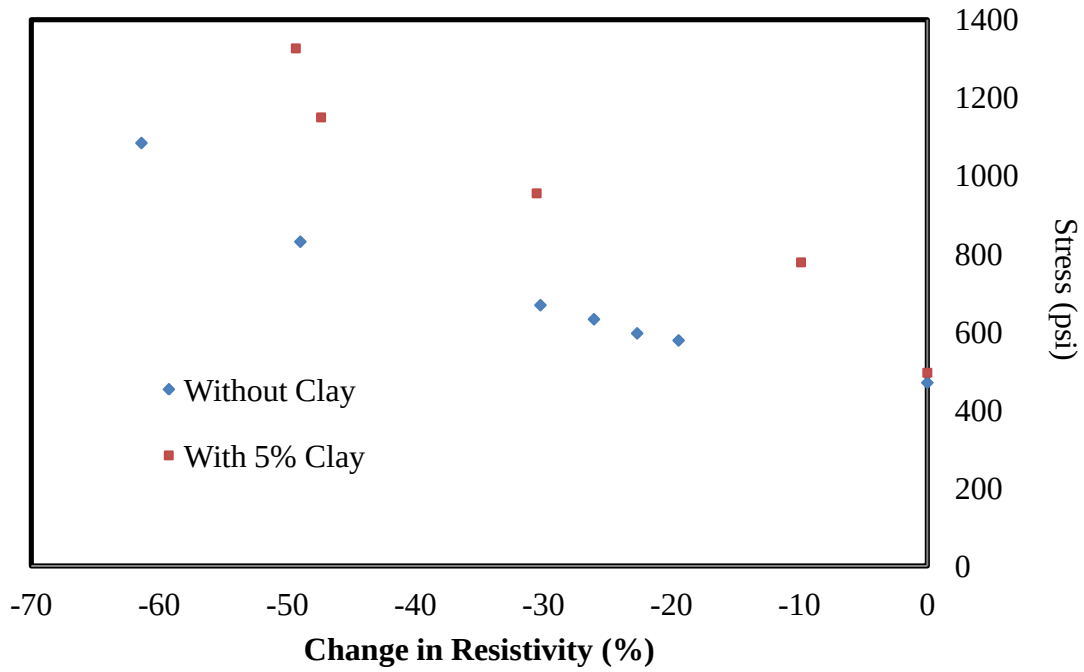

Figure 5-23: Piezo-resistive behavior of cement grout at W/C =0.6; Fiber content = 0.5%.

(g) Dielectric Constant Variation: Figure 5-24 and 5-25 show the dielectric constant variation on stress application. It is to be noted that, when the W/C is 1, on adding clay, the dielectric constant increases from a value of 23 to 4051 when the stress level increases from 0 to 1200 psi. But, the Er value increases from 23 to 10000 on increasing the stress from 0 to 1100 psi when 5% clay is added to the cement grout at W/C = 1. It is to be noted that, when the stress level is 800 psi, the Er value was 2958 when no clay was added to the grout. But the Er value increased by 167% to 8000 on adding 5% clay. However, the Er values were decreased on addition of clay when the W/C was 0.6 which is clearly evident from Figure 5-24. The Er values rose from 18 to 746 when no clay on increasing the stress level from 0 to 530 psi for cement grout without clay as opposed to an increase from 15.5 to 544 when the stress increased from 0 to 560 psi when 5% clay was added to the cement grout. At a stress level of around 390 psi, Er value decreased from 556 to 337 on adding 5% clay which is a 40% decrease in the Er value. Thus, it is observed that, as the W/C does have an effect on the dielectric variation.

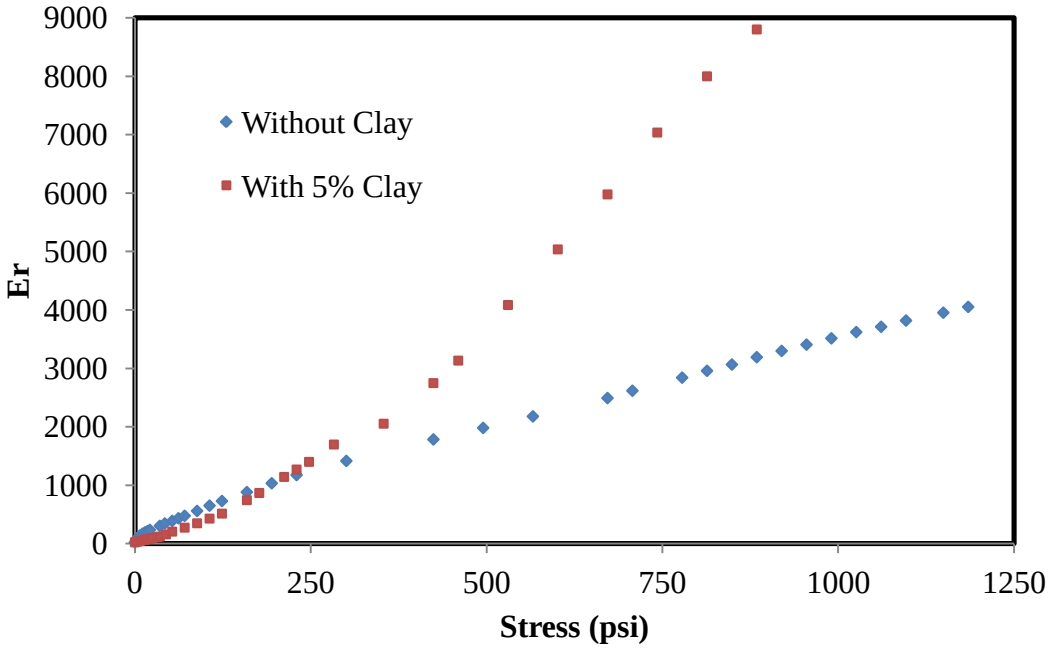

Figure 5-24: Dielectric behavior of cement grout at W/C =1; Fiber content = 0.5%.

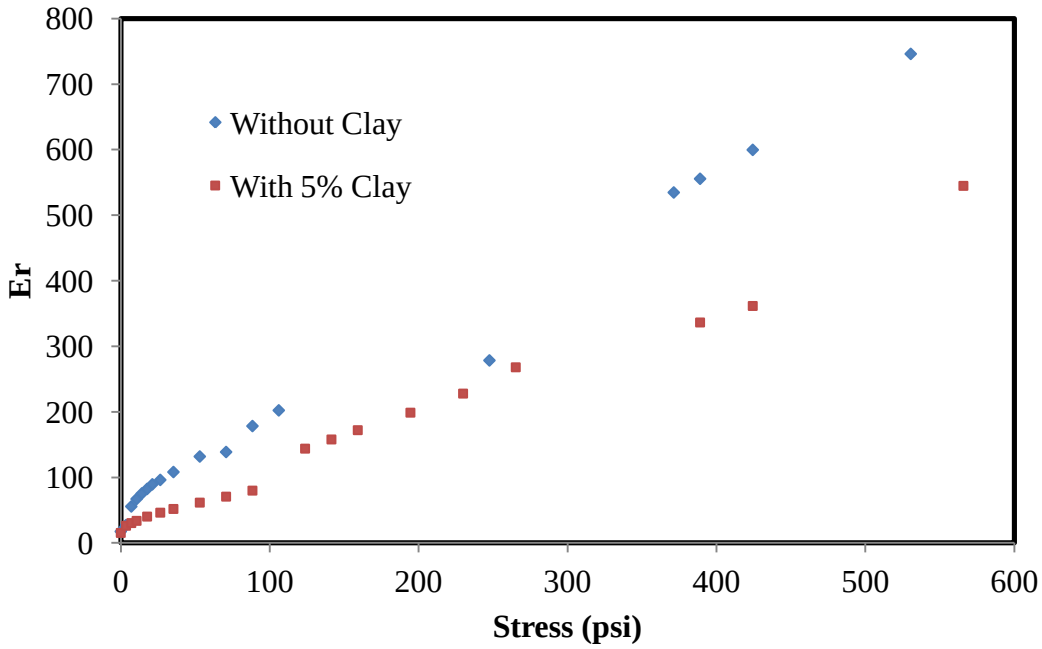

Figure 5-25: Dielectric behavior of cement grout at W/C =0.6; Fiber content = 0.5%.

5.3 Analysis of Setting, Flow, Dielectric and Strength Properties

When analyzing the final setting time, bleed and the static dielectric constant of the grout mixes, the following equations were assumed to predict the behavior og the grout,

$$T_f = A_0 + A_1*(\%Clay) + A_2/(W/C), \quad (5\text{-}1)$$

$$B = A_0 + A_1*(\%Clay) + A_2/(W/C), \quad (5\text{-}2)$$

$$E_r = A_0 + A_1*(\%Clay) + A_2*(W/C) + A_3*(\%C) + A_4*(S/C), \quad (5\text{-}3)$$

$$Pu = A_0 + A_1*(\%Clay) + A_2/(W/C). \quad (5\text{-}4)$$

Where T_f, B, E_r and Pu are final setting time, % Bleed, Dielectric constant and Pullout Strength of the grout mixes respectively. %Clay, W/C, %C and S/C stand for the percentages of clay, Water:cement ratio, Carbon Fiber and Sand used respectively. Table 5-3 gives the values of the model parameters $A_0 – A_5$ respectively.

Table 5-3: Model Parameters for Setting time, Bleeding and Dielectric Variation.

Property	Final Setting Time (t_f)	% Bleed (%B)	Dielectric Constant (E_r)	Pullout Strength (Pu)
A_0	1705	26	-2.9	111
A_1	-47	-1	-0.6	-6.8
A_2	-668	-12	43.7	164
A_3			-7	
A_4			-1.7	

Model parameters A_0, A_1 and A_2 suggest that the reduction in the final setting time of the grout is significantly contributed by the W/C ratio and is directly proportional to W/C and inversely proportional to %Clay. Opposite trend was observed with the pullout test result where, the increase in W/C decreased the pullout strength of the grout mix. It is to be noted that addition of clay decreased the pullout strength of the grout also.

Similar trend can also be found in Bleed, however the values of A_1 and A_2 have been reduced significantly. It is to be noted that the ratio of A_1/A_2 was 0.07 for the setting time and 0.08 for Bleeding this indicates that the addition of clay and W/C has similar impact on both the properties. Model Parameters A_1, A_2, A_3, A_4, A_5 indicate that addition of Carbon Fiber, Sand or Clay to the cement grout decreases the dielectric constant which tallies well with the experiment values. It is to be noted that increase in the W/C however increases the dielectric constant signicantly which is evident from A3 Value of 43.7. addition of Clay causes the least impact on the dielectric constant. Figure 5-26 and 5-27 show the model predictions of setting time and bleeding capacity.

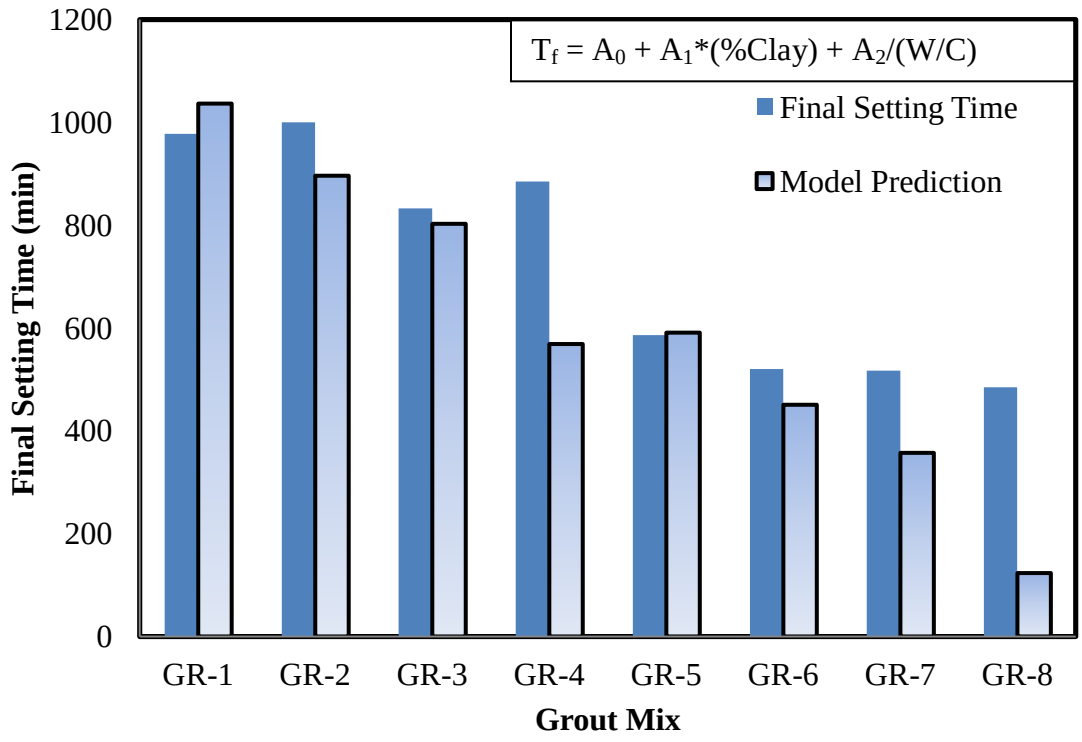

Figure 5-26: Final Setting Time Prediction for Cement Grout.

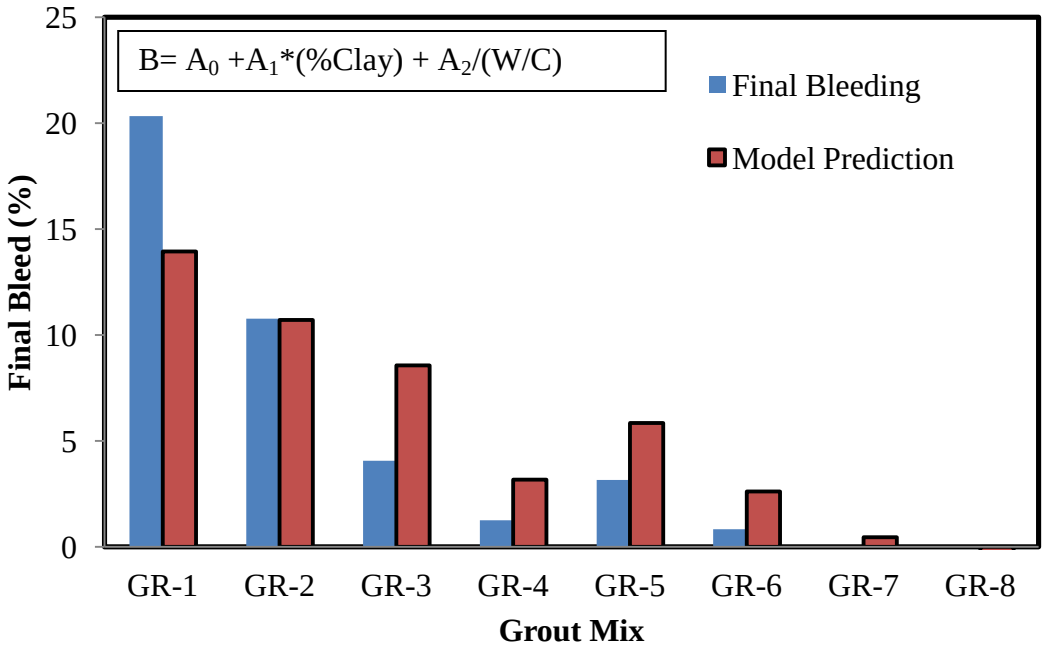

Figure 5-27: Bleeding Capacity Prediction for Cement Grout.

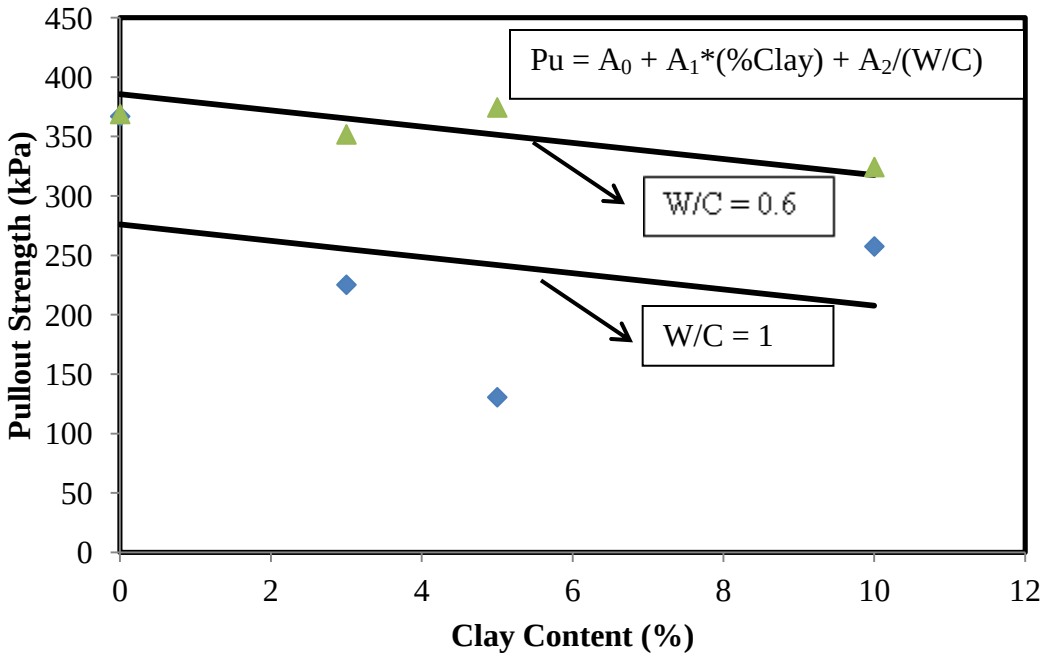

Figure 5-28: Pullout Strength Prediction for Cement Grout.

5.3 Summary

Effect of addition of various proportions of metakaolin clay on the flow ability, working and mechanical behavior of cement grout was investigated. Addition of 5% clay on the self sensing behavior of the cement grout was investigated in detail. Piezo resistive properties and dielectric variation on stress application was examined. The W/C ratios considered in this study were 0.6 and 1. The following observations can be determined from the above study:

1. The addition of clay decreased the bleeding capacity of the cement grouts with w/c ratio of 0.6 and 1. The flow-ability of the grout with w/c ratio of 0.6 was affected by the addition of clay. That was not the case with grout with w/c ratio of 1.
2. The initial and final setting time were affected by the addition of clay. The grouts with lower W/C ratio had set fast when compared to those with higher setting times and the difference between the initial and final setting times were also altered significantly on addition of clay. The electrical resistivity peaked before the initial setting of the grouts. The resistivity was affected by the w/c ratio and the clay content.
3. The general failure during the pull-out strength was interface shear. The pullout strength of the cement grout decreased with the addition of clay for the grouts with w/c ratio of 1. The changes were minimal for grouts with w/c ratio of 0.6. Grouts with w/c ratio 0.6 had a higher compressive strength than grouts with w/c ratio 1.

4. The addition of 5% clay to the cement grout had a noticeable impact on the relative dielectric constant of the cement grout with W/C 0.6 and 1. Addition of Sand decreased the Er of the grout. The void content in the grout has the greatest impact on the dielectric constant of the grout.
5. Piezo resistive behavior was observed with and without the addition of clay and, results suggest that, the resistance values reached very low values when C-fiber was added.
6. Clay addition did have an impact on the dielectric variation on stress application of the cement grout. W/C ratio plays a very vital role in determining the dielectric constant values of the cement grout especially when the material under study is subjected to stress.

CHAPTER 6 MODELING EXPANSIVE GROUT CURING AND GROUTED SAND BEHAVIOR

6.1 Introduction

In this chapter, a phenomenological model has been developed to predict the uniaxial expansive behavior of polyurethane grouts. Also, p-q model has been used to predict the stress-strain behavior of acrylamide and acrylic grouted sands. The effect of Grouting and Grouted bulb formation across the lateral leaking joint was also numerically studied.

6.2 Expansive Behavior of Polyurethane Grout

The hydrophillic polyurethane grouts, expand during curing. This expansion is a critical issue when it comes to repairs of infrastructure and offshore applications as the stress associated with the expansion grout are extremely high and also change rapidly. It is to be noted that, some polyurethane grouts expand more than 30 times their original volume, however the rate and amount of expansion is influenced by the grout constituents and the confined conditions in the field. The model takes into account the gas production and hardening of the grout during the curing process.

6.2.1 Model Development

A model has been developed to represent the curing of expanding polyurethane grout as shown in Figure 6-1. When the liquid grout mix cures, it expands and the chemical reaction produces gas and heat. Grout can expand freely or under confined condition.

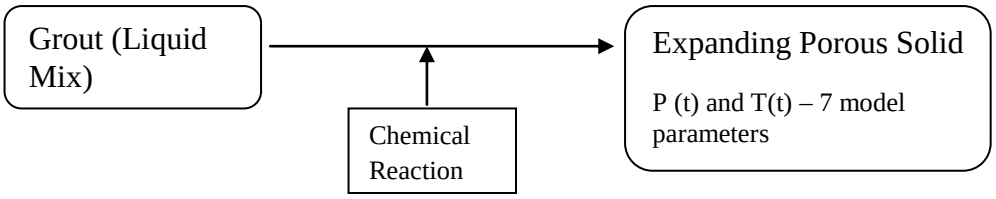

Figure 6-1: Expansion of Polyurethane Grout.

Figure 6-2 shows the physical model that describes the confined expansion (uniaxial) of the polyurethane grout. It is to be noted that, the expanding porous solid is a mixture of voids along with the strengthening semi-solid gell (grout). The shell represents the strengthening of the grout. The voids (bubbles) formed in the porous solid due to the evolution of carbon-di-oxide gas as a result of polymerization is lumped into a single void which is indicated in figure 6-2.

P_T is the uniaxial pressure exerted by the curing grout under confined conditions. With time the grout will gain strength ($\sigma_s(t)$ – tensile strength of the grout which increases with respect to time because of gelling of the grout till the P_T attains peak) and the P_g (t) which is attributed to the gas pressure exerted by the gas wrapped inside the void. The increase in gas pressure is because of the gas produced during the polymerization reaction, which is trapped inside the defined volume of the void. It must be noted that the temperature also will influence the P_T.

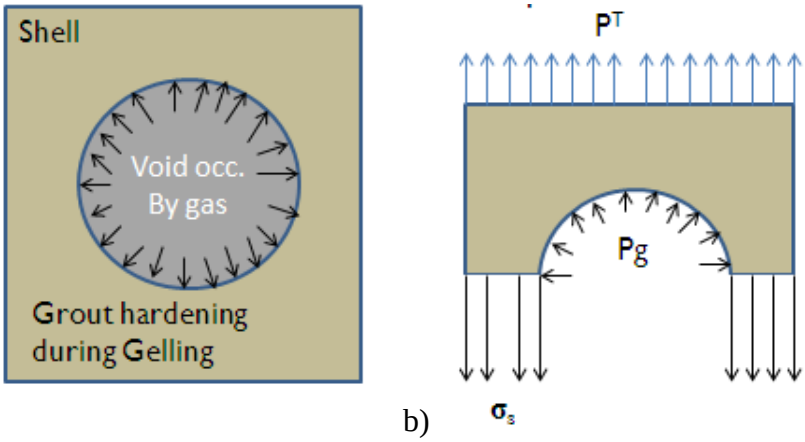

a) b)

Figure 6-2: a) Lumped model of porous solid, b) equilibrium condition of the lumped model.

6.2.2 Governing Equations and Assumptions

Governing Equations: In order to capture the uniaxial stress development during the curing of polyurethane grout, following governing equations were used,

1) Exothermic Chemical Reaction:

$$X + Y \longrightarrow CO_2 + PU. \qquad (6\text{-}1)$$

Typical Conditions: X = Isocyanate

Y = Water

In the current study: X = Diphenyl methyl diisocyanate + Toluene diisocyanate

Y = Water

The chemical reaction of isocyanate (Y) polymerization to polyurethane (PU) is described in chapter 2. It is an exothermic chemical reaction which attributes to the increase in the temperature of the grout during its phase transformation,

2) Total uniaxial stress developed is a function of time dependent pressure applied due to gas formation and grout strengthening

$$P_T(t) = f(P_g(t), \sigma_s(t)). \quad (6\text{-}2)$$

Where, P_T = total uniaxial pressure developed by the curing grout

P_g= Pressure developed by the gas formation in the void

σ_s = tensile strength of curing PU.

3) Modified ideal Gas law equation

For gas,

$$P.V = n.R.T. \quad (6\text{-}3)$$

In the case of grout hardening,

$P = P_g(t)$ which is pressure exerted by the gas trapped in the void.

$N = n_g(t)$ which is number of moles of the gas produced during the chemical reaction

T – T(t) which is change in the temperature with time during the setting of the grout.

Therefore,

$$p_{gas}(t) = (n_g(t)/V).\ R.\ T(t). \quad (6\text{-}4)$$

Which gives,

$$p_{gas}(t) = M(t).R.T(t), \quad (6\text{-}5)$$

where, R = universal gas constant = 8.314 J/K/mol and

$$M(t) = n_g(t)/V \text{ moles/m}^3. \quad (6\text{-}6)$$

Assumptions:

The following are the assumptions considering in developing this model:

- The produced CO_2 obeys the ideal gas law equation and M(t) represent the mass of CO_2 produced per unit volume of the gas.

- The tensile strength of the curing grout increases with time during the process of setting of the grout.

6.2.3 Modeling Procedure

Consider a system of curing grout (Semi liquid and gas phase) where gas is formed in the voids while grout is gelling. (lumped system shown in Figure 6-2). Considering the equilibrium condition,

$$p_T(t).A_T = p_{gas}(t).A_g - \sigma_s(t).A_s, \quad (6\text{-}7)$$

where,

A_T = total cross-sectional area of the lumped system.

A_g = area occupied the gas occupied lumped void.

A_s = area occupied by the shell (curing grout).

So, $$A_T = A_g + A_{s,} \quad (6\text{-}8)$$

therefore, $$As = A_T - Ag. \quad (6\text{-}9)$$

Dividing eqn. 6-7 by the total area, A_T, we get,

$$p_T(t) = p_{gas}(t)(A_g/A_T) - \sigma_s(t).(A_s/A_T), \quad (6\text{-}10)$$

substituting eqn 6-9 in eqn 6-10,

we get, $$p_T(t) = p_{gas}(t)(A_g/A_T) - \sigma_s(t).((A_T-A_g)/A_T). \quad (6\text{-}11)$$

Therefore, $$p_T(t) = p_{gas}(t)(A_g/A_T) - \sigma_s(t).(1-(A_g/A_T)). \quad (6\text{-}12)$$

Substituting $A_g/A_T = \alpha$, which is defined as the area ratio,

$$p_T(t) = p_{gas}(t).\ \alpha - \sigma_s(t).(1-\alpha). \quad (6\text{-}13)$$

In equation, 6-13, the first component on the RHS represents the gas production phase and the second component represents the grout hardening phase.

6.2.3.1 Gas Phase

Gas Production

From Equation 6-5 and 6-6,

$$p_{gas}(t) = M(t).R.T(t), \quad (6\text{-}5)$$

where,

$$M(t) = n_{gas}(t)/V \text{ moles/m}^3. \quad (6\text{-}6)$$

The pressure exerted by the gas production during the chemical reaction on the strengthening grout can be represented as shown in equation 6-5. It is important to note that, M(t) and T(t) are variables which are time dependent and needs to be modeled. Bikard et al. (2007) studied the polymerization reaction of a two component polyurethane chemical. On investigating the expansion of the grout during setting, it was found that, the evolution of gas was following the exponential decay path as indicated in Figure 2-2. It is to be noted that, the main factor that contributes to the variation of pgas(t) with respect to time is the production of CO_2 during the chemical reaction and hence it was observed that $P_g(t)$ follows an exponential decay path also. The rate of production of gas in this study is represented as follows.

$$\frac{dM}{dt} = B.(t) + C.D.e^{-Dt}, \qquad (6\text{-}14)$$

where, t = time

B, C and D are the model parameters which are related to the production of CO_2 that impacts in the exponential increase of $p_{gas}(t)$.

From eqn 6-14, we get the mass of gas produced M(t) varying with respect to time as follows.

$$M(t) = B(t-t_0)+C.e^{-Dt0}(1-e^{-D(t-t0)}), \qquad (6\text{-}15)$$

Where, t_0 = initial time used for mixing the grout component.

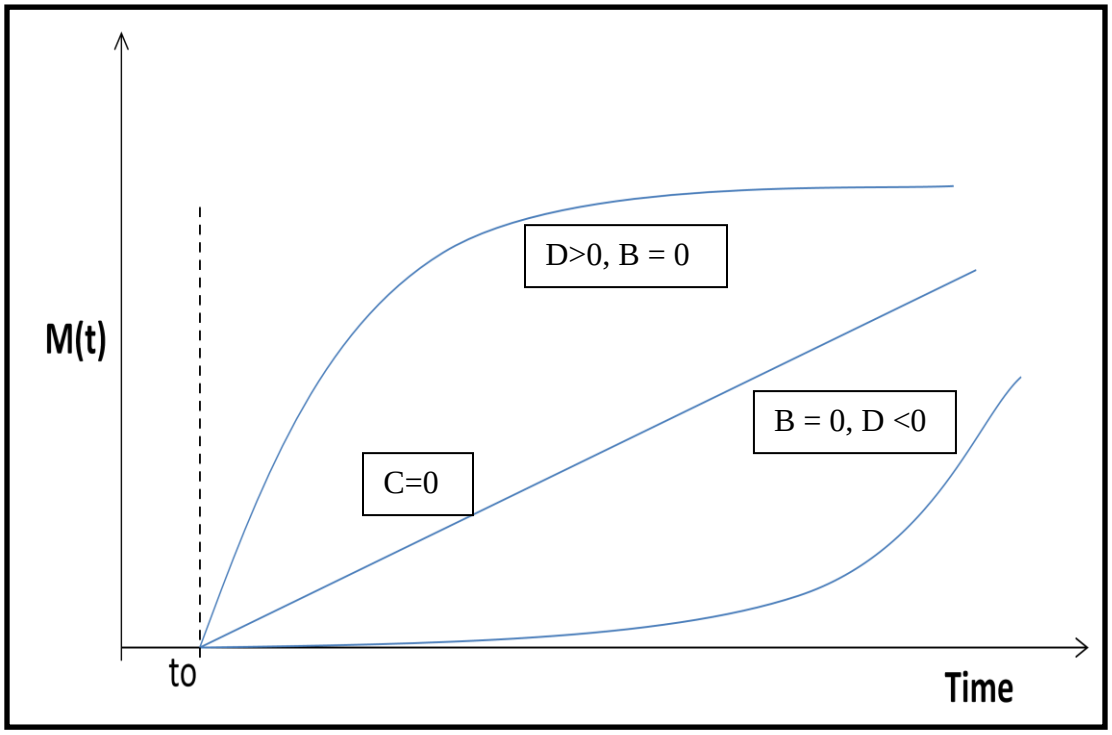

Figure 6-3: Typical Trends of M(t).

Figure 6-3 shows the typical trends in M(t) as predicted by the above equation 6-15. When D is positive, the trend of M(t) follows an exponential decay path which is typical of the production of the gas during the process of gelling of polyurethane grout. If

D was a negative value, the M(t) would follow the exponential increase which is unlikely because as the chemical reaction approaches completion, the rate of production of the gas should be trending towards zero which means that M(t) should attain a constant value. Also, if D was to take a value zero, then the M(t) is a linearly increasing value which does not come to a constant value. Hence, this equation holds good to predict the gas production phase to determine the mass of gas produced which varies with time when the value of the exponential model parameter D is positive.

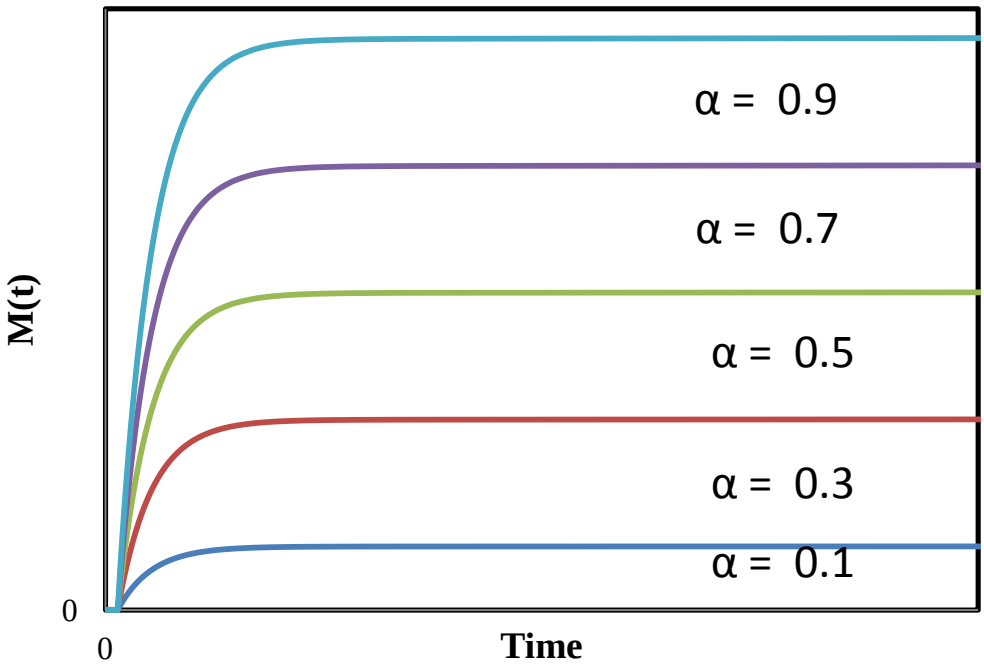

Figure 6-4 Variation of M(t) with the Area Ratio (α).

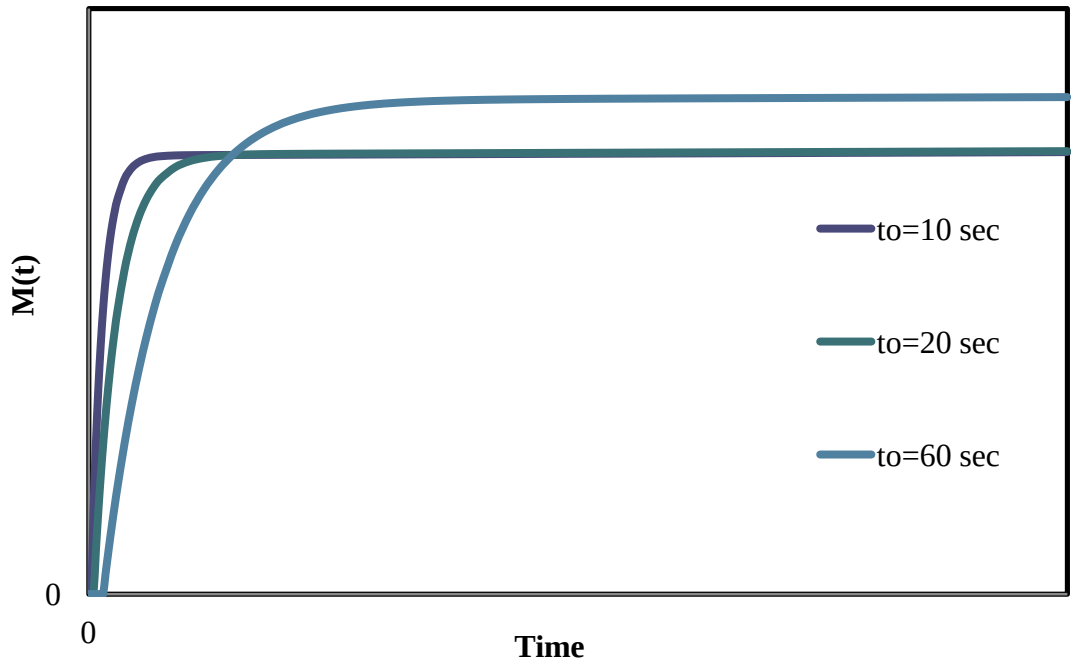

Figure 6-5: Variation of M(t) with time of mixing (t_o).

Figures 6-4 and 6-5 show the variation of M(t) with change in α and t_0. It is to be noted that as the area ratio increases, which means that the area occupied by the gas increases, M(t) decreases. This is because the smaller the area occupied by the gas, the more the pressure exerted by the gas as the number of moles of gas trapped in a smaller area exerts more pressure than that trapped in a larger area. Similarly, as t_0 increases M(t) increases. Two observations can be made from this result. It can be noted that as t_0 value increases, maximum value of M(t) increases which means that good mixing enhances complete usage of chemicals to participate in the reaction resulting the large production of gas. Similarly, it is interesting to note that as t_0 increases the peak value of M(t) is shifted to the right with time. Literature results (Mattey, 2001) show that as the resin:water ratio increases (conversely, as the water: resin ratio decreased) the total uniaxial pressure increases but this increase is delayed with time. The same trend can be

observed as t_0 changes. Hence this shift in time of the peak value can be attributed to the change in the composition of the grout mix.

Temperature Variation

Mattey (2001) proposed the T model to predict the variation of the temperature of the polyurethane grout material during the process of gelling. Eqn 6-16 gives the time-temperature relationship of polyurethane grout,

$$T = Tr + Tc(t/tc)/[q + (1 - p - q)(t/tc) + p(t/tc)\text{^}((p+q)/p)] \quad (6\text{-}16)$$

Where p and q are the material parameters to be determined, T_r is the initial grout mix temperature, T_c is the peak temperature during the chemical reaction and t_c is the time corresponding to the peak temperature. The parameter q is the ratio between the secant and the initial tangent moduli. Parameter p is obtained by minimizing the error to predict the time-temperature relationship. It is to be noted that q varies between 0 and 1 and $(p+q)/p \geq 0$.

Substituting eqn 6-16 and eqn 6-15 for T(t), and M(t) in eqn 6-5, we get,

$P_g(t) = B(t-t_0)+C.e^{-Dt_0}(1-e^{-D(t-t_0)}).R.$

$$Tr + Tc(t/tc)/[q + (1 - p - q)(t/tc) + p(t/tc)\text{^}((p+q)/p)] \quad (6\text{-}17)$$

6.2.3.2 Grout Strengthening Phase

In addition to the pressure exerted by the gas which results in the expansion of the grout, there is also an opposing force which is the tensile force of the grout due to strengthening of the grout mix during its transformation from liquid to solid resulting

because of the polymerization. It is assumed that this increase in tensile strength of the grout from zero and reaches the maximum value when the M(t) reaches a constant value indicating the completion of the chemical reaction. This increase is considered to be at an exponential rate in this study which can be represented as follows,

$$\sigma_s(t) = \sigma_{so}(1-e^{-F(t)}). \quad (6\text{-}18)$$

Figure 6-6 shows the variation of $\sigma_s(t)$ with time for different values of F, where F is the model parameter which depends on the mix proportion of the grout, σ_{so} is the peak tensile strength of the grout. It is to be noted that when F is greater than zero, the tensile strength is less than zero which is not practically possible. When F is lesser than zero, the change in tensile strength of the grout follows an exponential decay rate. If F = 0 then the tensile strength is zero at all times.

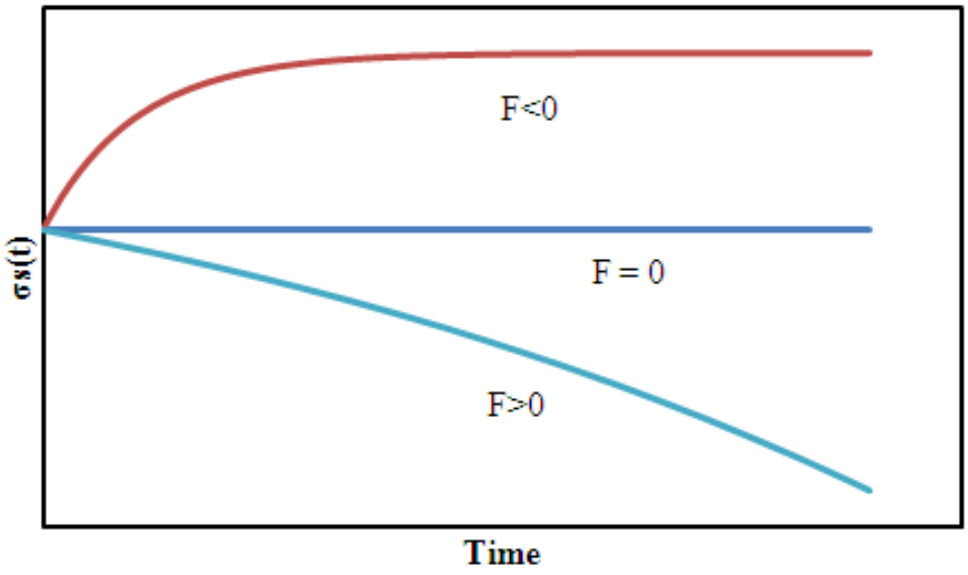

Figure 6-6: Variation of $\sigma_s(t)$ with varying values of F.

6.2.4 Confined Expansion Model

Thus combining the equations, 6-17 and 6-18 and substituting it in equation 6-13 we get,

$$P_T(T) = [[B(t\text{-}to) + C.e^{-Dto}(1-e^{-D(t-to)})] .R.$$
$$[T_r + [(t/t_c)/ (q +(1-p-q).(t/t_c) + p.(t/t_c)^{((p+q)/q))}T_c]] .\alpha$$
$$- \sigma_{so}(1-e^{-F(t)}).(1-\alpha) \quad . \quad (6\text{-}19)$$

Equation 6-19 is the proposed model to predict the uni-axial stress developed during the polyurethane grout expansion.

6.2.5 Experiment

Figure 6-7 shows the experimental setup to measure the uniaxial stress developed and the variation in temperature with time during the process of grout setting accompanied by grout expansion. It is to be noted that the thermocouple is inserted inside the cylindrical mold to capture the variation in temperature of the material during the polymerization. Similarly a load cell is placed over the top cap of the mold which is used to capture the increase in the stress developed during the expansion of the grout matrix. The experiment is allowed to take place in a confined space at allowable controlled volume of 20%. The apparatus is set and sealed as soon as the grout components are poured and have been hand mixed. Care is taken to ensure that there was minimum leak of the expanding grout during the polymerization as excessive leakage of the grout might

affect the uniaxial stress and might attribute to a significant loss in the stress values that might lead to inconsistent model predictions.

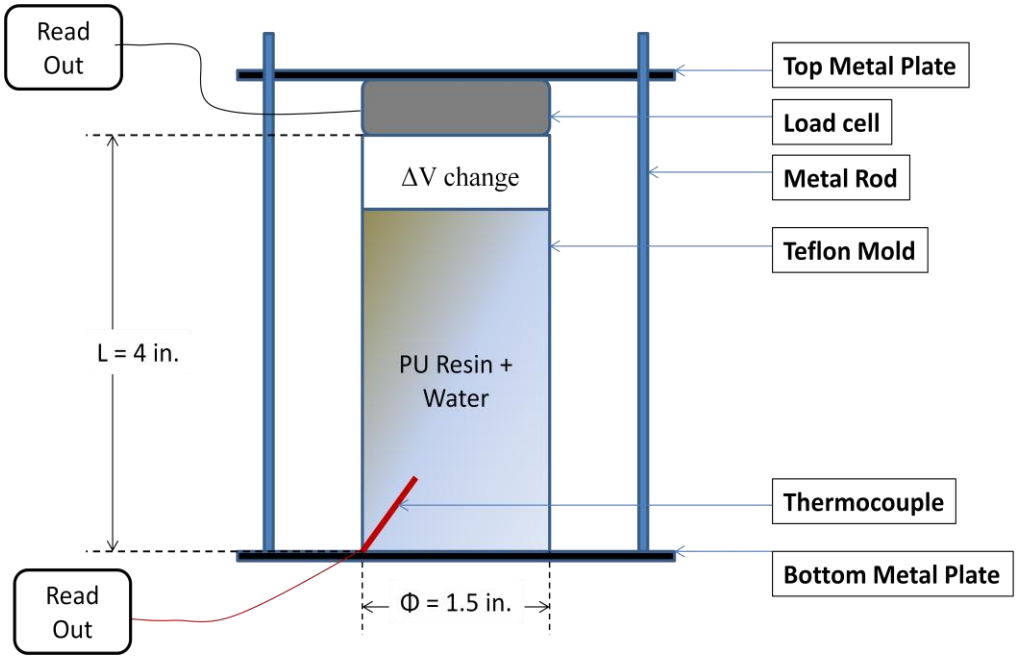

Figure 6-7: Experimental Setup to determine the uniaxial expansion stress and the temperature variation.

Figures 6-8 and 6-9 shows the experimental results on the uniaxial stress developed and the temperature change with respect to time during the process of grout setting for grout mixes with water:resin ratios of 1 and 0.25 respectively. Figures 6-10 and 6-11 shows the comparison of the modeled uniaxial stress curve with the experimental curve. It is to be noted that the model predicts the experimental observations for both cases of the grout mix. Hence the proposed model is applicable for the expansive grouts with varying compositions.

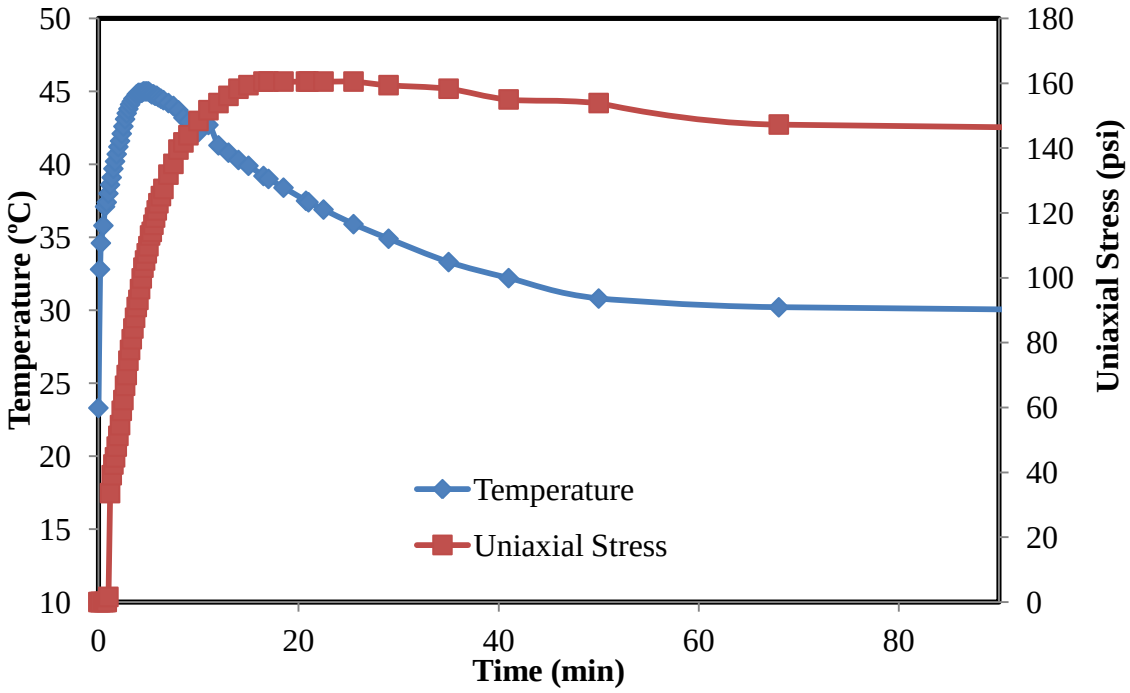

Figure 6-8 Experimental result: Variation of Uniaxial stress and Temperature with Time (W/R = 1).

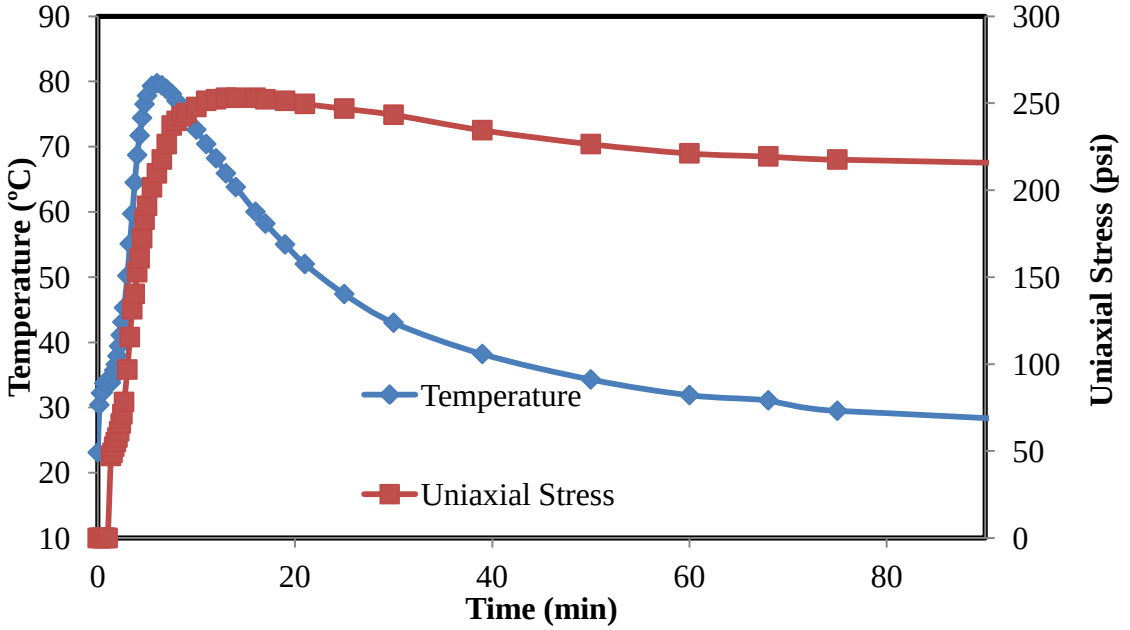

Figure 6-9 Experimental result: Variation of Uniaxial stress and Temperature with Time (W/R = 0.25).

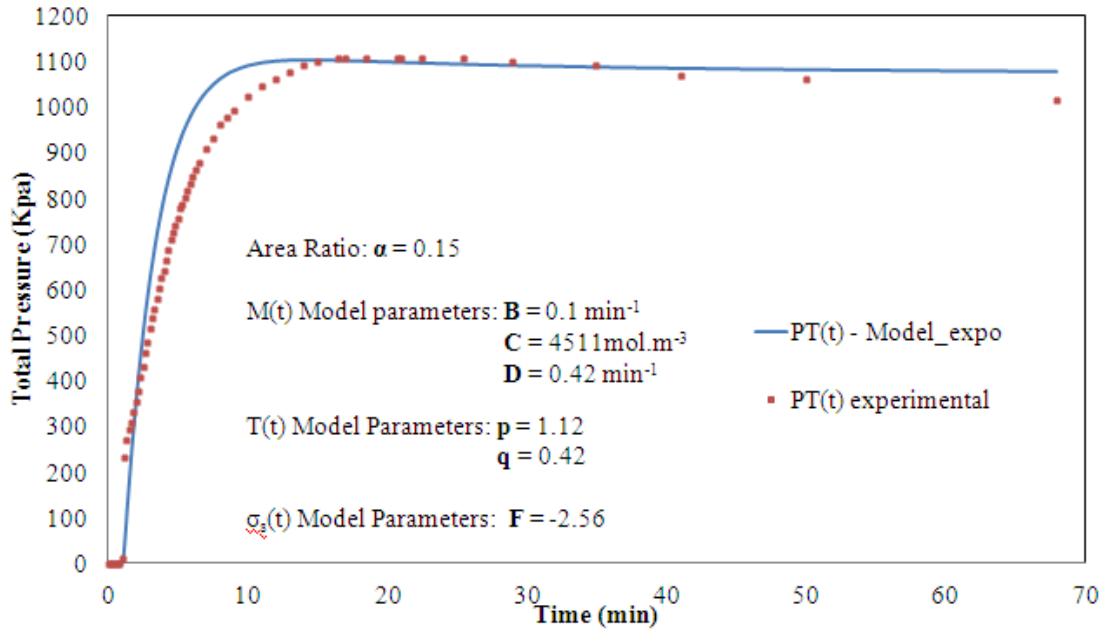

Figure 6-10: Model Prediction of uni-axial pressure development during grout expansion (W/R = 1).

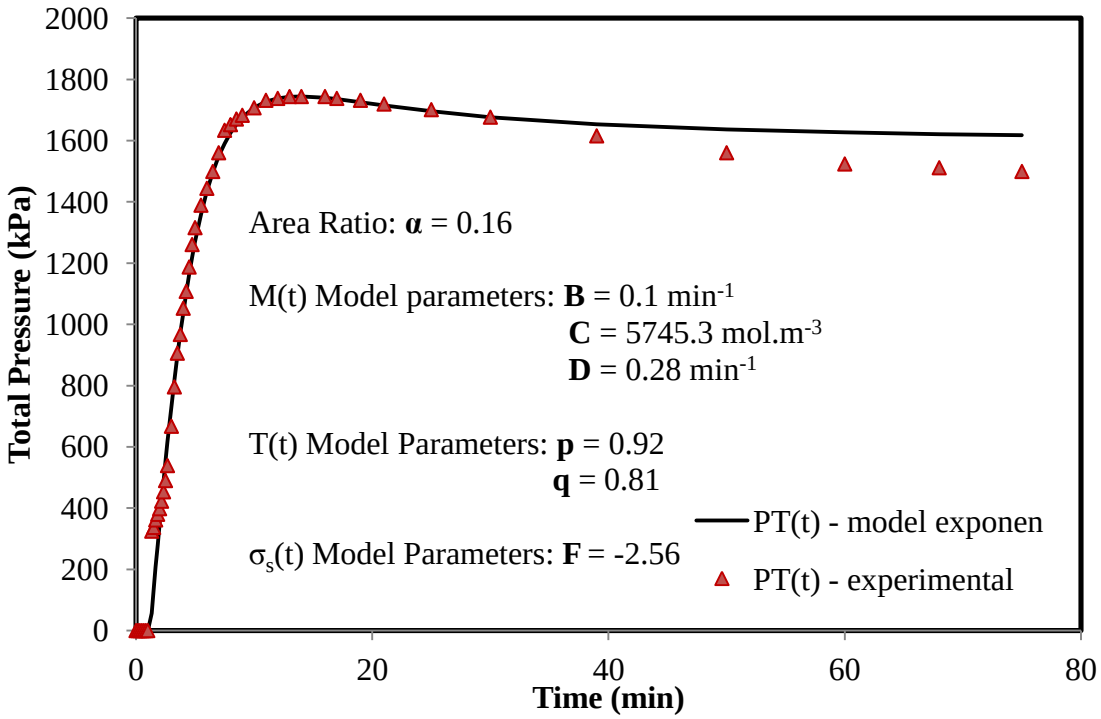

Figure 6-11: Model Prediction of uni-axial pressure development during grout expansion (W/R = 0.25).

6.3 Stress-Strain Model

A constitutive model was developed by Vipulanandan and Paul (1990) to predict the stress-strain behavior of polymer composite materials. The proposed model is given by the equation 6-20,

$$\sigma = \left\{ \frac{\varepsilon/\varepsilon c}{q+(1-p-q)\,\varepsilon/\varepsilon c+p(\varepsilon/\varepsilon c)^{((p+q)/p)}} \right\} \sigma c \,, \qquad (6\text{-}20)$$

where p and q are the material parameters, εc is the strain at peak stress and σc is the peak stress. P is the optimization parameter which is obtained by minimizing the error in predicting the relationship curve. q is the ratio between the secant and tangent moduli. The model parameter q has a significant role in defining the shape of the curve. the higher the value of q, more linear the curve is and vice versa.

Figure 6-12 to 6-16 gives the p-q model predictions of the stress strain relationship of acrylamide and surfactant modified acrylamide grouted sand. Figure 6-17 to 6-19 show the p-q model predictions of acrylic grouted sand after 3 day, 7 day and one month curing time. The p value for acrylamide grouted sand was 0.1 which was increased to 0.08 on adding 0.5% CTAB. The p value increased to 0.17 and 0.22 on adding o.5 and 4% SDS. Similarly the q values for the acrylamide and modified acrylamide grouted sand varied between 0.421 to 0.848. the maximum values for q was observed when 4% CTAB and SDS were added indicating that addition of surfactants tend to linearize the stress-strain curve of the acrylamide grouted sand. Addition of 0.5% surfactants did not cause significant variation to q value. Similarly, the p value for acrylic grout was 0.15 after 3 days of curing and reamined constant at 0.15 after 7th day. However, it was increased to

0.26 after one month of curing. The q value was increased at the 7th day of testing and marginally was decreased for the one month cured sample. However acrylic grout had a higher q value when compared to acrylamide grout.

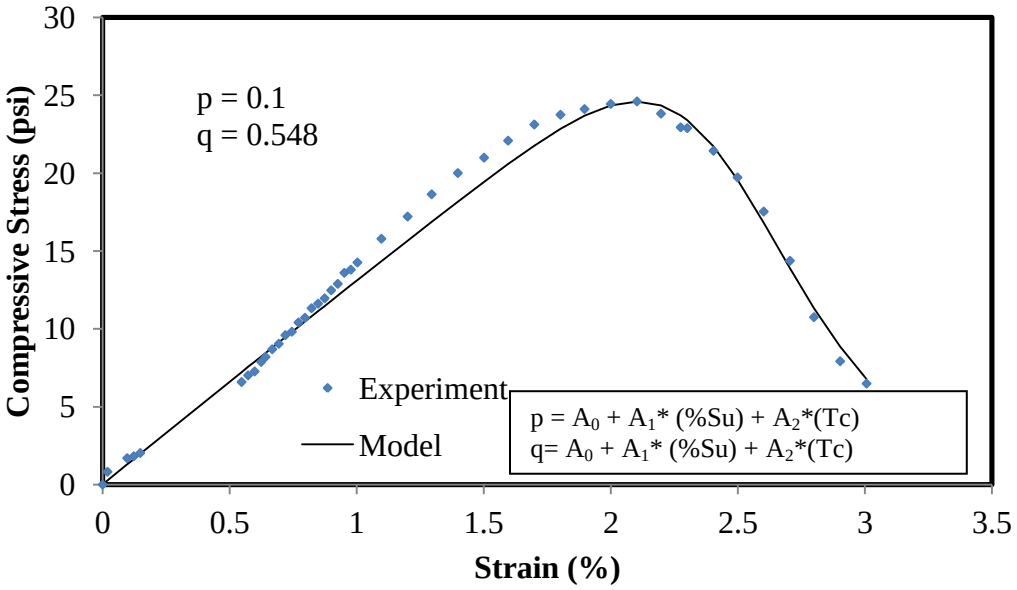

Figure 6-12: Stress- Strain Relationship for acrylamide grouted Sand.

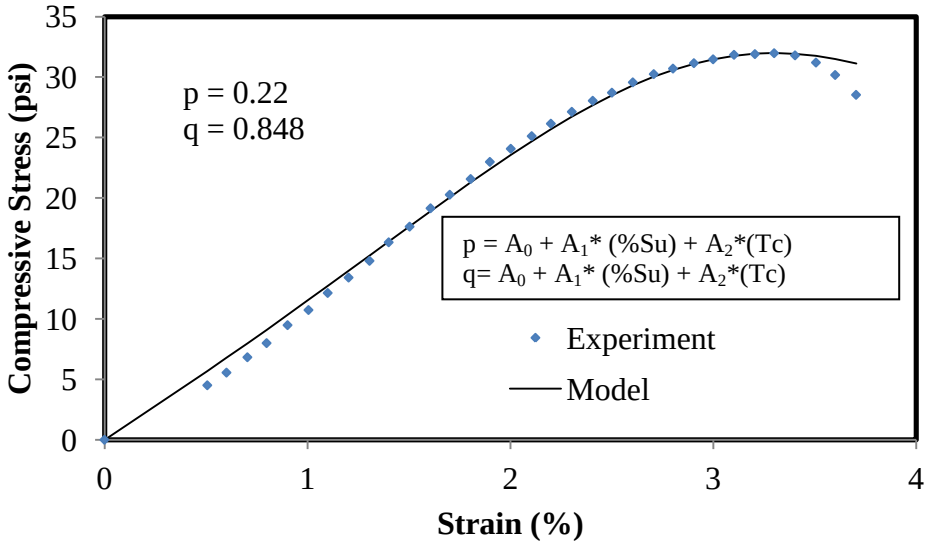

Figure 6-13: Stress- Strain Relationship for acrylamide grouted sand modified with 4% CTAB.

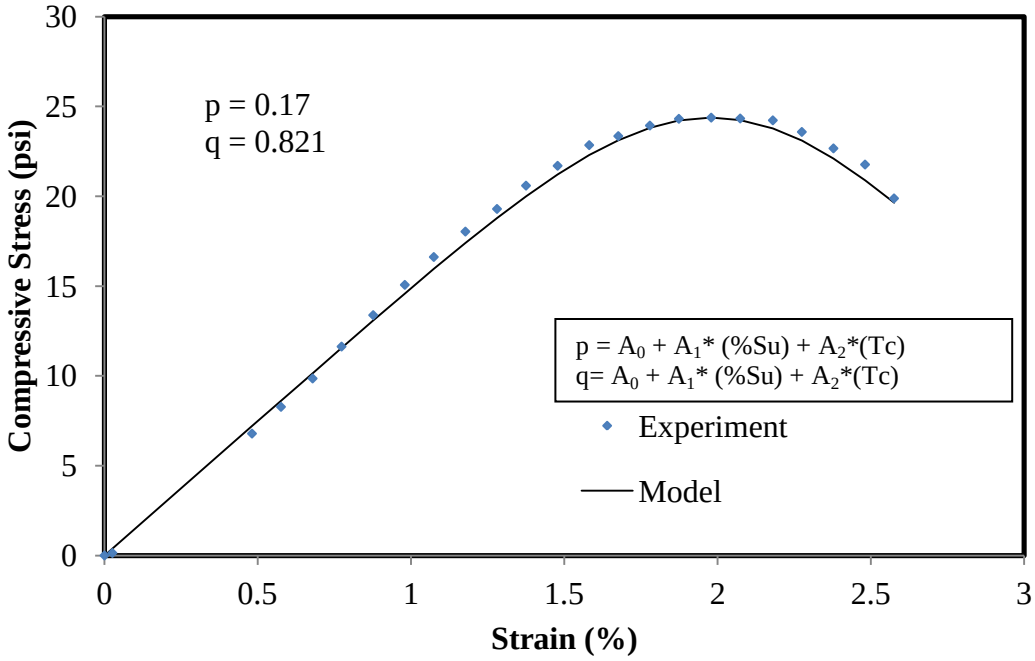

Figure 6-14: Stress- Strain Relationship for acrylamide grouted sand modified with 4% SDS.

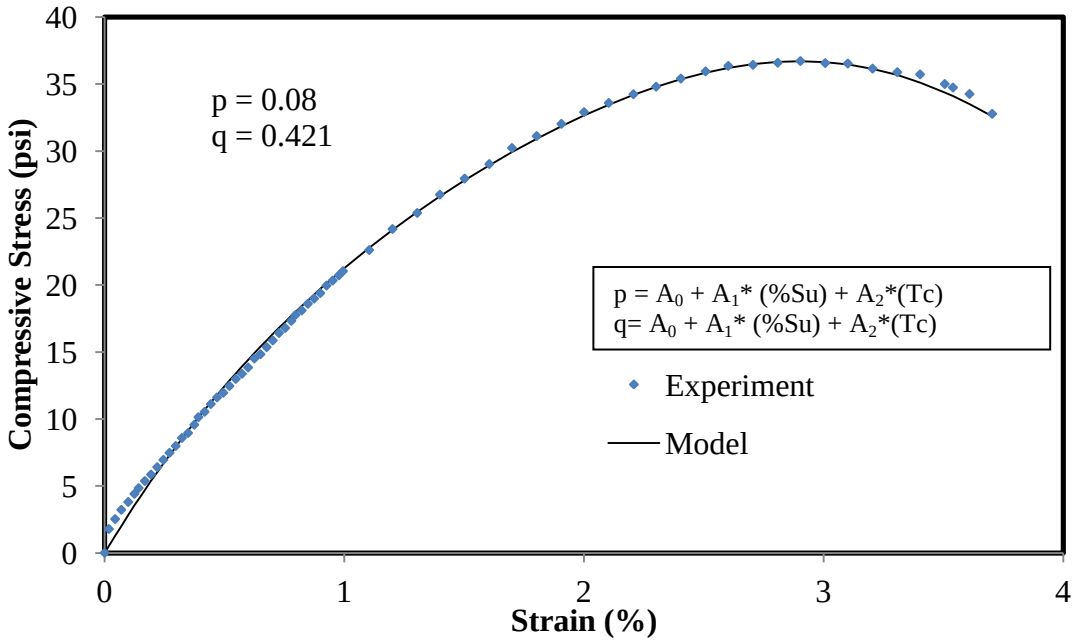

Figure 6-15: Stress- Strain Relationship for acrylamide grouted sand modified with 0.5% CTAB.

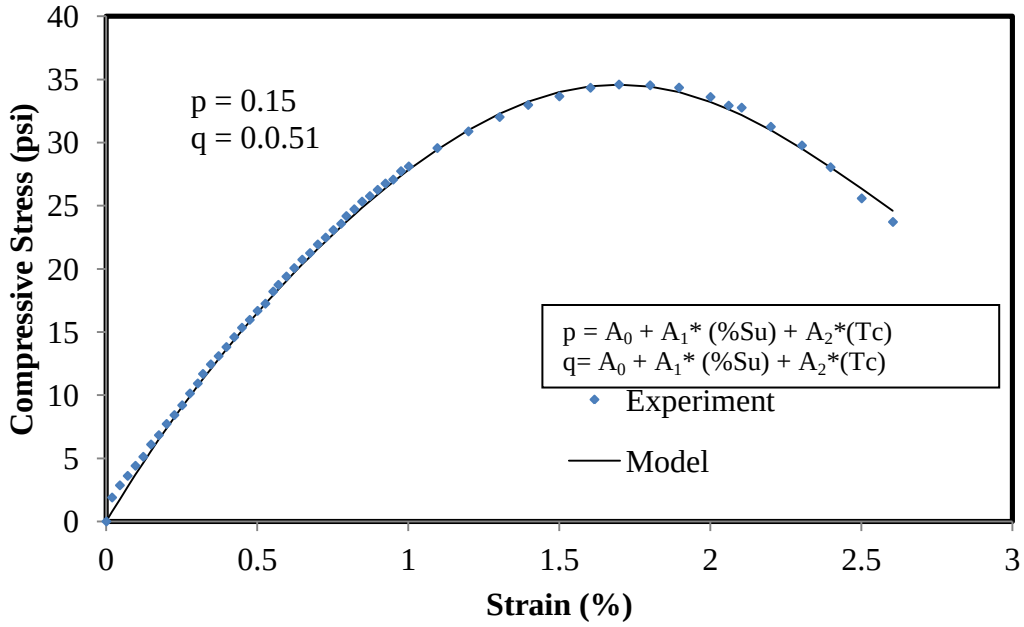

Figure 6-16: Stress- Strain Relationship for acrylamide grouted sand modified with 0.5% SDS.

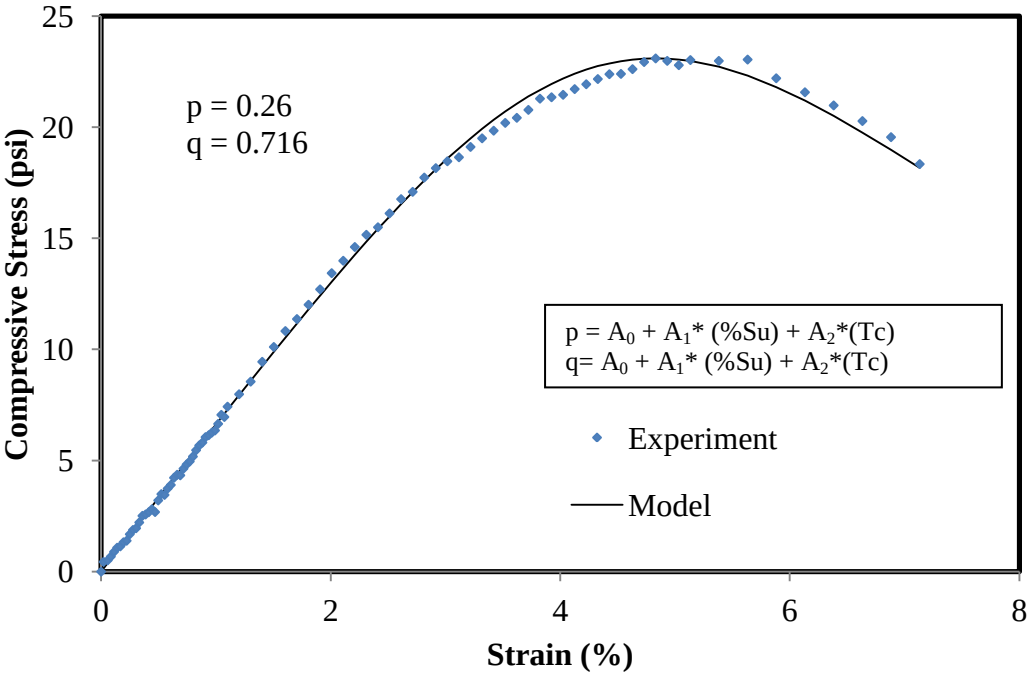

Figure 6-17: Stress- Strain Relationship for acrylic grouted sand after 3 days of curing.

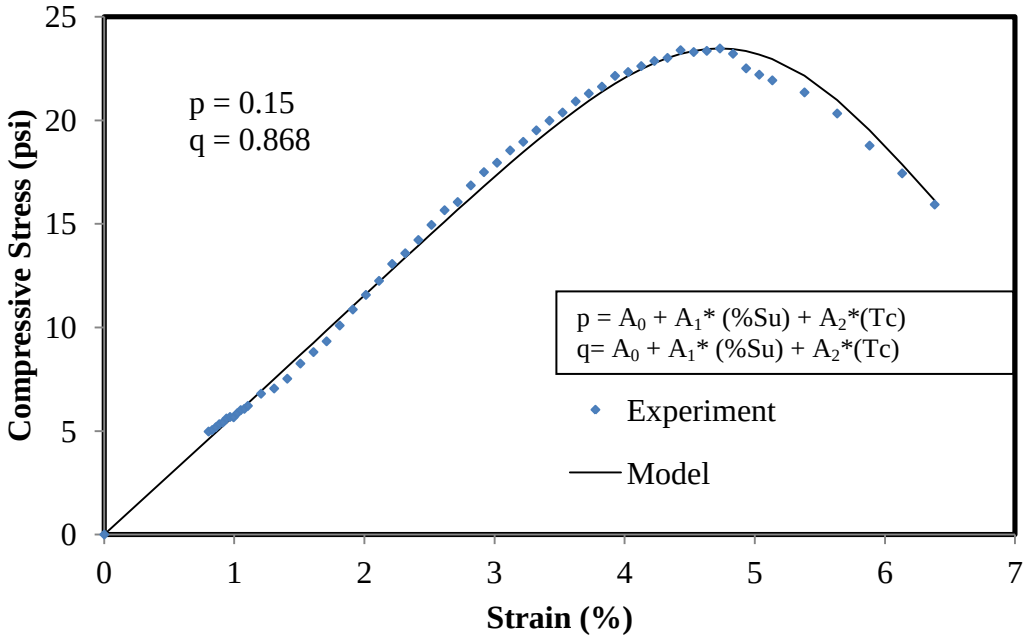

Figure 6-18: Stress- Strain model for acrylic grouted sand after 7 days of curing.

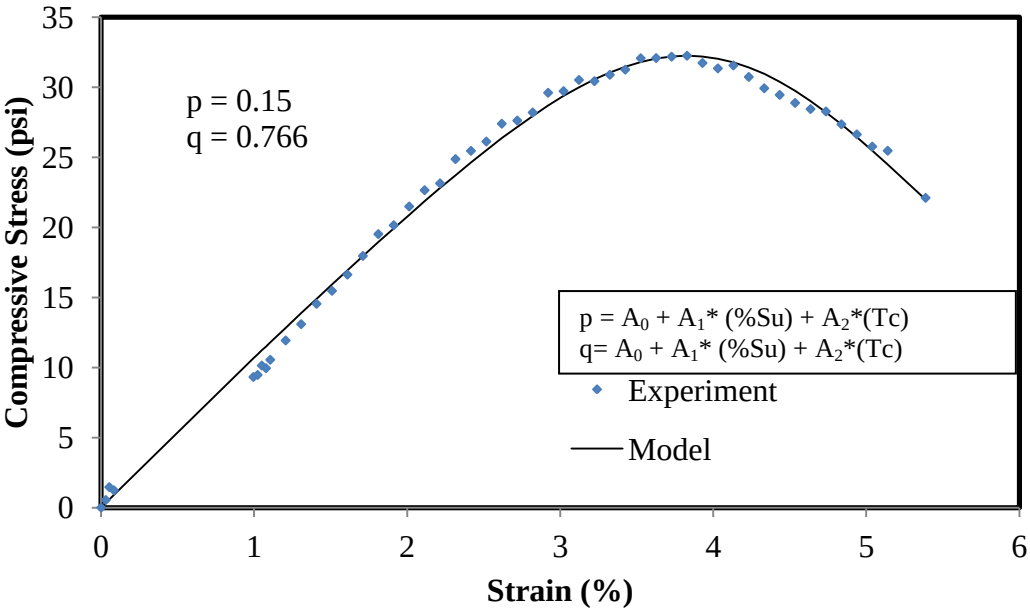

Figure 6-19: Stress- Strain model for acrylic grouted sand after one month of curing.

When analyzing the variation in model parameters p and q, it was noted that, the following relation can be used to predict the values of p and q,

$P = A_0 + A_1*(\%Surfactant(\%Su)) + A_2*(Curing\ Time\ (Tc))$, (6-21)

$q = A_0 + A_1*(\%Surfactant(\%Su)) + A_2*(Curing\ Time\ (Tc))$. (6-22)

Table 6-1 shows the value of A0, A1 and A2 for p and q. it can be noted that, the amount of surfactant added has a greated effect on p and q values when compared to the curing time as A1 values are greater than A2 values. It is also observed that the surfactant concentration has a greater effect on the q values as the A2 value for predicting q is 0.47 which is more than three times the value of A2 (0.013) to predict p.

Table 6-1: Model parameters to predict p and q behavior

	p	**q**
A0	0.187	0.652
A1	0.013	0.047
A2	-0.003	-0.002

6.4 Modeling the lateral leak joint

In chapter 3, the large scale 3D model experiment of lateral leaking joint was discussed and acrylic grout was injected into the soil surrounding the leak and it was noted that the leak was reduced to 0 gallons/day from around 1250 gallons per day at 3 psi water pressure after just one day of grouting. About 2-6 gallons of the grout were used. The method of chemical grouting with acrilic grout proved to be an effective tool to solve the problem of lateral leaking joint. However it is to be noted that this might be uneconomical if the amount of grout injected was way more than what was required to solve the leak. Thus, this study emulates the development of grouted bulb around the leaking joint which is used to reduce the leak. An increase in the grouted bulb indicates a

larger usage of grout. This study was investigated the amount of leakage with the increase in the dimension of the grouted bulb. Figure 6- 20 shows the 2D PLAXIS model of the experimental setup. It is to be noted that all the dimensions have been strictly followed according to the real experimental setup. The horizontal and vertical gap for the leak between the two pipes was approximated to 0.5 in.

The mesh size was 30 in. x 30 in. A total of 286, 6 node elements were used. A water pressure of 3, 4 and 5 psi was applied to emulate the real experimental setup. The base and the sides were all fixed. The horizontal PVC pipe had impervious layer with porous space inbetween to let the discharge to flow. Figure 6-21 shows the typical flow of infiltration/inflow effluent through the lateral leak.

In order to study the influence of properties of sand on the infiltration/ inflow leak in the lateral joint a study was done to investigate the variation in discharge by changing the permeability of the sand from 0.015 cm/s to 0.118 cm/s. To study the effect of grouted bulb increase, the cross-sectional dimensions of the triangular grouted bulb varied from 1.5 in x 1.5 in, 4 in x 4 in. and 9 in.x 5 in. with cross sectional areas (1.1 sq.in, 8 sq.in. and 22.5 sq.in. respectively.

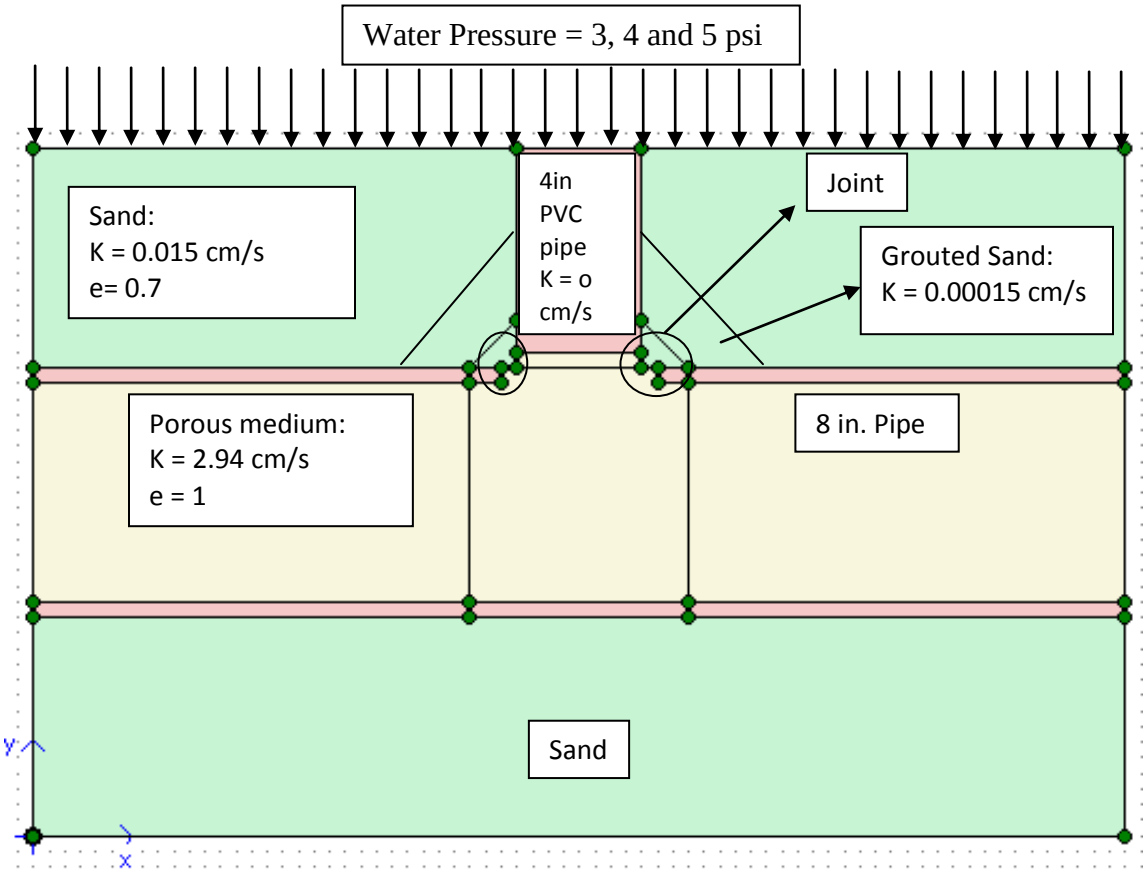

Figure 6-20: 2D PLAXIS Model of Lateral Leaking Joint.

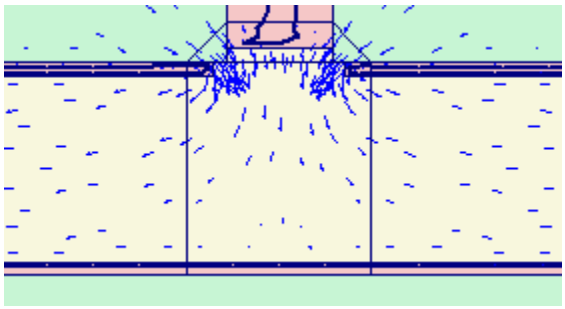

Figure 6-21: I/I Flow through lateral leaking joint.

Figure 6-22 shows the change in discharge on varying the permeability of the soil at a void ratio was 0.7. it is to be noted that as the permeability of the soil increases, the discharge also increases and the slope of the discharge also increases on increasing the

water pressure from 3 to 5 psi in all cases. When the coefficient of permeability (k) of the soil was set to 0.015 cm/s, the maximum discharge observed at 3, 4 and 5 psi were in the order of 1000, 1400 and 1700 gpd respectively. However on increasing the k value to 0.118 cm/s, the discharge values at 3, 4 and 5 psi were found to be 7700, 10300 and 13000 gpd respectively.

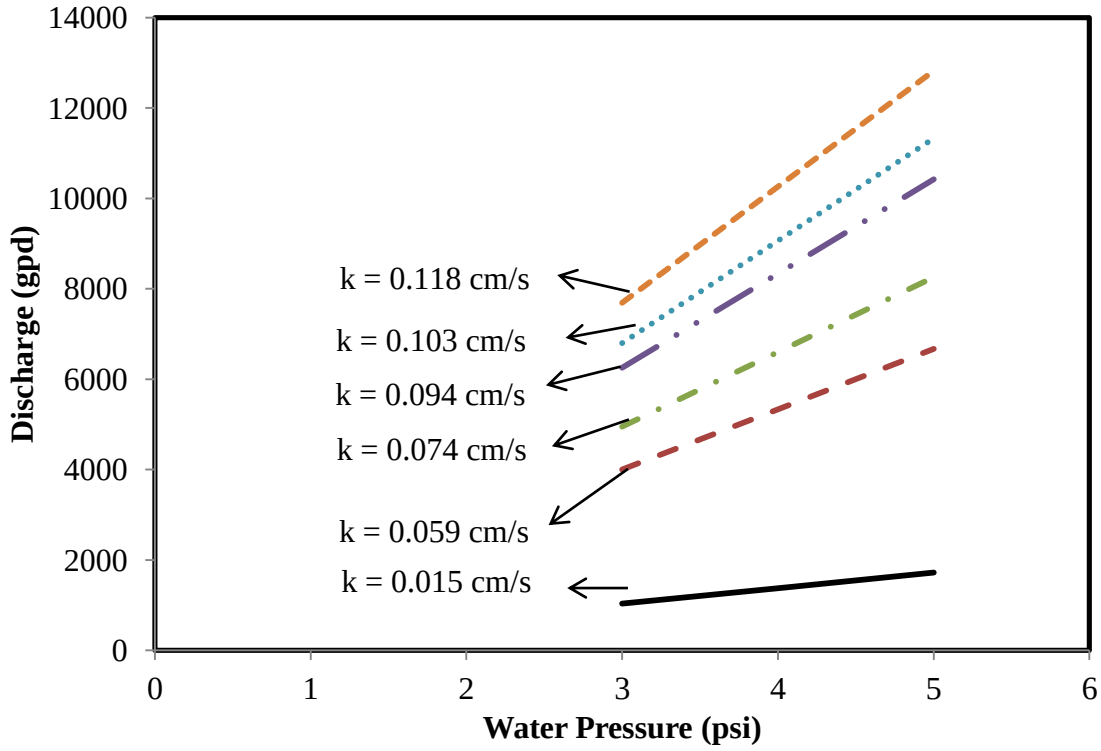

Figure 6-22: Discharge values on varying the coefficient of permeability (k) of soil.

On investigating, it was observed that when the k value of the soil was set to 0.015 cm/s at void ratio (e) = 0.7, the numerical model gives a close approximation to the experimental result. Figure 6-23 shows the selected numerical model result with the experimental result.

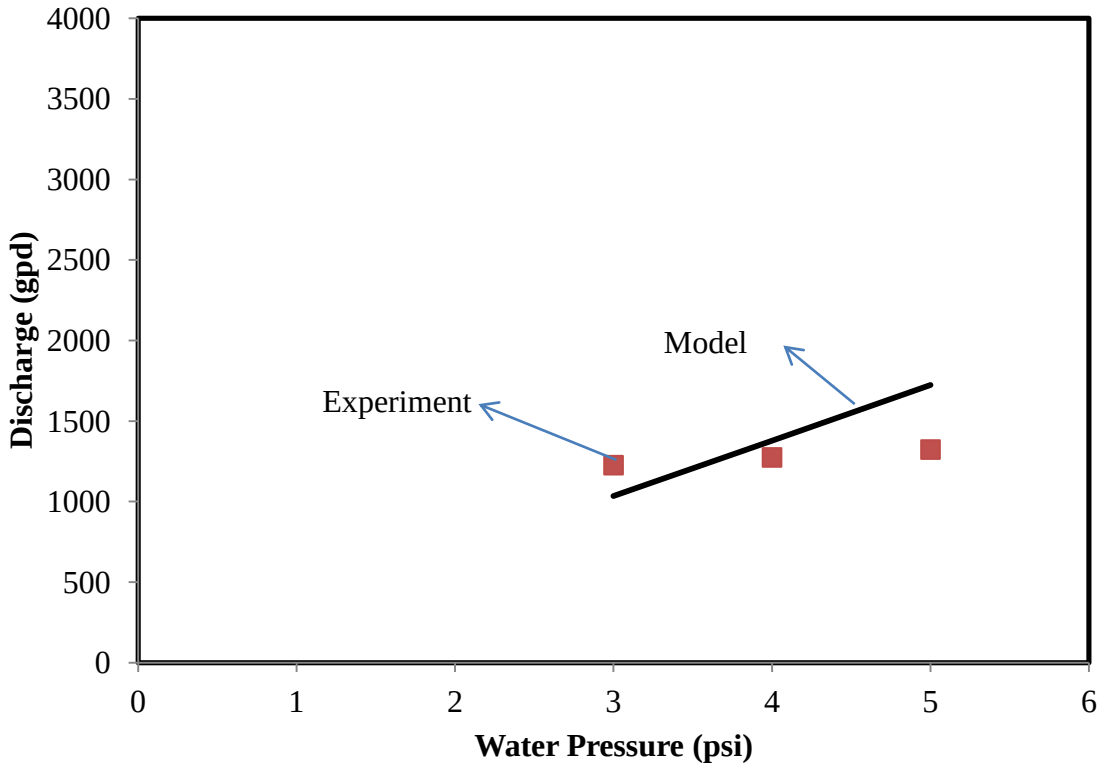

Figure 6-23: Experiment Result vs Model Values for Discharge.

On further studying the impact of grouting, the effect of the growth of grouted bulb around the lateral leaking joint on the discharge was investigated. For this purpose, 3 cases of the grouted bulb dimensions were studied. The first case had the triangular cross sectional grouted bulb with the height and width of 1.5 in. the second and third cases studied had dimensions of 4 in x 4 in. and 9 in. x 5 in. respectively. Thus the grouted bulb had a cross sectional area (elevation view) of 1.125 in^2, 8 in^2 and 22.5 in^2 respectively. In all the cases the k of grouted sand (grouted bulb) was set to a low value of 0.00015 cm/s. The effect of grouted bulb formation on the discharge is shown in Figure 6-25.

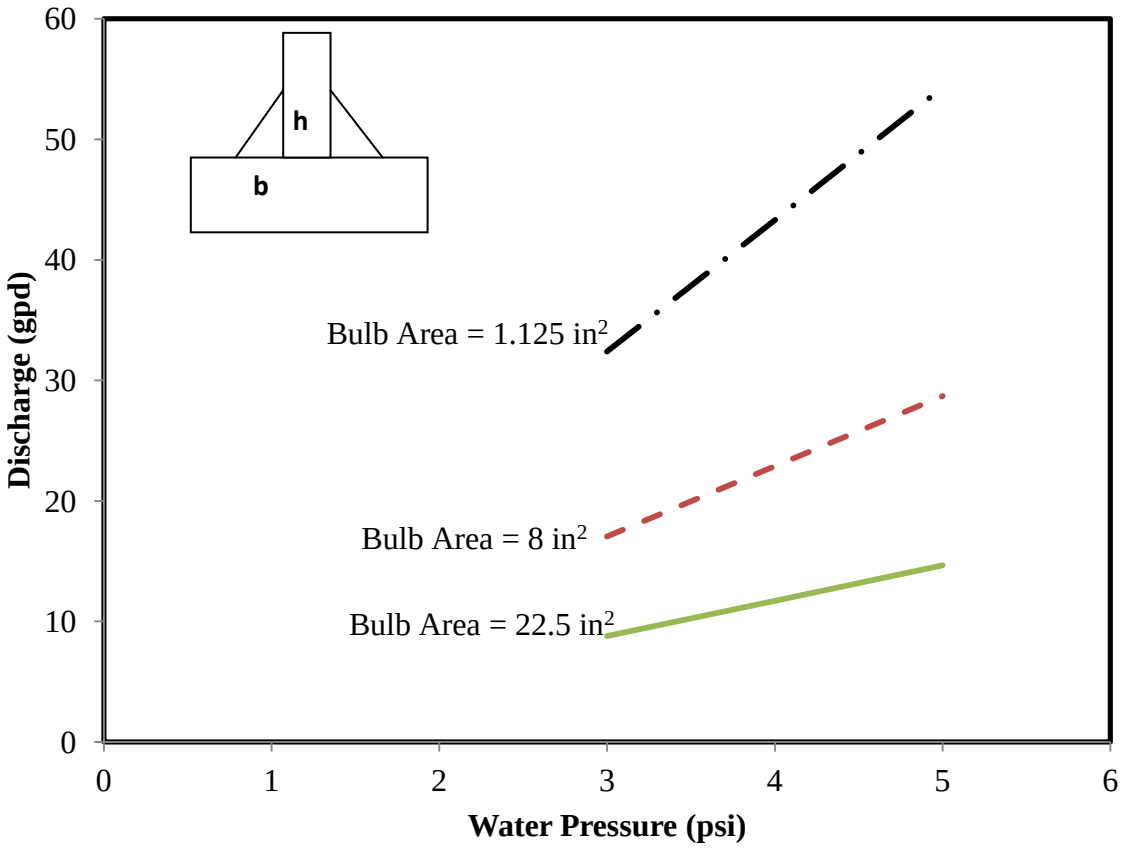

Figure 6-24: Variation of Discharge with Different Grouted Bulb Dimensions.

When the grouted bulb was 1.5 in x 1.5 in. the discharge from the leaking joint was reduced from 1000 gpd to 32 gpd, 1400 gpd to 43 gpd and 1700 gpd to 54 gpd at 3, 4 and 5 psi respectively. However on increasing the grouted bulb dimensions to 4 in. the discharge was further reduced to 17, 23 and 29 gpd at 3,4 and 5 psi respectively. When the dimensions of the grouted buld were 9 in x 5 in, the discharge at 3, 4 and 5 psi were 9, 12 and 15 gpd respectively. Thus it is noted that on increasing the grouted bulb dimensions, the discharge is significantly reduced.

6.5 Summary

Based on the modeling of grout curing, stress-strain relationship and leak control, following conclusions can be determined.

1. The uni-axial stress developed during the expansion of the polyurethane grout during its setting has been modeled. Expulsion of the bi-product, carbon-dioxide during the polymerization reaction, increase in temperature of the material owing to the exothermic reaction and increasing tensile strength of the grout affect the uni-axial stress developed during the grout expansion.
2. In order to characterize the stress-strain behavior of the grout, p-q model was used to fit the experimental results. It was noted that more addition of surfactants increased the q value indicating the behavior of the grouted sand tending towards linear order. However, the curing time of the grouted sand does not have much impact on the stress-strain trend.
3. The 2D Plaxis model emulated well lateral leaking joint. The increase in permeability of the sand increased the discharge. It was also observed that the increase in the grouted sand dimensions decreased the discharge.

CHAPTER 7 CONCLUSIONS AND RECOMMENDATIONS

7.1 Conclusions

This study investigated the use of chemical and cementitious grout materials for different applications such as sealing and sensing. Acrylamide and acrylic grout were modified with cationic and anionic surfactants and the effect of this modification on the grout workability and strength properties have been addressed. Similarly, the cement grout with W/C 0.6 and 1 were modified with metakaolin clay. The test methods were developed to evaluate the self sensing capability of the grout material. Large scale model tests were used to evaluate the performance of grout in sealing lateral leaks and in sealing pipes for decommissioning. A phenomenological model was developed to predict the uni-axial stress developed during the expansion of the injected polyurethane grout during application. Based on the study following conclusions can be advanced:

1. Addition of CTAB and SDS up to 4% by weight of the acrylamide grout solution did not affect the viscosity of the grout solution. The viscosity of the acrylic grout resin was 5.2 centipoise (cP). The gelling time of the grout was increased with the addition of CTAB at all initial temperatures investigated in this study. Addition of SDS increased the gelling time at higher temperatures but reduced the gelling time when the test was conducted at an initial temperature of 40^{o}F. Maximum curing temperature decreased with the addition of surfactants for most cases investigated. The setting time of the acrylic grout at room temperature (70^{o}F) varied from 20 to 30 seconds.

2. The pullout strength of the grout and grouted sand decreased with the addition of surfactants. The pullout strengths in the grouted sand were higher than the grout. The failures in the grout and grouted sand were at the interface, shear failure. Addition of surfactants increased the compressive strength of the grouted sand however the failure strain was increased when CTAB was added to the grout.

3. Volume of the grout used for sealing applications is an important factor as more the volume of the grout used, more the extrusion pressure needed to expel the grout during sealing applications. Addition of carbon fiber caused a significant change in the dielectric constant value of the chemically grouted sand. Grouted sand with carbon fiber exhibits both piezo-resistive as well as dielectric variation behavior on stress application.

4. The average weight change of grouted sand due to water absorption in 7 days was negligible. The shrinkage, change in length, at 90% humidity was zero. The permeability of the grouted sand was zero, impermeable under a hydraulic gradient of 100. The compressive strength increased with curing time. The average compressive strength after 28 days of curing was 19 psi; The average change in weight in pH 2, 7 and 10 after six months was less than 3% on all three cases.

5. The average leak rate at the 4-inch diameter lateral pipe joint was 1300 gallons/day before grouting. Model tests showed that grouting with acrylic grout was effective in eliminating the leak at the lateral joint (zero water leak at 5 psi

water pressure) immediately after grouting and after two wet and dry cycles over period of one month.

6. The gelling time of the polyurethane grout was not altered when subjected to oil environment. The surfactants and cement had a significant effect in altering the gelling time of the grout.
7. The uniaxial pressure exerted by the polyurethane grout was more in oil environment indicating greater expansion of the grout whereas, the peak temperature was low in oil environment compared to water.
8. The polyurethane grout was totally impervious to water at a hydraulic pressure as high as 14.5 (hydraulic gradient, I = 100). The strength of the grout increased on subjecting the ample to permeability (interaction with water). The coefficient of permeability was zero for a hydraulic gradient of 100 even after three months.
9. The confined compressive strength of the polyurethane grout increased when it was exposed to the oil environment. The strength after permeability is more than the strength before permeability indicating the continued chemical reaction of the grout with water.
10. The polyurethane grout has excellent bonding with the PVC pipe which is evident from the extrusion test results. It is to be noted that the larger the contact area of the grout with the pipe wall, the more the extrusion strength.

11. It was observed that enclosing an impermeable barrier of grouted sand in-between grouted balloons gave best results however sealing and eliminating the interface leak at high pressures are still a challenge.
12. Addition of clay decreased the bleeding capacity of the cement grouts with w/c ratio of 0.6 and 1. The flow-ability of the grout with w/c ratio of 0.6 was affected by the addition of clay. That was not the case with grout with w/c ratio of 1. The initial and final setting time were affected by the addition of clay. The grouts with lower W/C ratio had set fast when compared to those with higher setting times and the difference between the initial and final setting times were also altered significantly on addition of clay. The electrical resistivity peaked before the initial setting of the grouts. The resistivity was affected by the w/c ratio and the clay content.
13. The general failure during the pull-out strength for the cement grout was interface shear. The pullout strength of the cement grout decreased with the addition of clay for the grouts with w/c ratio of 1. The changes were minimal for grouts with w/c ratio of 0.6. Grouts with w/c ratio 0.6 had a higher compressive strength than grouts with w/c ratio 1.
14. The addition of 5% clay to the cement grout had a noticeable impact on the relative dielectric constant of the cement grout with W/C 0.6 and 1. Addition of Sand decreased the Er of the grout. The void content in the grout has the greatest impact on the dielectric constant of the grout. Piezo resistive behavior was observed with and without the addition of clay and, results suggest that, the resistance values reached very low values when C-fiber was added. Clay addition

did have an impact on the dielectric variation on stress application of the cement grout. W/C ratio plays a very vital role in determining the dielectric constant values of the cement grout especially when the material under study is subjected to stress.

15. The proposed phenomenological model predicted well, the uniaxial stress developed during the confined expansion of the polyurethane grout during curing. The gas formation, grout strengthening and temperature change during the polymerization reaction are the key governing factors responsible for the expansion of the polyurethane grout.
16. The stress – strain properties of the chemically grouted sand were predicted well with the p-q model. It was observed that addition of 4% surfactants tend to linearize the stress strain curve indicated by the increase in q value.
17. The lateral leaking joint was numerically studied using a finite element model. It was possible to quantify the effect of grouted mass and permeability on the leak at the pipe joint. On grouting the joint the leak was significantly reduced. The leak was reduced to less than 20 gallons/day when the grouted sand bulb formation was 22.5 sq.in in cross section.

7.2 Recommendations

Based on the experimental analysis and study, following suggestions are recommended:

1. It is essential to study the impact of surfactant on the sensing capabilities of the grout. Also, since one of the component of the acrylamide and acrylic grout have a small amount of non-ionic surfactant (tri-ethanol amine), it is essential to investigate the effect of addition of different types of non-ionic surfactants to the grout. Studying the behavior of the grout on addition of organic surfactants is also recommended as the grout under study was polymeric by itself.

2. It is essential to characterize the different types of polyurethane grouts in market for the purpose of decommissioning pipelines as, it has been proven that the use of hydrophyllic polyurethane grout is effective for the same. It is also recommended to develop testing methods to inject the grout in the pipeline at certain confined condition because, the expansion feature of the grout also would possess better strength if the expansive grout is condensed (improvement of permeability properties).

3. Measurement of dielectric constant has proven to be a very good tool to catagorize the stress related – sensing behavior. However more innovative methodologies should be developed to implement the use of the grout with enhanced sensing capabilities in the field.

REFERENCES

Akbulut, S., Saglamer, A., (2002) "Estimating the Groutability of Granular Soils: A New Approach." Journal of Tunnelling and Underground Space Technology, Vol 17, No 4, pp 371-380.

Akiyama, M., Kawasaki, S., (2012) "Novel grout material comprised of calcium phosphate compounds: In vitro evaluation of crystal precipitation and strength reinforcement." Engineering Geology, Vol 125, pp 119-128.

Anagnostopoulos, C., and Hadjispyrou, S., (2004) "Laboratory Study of an Epoxy Resin Grouted Sand." Ground Improvement, Vol 8, No.1, pp 39-45.

Anagnostopoulos, C. A., (2005) "Laboratory study of an injected granular soil with polymer grouts." Tunnelling and Underground Space Technology, Vol 20, pp 525-533.

Anagnostopoulos, C. A., (2007) "Cement-clay grouts modified with acrylic resin or methyl methacrylate ester: Physical and mechanical properties." Construction and Building Materials, Vol 21, pp 252-257.

Ata, A., and Vipulanandan, C., (1998) "Cohesive and Adhesive Properties of Silicate Grout on Grouted - Sand Behavior." Journal of Geotechnical and Geoenvironmental Engineering, ASCE, Vol 124, No.1, pp 38-44.

Axelsson, M., (2006) "Mechanical tests on a new non-cementitious grout, silica sol: A laboratory study of the material characteristics." Tunnelling and Underground Space Technology, Vol 21, pp 554-560.

Baltazar, L. G., Fernando, M.A. H., Fernando J., (2012) “Optimisation of flow behavior and stability of superplasticized fresh hydraulic lime grouts through design of experiments.” Construction and Building Materials, Vol 35, pp 838-845.

Christopher, B.R., Atmatzidis, D.K., Krizek, R.J., (1989) “Laboratory Testing of Chemically Grouted Sand,” Geotechnical Testing Journal, Vol 12, No.2, pp 109-118.

Domone, P., L., (1988) “The Properties of Low Strength Silicate/Portland Cement Grouts.” Journal of Cement and Concrete Research, Vol 20, No 1, pp 25-35.

Ericksson, M., Friedrich, M., Christoph, V., (2004) “Variations in the rheology and penetrability of cement-based grouts – an experimental study.” Cement and Concrete Research, Vol 34, pp 1111-1119.

Gallavresi. F.,(2009) “Grouting Improvement of Foundation Soils,” Keynote Lecture, pp 1-39, Grouting, Soil Improvement and Geosynthetics, Conference Proceedings, February 28.

Gallagher, P. M., Mitchell, J. K., (2002) “Influence of colloidal silica grout on liquefaction potential and cyclic undrained behavior of loose sand.” Soil Dynamics and Earthquake Engineering, Vol 22, pp 1017-1026.

Harendra, S, and Vipulanandan, C.(2008) "Degradation of High Concentrations of PCE Solubilized in SDS and Biosurfactant with Bimetallic Fe/Ni Particles," Colloids and Surfaces A: Physicochemical and Engineering Aspects, Vol. 322, No. 3, pp. 6-13.

Haug, M.D., Al-Manaseer, A.A., and Coode, A.M., (1998) "Impact of Confining Pressure on Long-Term Performance of Chemical Grout in Salt Water." Journal of Materials in Civil Engineering, ASCE, Vol 10, No.2, pp 70-75.

Huang, W., H., (2001) "Improving the Properties of Cement-Fly ash Grout Using Fiber and Superplasticizer." Journal of Cement and Concrete Research, Vol 31, No 7, pp 1033-1041.

Hutagalung,S. D., Sahrol, N. H., Ahmad, Z. A., Ain, M. F., Othman, M., (2012) "Effect of MnO2 Additive on the Dielectric and Electromagnetic Interference Shielding Properties of Sintered Cement Based Ceramics." Ceramics International, Vol 38, pp 671-678.

Karol, R.H., (1982) "Seepage Control with Chemical Grout." Conference Proceedings on Grouting in Geotechnical Engineering, ASCE, pp 564-575.

Karol R. H., (1990), Chemical Grouting, Marcel Dekker, Inc., New York, 2nd edition, pp 465.

Kilic, A., Yasar, E., Celik, A., G., (2002) "Effect of Grout Properties on the Pull-Out Load Capacity of Fully Grouted Rock Bolt." Journal of Tunnelling and Underground Space Technology, Vol 17, No 4, pp 355-362.

Krishnamoorthy, T.S., Gopalakrishnan, S., Balasubramanian, K., Bharatkumar, B.H., Rama Mohan Rao, P., (2002) "Investigations on Cementitious Grouts Containing Supplementary Cementitious Materials." Cement and Concrete Research, Vol 32, pp 1395-1405.

L. Lefebre, "Simulation numerique de l'expansion des mousses en ´polyurethane." Ph.D. Thesis, Louvain-la-Neuve, 1993.

Lubeck, A., Gastaldini, A. L. G., Barin, D. S., Siqueira, H. C., (2012) " Compressive Strength and Electrical Properties of Concrete with White Portland Cement and Blast-Furnace Slag." Cement and Concrete Composites, Vol 34, pp 392-399.

Maalej, Y., Dormieux, L., Canou, J., Dupla, J.,C., (2007) "Strength of a Granular Medium Reinforced by Cement Grouting." Journal of Comptes Rendus Mecanique, Vol 335, No 2, pp 87-92.

Maher, M. H., Ro, K. S., Welsh, J. P., (1994) "High strain dynamic modulus and damping of chemically grouted sand." Soil Dynamics and Earthquake Engineering, Vol 13, pp 131-138.

Mattey, Y., (2001) " Mechanical Properties and Microstructure of Polyurethane Grout." M.S. Thesis, University of Houston

Mesbah, H. A., Yahia, A., Khayat, K. H., (2011) "Electrical Conductivity Method to Assess Static Stability of Self-Consolidating Concrete." Cement and Concrete research, Vol 41, pp 451-458.

Ozgurel, H. G., (2004) "Mechanical Behavior of Grout and Groutability of Acrylamide Grout used in Leak Control at Lateral Pipe Joints." M.S. Thesis, University of Houston.

Ozgurel, H. G. and Vipulanandan, C. (2005) "Effect of Grain Size Distribution on Permeability and Mechanical Behavior of Acrylamide Grouted Sand," Journal of Geotechnical and Geoenvironmental Engineering, Vol. 131, No. 12, pp.1457-1465

Nguyen, V., Sebastien, R., Gallias, J., (2011)"Influence of cement grouts composition on the rheological behaviour." Cement and Concrete Research, Vol 41, pp 292-300.

Papadakis ,V.G., Vayenas, C. G., and Fardis, N. (1991) "Physical and Chemical Characteristics Affecting the Durability of Concrete," ACI Materials Journal, Vol 8, No. 2, pp. 186-196.

Paul, E.C., (1988) " Mechanical Behavior of Polyester and Epoxy Polymer Concrete Systems," M.S. Thesis, University of Houston.

Potong, R., Rianyoi, R., Jaitanong, N., Yimnirun, R., Chaipanich, A., (2012) "Ferroelectric Hydterisis Behavior and Dielectric Properties of 1-3 Lead Zirconate Titanate-Cement Composites." Ceramics International, Vol 38S pp S267-S270.

Sabir BB, Wild S, Bai J. Metakaolin and calcined clays as pozzolans for concrete: a review. Cement Concrete Compos 2001;23(6):441–54

Sahmaran, M., Ozkan, N., Keskin, S.B., Uzal, B., Yaman, I.O., Erdem, T.K., (2008) "Evaluation of natural zeolite as a viscosity-modifying agent for cement-based grouts." Cement and Concrete Research, Vol 38, pp 930-937.

Schwarz, N., Dubois, M., Neithalath, N., (2007) " Electrical Consudtivity based characterization of Plain and Coarse Glass Powder Modified Cement Pastes." Cement and Concrete Research, Vol 29, pp 656-666.

Shannag, M. J., (2002) "High-performance cementitious grouts for structural repair." Cement and Concrete Research, Vol 32, pp 803-808.

Shenoy, S. G., (1991) “Behavior of cement-Based Grouts and Grouted Sands.” M.S. Thesis, University of Houston.

Snuparek, R., Soucek, K., (2000) “Laboratory Testing of Chemical Grouts.” Tunnelling and Underground Space Technology, Vol 15, No 2, pp 175-185.

Somasundaram, S., (2003) “Behavior of Flexible and Rigid Polyurethane Grouts Used for Controlling Water Leaks”, M.S. Thesis, University of Houston.

Sonebi, M., Lachemi, M., Hossain, K.M.A., (2013) “Optimisation of rheological parameters and mechanical properties of superplasticised cement grouts containing metakaolin and viscosity modifying admixture.” Construction and Building Materials, Vol 38, pp 126-138.

Svermova, L., Mohammed S., Bartos, P. J.M., (2003) “Influence of mix proportions on rheology of cement grouts containing limestone powder.” Cement & Concrete Composites, Vol 25, pp 737-749.

Tan, O., Sahin Zaimoglu, A., Hinislioglu, S., Altun, S., (2005) “Taguchi approach for optimization of the bleeding on cement-based grouts.” Tunnelling and Underground Space Technology, Vol 20, pp 167-173.

Taylor, M. A., Arulanandan, K., (1974) “Relationships between Electrical and Physical Properties of cement Pastes” Cement and Concrete Research, Vol 4, pp 881 - 897.

Vintzileou, E., Miltiadou-Fezans, A., (2008) “Mechanical properties of three-leaf stone masonry grouted with ternary or hydraulic lime-based grouts.” Engineering Structures, Vol 30, pp 2265-2276.

Vipulanandan, C. and Shenoy, S. (1992) "Properties of Cement Grouts and Grouted Sands with Additives," Proceedings, Grouting, Soil Improvement and Geosynthetics, ASCE, pp. 500-511.

Vipulanandan, C., Jasti, V., Magill, D. and Mack, D. (1996), "Shrinkage Control in Acrylamide Grouts and Grouted Sands," Proceedings, Materials for the New Millennium, ASCE, Washington D.C., pp.840-850.

Vipulanandan, C. and Jasti, V. (1996), Behavior of Acrylamide and N-methylolacrylamide (NMA) Grouts and Grouted Sands, Research Report No. CIGMAT/UH 96-2, University of Houston, Houston, Texas.

Vipulanandan, C. Mattey, Y., Magill, D. and Mack, D. (2000) "Characterizing the Behavior of Hydrophilic Polyurethane Grout," Proceedings, Advances in Grouting Technologies ASCE, GSP 104, Denver, CO, pp. 234-245.

Vipulanandan, C., and Ozgurel, H. G. (2009) "Simplified Relationships for Particle-Size Distribution and Permeation Groutability Limits for Soils," Journal of Geotechnical and Geoenvironmental Engineering, Vol. 135, No. 9, pp. 1190-1197.

Vipulanandan, C., and Sunder, S. (2011) "Effect of cationic Surfactant on the Behavior of Acrylamide Grout and Grouted Sand," Conference Proceedings, Geo-frontiers, pp. 687-696.

Vipulanandan, C., and Sunder, S. (2012) "Anionic and Cationic surfactant modified Acrylamide Grout," Conference Proceedings, Grouting and Deepmixing Conference, March 2012.

Vipulanandan, C., and Sunder, S. (2012) "Anionic and Cationic surfactant modified Acrylamide Grout," Conference Proceedings, Grouting and Deep mixing Conference, March 2012.

Vipulanandan, C., and Sunder, S. (2012) "Effect of Metakaolin on the Working and Strength Properties of Cement Grout," Conference Proceedings, Grouting and Deep mixing Conference, March 2012.

Wang, X., Zhou, H., (2001) "An Improved Hyperbola Rheological Model for Fresh Cement-Clay Grouts." Journal of Tunnelling and Underground Space Technology, Vol 16, No 4, pp 353-357.

Weidenborg, M., Kallqvist, T., Odegard, K., Sverdrup, L.E., and Vik, E.A., (2001) "Environmental Risk Assessment of Acrylamide and Methylolacrylamide From a Grouting Agent Used in Tunnel Construction of RomerikSporten, Norway." Water Resources, Vol 35, No.11, pp 2645-2652.

Wen, S., Chung, D. D. L., (1998) "Piezoresistivity in Continuous Fiber Cement-Matrix Composite." Cement and Concrete Research, Vol 29, pp 445-449.

Wen, S., Chung, D. D. L., (2000) "Damage Monitoring of cement Paste by Electrical Resistance Measurement." Cement and Concrete Research, Vol 30, pp 1979-1982.

Wen, S., Chung, D. D. L., (2001) "Effect of Admixtures on the Dielectric Constant of cement Paste." Cement and Concrete Research, Vol 31, pp 673-677.

Wen, S., Chung, D. D. L., (2002) "Cement-based Materials for Stress Sensing by Dielectric Constant." Cement and Concrete Research, Vol 32, pp 1429-1433.

Xinghua, W., Quqing, G., (1997) "Study of a New Cheap Grouting Material: Clay Hardening Grout." Journal of Tunneling and Underground Space Technology, Vol 12, No 4, pp 497-502.

Zelanko, J. C., Karfakis, M. G., (1997) "Development of a Polyester-based Pumpable Grout." Int. J. Rock Mech. & Min. Sci., Vol 34:3-4, No 357.

APPENDIX

Designation: CIGMAT GR 8-09

Standard Test Method for Measuring the Gelling Time of Grout Mix.

1. Scope

1.1 This test method describes the determination of gelling time of chemical grouts.

1.2 The values are stated in British and SI units.

1.3 This standard does not address the safety concerns associated with the handling of grouts. It is the responsibility of the user of this standard to establish appropriate safety and health practices, and determine the applicability of regulatory limitations prior to use the grout/polymer with the help of material manufacturer/supplier.

1.4 MSDS sheet must be reviewed before testing the grout.

2. Referenced Documents

1.1 ASTM Standard C0953 -06 "standard test method for time of setting of grouts for Preplaced-Aggregate Concrete in the Laboratory".

3. Terminology

3.1 Gelling time – It is the time taken for the free radical polymerization reaction of the grout mix to change. It is also referred to as setting time in the literature.

4. Summary of Test Method

4.1 When the grout mix is prepared by adding the subscribed ingredients of chemicals in required proportions, the chemicals being the grout under study, initiator, activator and other chemicals that has a tendency to participate in the reaction, the polymerization reaction takes place and the grout begins to set. Then the gelling time is observed by careful visual observation.

5. Significance and Use

5.1 The purpose of this test method is to provide a means for measuring the gelling time of the grouts at different conditions (like with temperature and varying proportions of the chemicals).

5.2 The test procedure described in here provides a standard method of obtaining data for research and development, quality control, acceptance and rejection under specifications, and special purposes.

5.3 The data obtained by this test method is applicable to the material under conditions of the particular test and are not necessarily the same as obtained in other environments.

6. General Test Conditions

6.1 Tests shall be conducted under known conditions of temperature and humidity. However since the observation of gelling time is associated with the change in the temperature owing to the progress in the chemical reaction of the grout mix, the initial temperature is taken into consideration. In case of dispute, test will be performed at room temperature ($23\pm2\ ^{0}C$) and relative humidity (50 ± 5)%.

6.2 It is recommended that all tests shall be performed with minimum contact with air.

7. Sampling and Test Specimen

7.1 The minimum requisites to run this test are the grout (under study), catalyst and the activator and the solvent, mostly water. (Representative samples of the grout/polymer being examined shall be selected at random as required.

7.2 It is advisable to repeat the experiment with 2 samples of the same mix of the grout.

8. Apparatus

8.1 Glass Beaker (600 mL) – The beakers are used for preparing the mix of grouts.

8.2 Thermometer/Thermocouples – it is used to measure the temperature variation with respect to time.

8.3 Stop watch – the watch accuracy will be based on the gelling time of the grout. Generally a stop watch with an accuracy of 1 second is used to measure the time and accurately note the time at which the grout gels or sets.

9. Procedure

9.1 In one beaker, prepare a solution of the required percentage by weight of catalyst and solvent which is generally water. It is essential to prepare 50 g of this solution.

9.2 In the second beaker, prepare a solution containing the required percentage by weight of grout and activator in the solvent which is generally water.

9.3 While preparing the second specimen care should be taken to weigh the grout first and put it in the beaker and then add sufficient solvent and mix it well such that the grout gets dissolved completely in it. Then the required percentage of activator should be added and then additional water should be added to bring the total weight of the beaker to 50 g.

9.4 Finally when two beakers are fully prepared, it is ensured that the beakers contain a perfectly homogenous solution of catalyst and grout and activator, that is, they are perfectly mixed until the chemicals are fully dissolved.

9.5 Then the solution in the second beaker is transported into the first beaker to initiate the reaction.

9.6 After mixing the solutions the stop watch is immediately turned on and the time initial time is noted.

9.7 The beaker is kept at an inclined position of 45 degrees to the vertical to check the flow of the solution.

9.8 When the solution cannot flow at this position of the beaker, the time is noted. This time corresponds to the gelling time of the grout mix.

9.9 Simultaneously temperature is also noted from the beginning of the reaction by inserting the thermocouple into the solution to ensure that the reaction is taking place

because the sudden rise in the temperature indicates the ending of the reaction and it is at this point of time that the gelling time is observed.

9.10 One more reason for observing the temperature is that, a rise in temperature is a clear indication of the smooth progress in the exothermic chemical reaction and later on the temperature falls to room temperature after attaining a peak.

10. Schematic Diagram

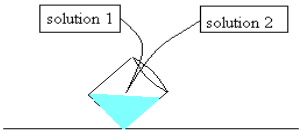

Figure A1: A Schematic Diagram of the Apparatus Set Up.

11. Report

11.1 Report the following information:

11.1.1 Type of grout

11.1.2 Weight of the grout in grams

11.1.3 Weight of the catalyst in grams

11.1.4 Weight of the activator in grams

11.1.5 Weight of the solvent in grams

11.1.6 Initial or the beginning temperature of the experiment in degree Fahrenheit

11.1.7 Gelling time in seconds

11.1.8 Graph of time in seconds and variation in temperature in degree Fahrenheit with the gelling time indicated in it

12. Precision and Bias

15.1 Since there is no reference material available for determining the precision and bias, no statement is being made at this time. There is ongoing research at CIGMAT on this topic and once the results become available more information will be added to this standard.

13. Keywords.

Grout mix, activator, catalyst, gelling time.

14. References

14.1 ASTM Standard C0953 -06 “standard test method for time of setting of grouts for Preplaced-Aggregate Concrete in the Laboratory”.

14.2 Reuben H.Karol, “Chemical grouting and Soil Stabilization, third edition.